



Lithium solid-state batteries: State-of-the-art and challenges for materials, interfaces and processing

Nicola Boaretto^{a,1}, Iñigo Garbayo^{a,1}, Sona Valiyaveetil-SobhanRaj^{a,b}, Amaia Quintela^{a,b}, Chunmei Li^a, Montse Casas-Cabanas^{a,c,**}, Frederic Aguesse^{a,*}

^a Centre for Cooperative Research on Alternative Energies (CIC energiGUNE), Basque Research and Technology Alliance (BRTA), Alava Technology Park, Albert Einstein 48, 01510, Vitoria-Gasteiz, Spain

^b University of the Basque Country (UPV/EHU), Barrio Sarriena, s/n, 48940, Leioa, Spain

^c Ikerbasque, The Basque Foundation for Science, Maria Diaz de Haro 3, 48013, Bilbao, Spain

HIGHLIGHTS

- Next steps towards solid state batteries.
- Potential and most probable candidates as solid electrolytes, cathode active materials.
- Challenges to develop electrochemically stable interfaces.
- Overview of the existing processing technology for cell production.

ARTICLE INFO

Keywords:

Solid state batteries
Processing technology
Interfacial challenges
Solid electrolytes

ABSTRACT

Lithium solid-state batteries (SSBs) are considered as a promising solution to the safety issues and energy density limitations of state-of-the-art lithium-ion batteries. Recently, the possibility of developing practical SSBs has emerged thanks to striking advances at the level of materials; such as the discovery of new highly-conductive solid-state electrolytes. Consequently, the focus in research has progressively shifted towards the integration of the various components, the battery's functionality at full cell level, and the scalability of the fabrication processes. Considering these points, the development of SSBs still faces formidable challenges. This review covers the recent advances in SSB development, stressing the importance of full cell integration. The most relevant materials and fabrication processes are briefly summarized and their potential applications in SSBs are examined. The main challenges and strategies for full cell integration are then discussed highlighting the most promising materials and the best suited processing techniques. Particular attention is paid on the mutual compatibility of the cell components, the properties of the interfaces within the cell (anode-electrolyte, cathode-electrolyte, intra-electrolyte) and the strategies applied to stabilize and minimize the resistance of these interfaces via compatible processing.

1. Introduction

Modern society is demanding, more than ever, solutions for advanced energy storage systems that require higher energy and/or power densities, better safety, and improved sustainability. This is mainly due to the increasing demand for electric vehicles, the main

driving force of energy storage solutions, and the technological push for other applications such as drones, portable electronic devices or stationary applications [1]. Climatic and environment considerations are other factors that urgently need advanced energy storage solutions. Among rechargeable technologies, lithium ion batteries (LIBs) are the most mature technology, currently leading as the power and energy

* Corresponding author.

** Corresponding author. Centre for Cooperative Research on Alternative Energies (CIC energiGUNE), Basque Research and Technology Alliance (BRTA), Alava Technology Park, Albert Einstein 48, 01510, Vitoria-Gasteiz, Spain.

E-mail addresses: mcasas@cicenergigune.com (M. Casas-Cabanas), faguesse@cicenergigune.com (F. Aguesse).

¹ Authors with an equal contribution to the manuscript.

supplier for technological applications due to the comparatively superior performance in most aspects [2,3].

State-of-the-art (SoA) LIBs technology, which is based on liquid, organic electrolyte, is generally believed to have already reached theoretical maximum energy density ($250 \text{ Wh}\cdot\text{kg}^{-1}$ and $600 \text{ Wh}\cdot\text{L}^{-1}$) [4]. However, this does not meet the emerging energy requirements of new applications. Also the safety of SoA LIBs faces challenges associated with the use of toxic and flammable liquid electrolytes [5–7]. The solid-state battery approach, which replaces the liquid electrolyte by a solid-state counterpart, is considered as a major contender to LIBs as it shows a promising way to satisfy the requirements for energy storage systems in a safer way. Solid Electrolytes (SEs) can be coupled with lithium metal anodes resulting in an increased cell energy density, with low or nearly no risk of thermal runaway [8,9]. Further increase of the energy density up to $400 \text{ Wh}\cdot\text{kg}^{-1}$ and $900 \text{ Wh}\cdot\text{L}^{-1}$ is thus possible with the use of high capacity and high voltage cathode active materials [10, 11]. Nonetheless, the maximum thickness of electrolyte and its loading in the cathode should be precisely assessed, depending on the density of each material, in order to obtain full cells with competitive and desired energy density.

SEs fulfil a dual role in solid-state batteries (SSBs), viz. i) being both an ionic conductor and an electronic insulator they ensure the transport of Li-ions between electrodes and ii) they act as a physical barrier (separator) between the electrodes, thus avoiding the shorting of the cell. Over the past few decades, remarkable efforts were dedicated to the development of SEs, and the most relevant results have been summarized in several reviews [10,12,14–16]. SEs are typically comprised of polymer materials, famous for their integration in the Blue Car® [17], the first industrially developed electric vehicle based on the solid-state technology, and ceramic materials [18]. Recently, new high performing inorganic SEs [19,20] as well as mixtures between organic and inorganic electrolytes [21–23] have also been proposed and attract a lot of attention. The development of the SSBs is not only limited to the development of new SEs, as the replacement of the liquid component by a solid one represents a challenge for current cell production processes, whose steps need to be adapted and even redesigned. Over the last few years, research activities have oriented towards the adaptation of novel cell processing routes and the integration of components from these new routes towards the production to solid-state technology [24]. Processing of the different components should be revisited to ensure efficient cell fabrication in terms of performance, production speed, and sustainability. The processing of SSBs includes the development of the SE, and the solid cathode and anode. It is worth highlighting that processing routes to fabricate cathode, SE and final assembly of the full cell represent a critical step to achieve the promised cell performances. The utilization of ultra-thin electrolyte separators [25], and the increase of the packing density of the positive electrode [26] will further push the limits of the energy density towards high values. It is thus highly possible that the processing route of SSBs will be different from the current ones applied to LIB production.

Another challenge is related to the potential current density limits; which are due to the lower conductivity of solid-state electrolyte, and due to the presence of highly resistive solid-solid internal interfaces. Thus, the development of highly conducting electrolytes and of low resistive interfaces is one of the most important challenges facing the SSBs. Another challenge is represented by the stability of such interfaces [27]. Mechanical instability upon cycling and, importantly, chemical and electrochemical instability within the cells, results in the formation of undesired reactions at the interfaces [28–30]. This is also translated into large internal resistances and mechanical failures derived from volume changes or interfacial stresses [31]. Solving the interfacial issues requires finding the balance between the material and the processing technique that will resolve the technical issue while making processing at production level a reality [32–36].

Several recent reviews on SSBs are revisiting the performance on individual cell components, such as cathode materials [14,37,38], solid

electrolytes [12,21–23,39–45], or the use of lithium metal as the anode [46–48], as well as analysing the main challenges faced related to solid-solid interfaces formation [27,32–34,36,49–53]. Recent studies have focused on full cell integration and fabrication [24,28,36,53–56]. However, these mostly regard specific classes of SEs, usually inorganic solid-state electrolytes, and a complete landscape of SSBs is still missing. Here, we propose an analysis of the current status of SSBs putting the attention on the full cell development, covering SoA materials and most promising processing techniques, and the main challenges to overcome with respect to their integration in functional SSBs. This review aims to help the development of practical lithium SSBs, by focusing the attention on the most important challenges for the near future, and by summarizing the latest and most notable developments in the field.

2. Materials for solid-state batteries

2.1. Solid electrolyte materials

This section reviews the most relevant solid electrolyte (SE) materials for SSBs. A simple classification based on chemical composition is followed, differentiating between inorganic and organic (polymer-based) electrolytes [11,18,41,42]. The combination of both groups gives rise to a third intermediate class, namely hybrid solid electrolytes. Most relevant parameters are briefly discussed, including ionic conductivity, thermal stability and electrochemical stability window. Since the main focus of the review is on full cell integration, for a more detailed information on SE properties the reader is referred to the numerous reviews devoted to SEs [12,21–23,39–44,57–65].

2.1.1. Inorganic electrolytes

2.1.1.1. Oxide and polyanionic compounds. Lithium Superionic Conductors (LISICONs) were first reported by the composition $\text{Li}_{14}\text{Zn}(\text{GeO}_4)_4$, giving an ionic conductivity of 0.13 S cm^{-1} at 300°C (Fig. 1) [66]. $\text{Li}_{14}\text{Zn}(\text{GeO}_4)_4$ exhibits a crystal structure similar to $\gamma\text{-Li}_3\text{PO}_4$ [67] in which $\text{Li}_{11}\text{Zn}(\text{GeO}_4)_4^{3-}$ units form a three-dimensional network where three additional Li-ions occupy interstitial positions, providing Li-ion diffusion carriers. A certain anisotropy with preferential Li-ion mobility through the *ab* plane is reported [68]. An interesting material within this family is the $(1-x)\text{Li}_4\text{SiO}_4\text{-}(x)\text{Li}_3\text{PO}_4$ solid solution. Efficient ion transport was suggested by ab-initio calculations associated to a larger amount of Li interstitials [69]. A wide range of compositions was explored by varying the value of *x*: $0 < x < 1$ and appreciable ionic conductivities were reported for $x = 0.25, 0.5$ and 0.75 [70] as well as adding different dopants to the structure such as Al, Ge, As and V [71, 72]. LISICONs are stable against water and their thermal stability and near zero vapor pressure make them operational at high temperatures. The main drawback is typically associated to a low ionic conductivity at room temperature (ca. $10^{-7} \text{ S cm}^{-1}$) [66], although enhanced Li-ion conduction could be achieved by strategic substitution (recently, Deng et al. proved by molecular dynamics simulations a conductivity of $9\cdot 10^{-4} \text{ S cm}^{-1}$ at room temperature for $\text{Li}_4\text{Al}_{1/3}\text{Si}_{1/6}\text{Ge}_{1/6}\text{P}_{1/3}\text{O}_4$ [71]). Still, LISICONs are highly reactive with lithium metal and atmospheric CO_2 [18] and their electrochemical stability window is limited within the range of 1.4 V and 4 V [73].

Sodium Superionic Conductors (NASICONs) were first reported in 1976, by partial substitution of P by Si in the $\text{NaM}_2(\text{PO}_4)_3$ (*M* = Ge, Ti, Zr) structure [18]. Their crystal structure is characterized by corner-sharing P/SiO_4 tetrahedra and MO_6 octahedra [74] in which Na-ions occupy interstitial positions and preferentially diffuse along the *c*-axis [75]. Later on, the substitution of Na by Li was explored aiming to develop advanced Li-ion conductors. However, this substitution was found to entail a reduction of the ionic conductivity due to a large mismatch in the ionic radii between Li and Na ions and large covalency of Li–O bond when compared to Na–O [66]. Partial substitutions were

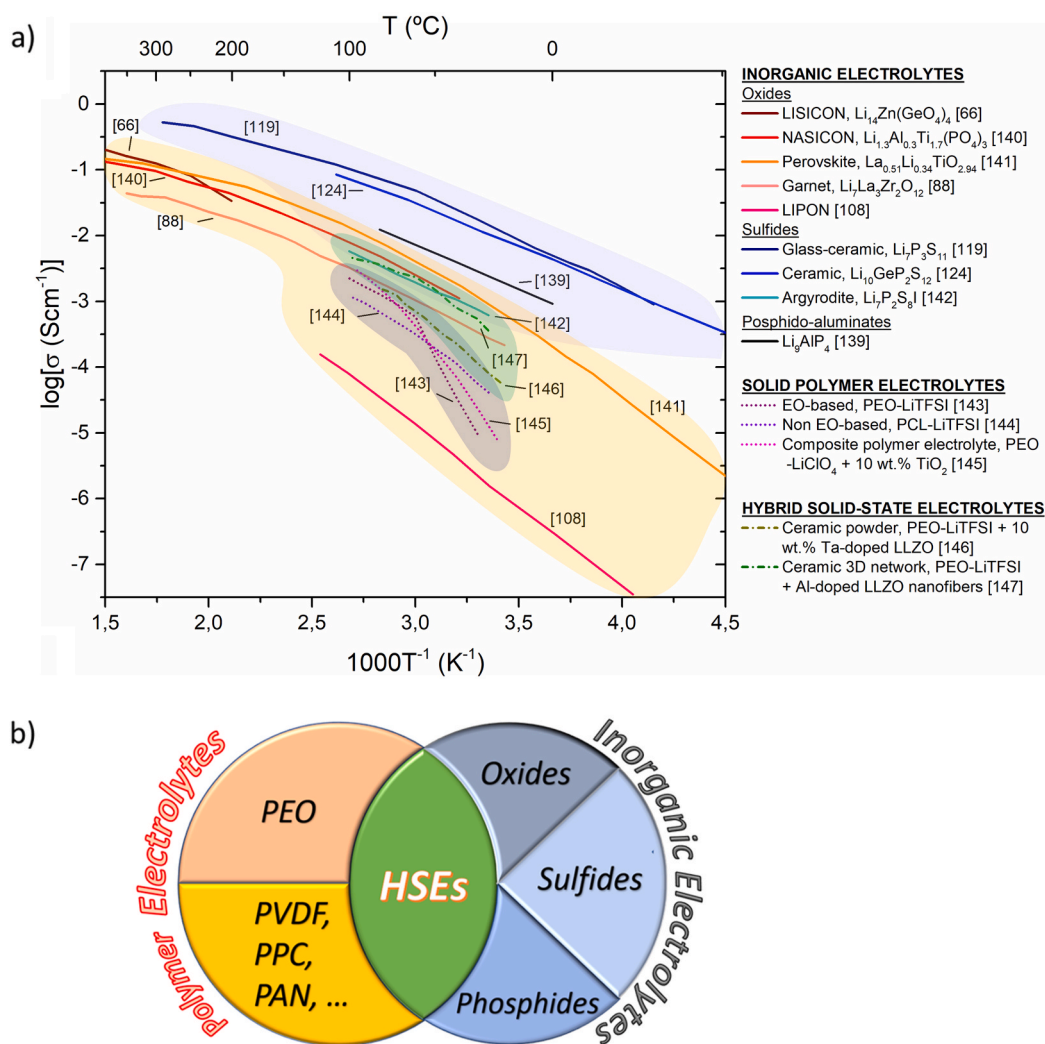


Fig. 1. a) Arrhenius plot of the ionic conductivity range of most representative inorganic, solid polymer and hybrid SEs, grouped per family. Data have been plotted from experimentally reported values to include inorganic (LISICON [66], NASICON [140], perovskite [141], garnet [88], LIPON [108], sulfide glass-ceramic [119], sulfide ceramic [124], argyrodite [142], phosphide-aluminate [139]), solid polymer (EO-based [143], non EO-based [144], composite polymer electrolyte, PEO-LiClO₄ + 10 wt.% TiO₂ [145]) and hybrid solid-state (ceramic powder [146], ceramic 3D network [147]) electrolyte families. The colored areas are indicative of the range of ionic conductivity that can be obtained within these families of compounds and varying the composition. b) Schematic summarizing the classification of the different existing solid-state electrolytes for solid-state batteries.

experimentally realized with different elements and valences to compensate the ionic radii mismatch and hence boost the ionic conductivity. In particular, trivalent Al is preferable for partial substitution thanks to its smaller ionic radius and the compositions made with $M = \text{Ti, Ge}$ with partial substitution of Al ($\text{Li}_{1+x}\text{Al}_x\text{Ti}_{2-x}(\text{PO}_4)_3$ – LATP and $\text{Li}_{1+x}\text{Al}_x\text{Ge}_{2-x}(\text{PO}_4)_3$ – LAGP, respectively) were reported showing higher ionic conductivity than the corresponding parent compounds [76,77]. The highest reported conductivities of LATP and LAGP are $1.09 \cdot 10^{-3} \text{ S cm}^{-1}$ [78] and $6.18 \cdot 10^{-3} \text{ S cm}^{-1}$ [75], respectively, at room temperature (Fig. 1). In general, the high conductivity added to moisture stability and wide thermodynamic electrochemical stability window make NASICONs competitive SE materials for SSBs. NASICONs have high elastic modulus, e.g. 115 GPa for LATP [79] and 125 GPa for LAGP [96], but they have also low fracture toughness, which results in overall unfavourable mechanical properties (as is the case of all oxide-based materials). Moreover, interaction with Li metal limits their direct combination unless protective layers are added [81]. Reduction of Ti/Ge in contact with Li metal leads to the formation of an unstable mixed (ionic/electronic) conductive interface which has been compared to the SEI layer in liquid electrolytes [82]. It results in a lower voltage limit of 2.17 V (LATP) and 2.7 V (LAGP) [73]. It is important to note that, despite the improved properties, LAGP is nearly 100 times more expensive than LATP owing to the high cost of Ge compared to Ti.

Li-based perovskites respond to the general formula ABO_3 ($A = \text{Li, Ca, Sr, La}$, and $B = \text{Al, Ti}$) [76,77]. In these materials, Li-ions hop from site to site through the bottleneck formed by face sharing dodecahedra.

Ionic conductivity in perovskites depends on different factors like i) Li, La and vacancy content, ii) composition, iii) size of A and B cations and of the bottleneck, iv) covalent nature of Ti–O bond and v) quenching temperature and atmosphere. One of the most promising materials is the $\text{Li}_{3x}\text{La}_{(2/3-x)\gamma(1/3-2x)}\text{TiO}_3$ (LLTO), where $0.04 < x \leq 0.17$ and γ is the number of cationic vacancies, obtained by aliovalent substitution of both metal ions in the A site [83]. A high bulk conductivity of $10^{-3} \text{ S cm}^{-1}$ was reported, owing to the larger radius and higher valence of La (Fig. 1) [18]. These are hard materials, reported with an elastic modulus value of 200 GPa [79]. Despite the high ionic conductivity at room temperature, the application of LLTO is also limited due to the reduction of Ti^{4+} to Ti^{3+} in contact with metallic lithium, similar to LATP, LAGP and LISICON. Hence the lower voltage limit is set at 1.8 V [73]. Moreover, processability of this material is also challenging as grain boundary resistivity can reduce by two orders of magnitude the total conductivity down to $10^{-5} \text{ S cm}^{-1}$ [84]. Through the use of dopants such as Nb^{5+} , the grain boundary resistance can be decreased as it reduces the positive charges accumulation at the grain boundary, which in turn reduces the space-charge layer formed between two grains [85,86]. Hence, proper interfacial engineering is indispensable to permit the integration of LLTO material in a battery technology.

The garnet family is characterized by the general formula $\text{A}_3\text{B}_2(\text{XO}_4)_3$, with eight, six and four coordinated cations [40]. Li-ion conducting garnets were initially reported within the compositions of $\text{Li}_5\text{La}_3\text{M}_2\text{O}_{12}$ ($M = \text{Nb, Ta}$) and $\text{Li}_6\text{Ala}_2\text{M}_2\text{O}_{12}$ ($A = \text{Ca, Sr, Ba}$ and $M = \text{Nb, Ta}$), reaching conductivity values of $10^{-6} \text{ S cm}^{-1}$ and $10^{-5} \text{ S cm}^{-1}$ at

room temperature, respectively [87]. The Li-ion conductivity was then significantly enhanced by maximizing the Li content with the so-called Li-stuffed garnets, responding to the parent formula $\text{Li}_7\text{La}_3\text{Zr}_2\text{O}_{12}$ (LLZO) [88,89]. The conductivity of this material exhibits high dependency on the crystalline structure, showing difference of two orders of magnitude in ionic conductivity between the cubic and the tetragonal phases [90,91]. Controlling Li loss during high temperature treatments as well as a doping strategy in either the Li, La or Zr sites have been reported to be fundamental for the stabilization of the cubic garnet phase with high Li-ion conductivity even at room temperature, see Fig. 1 [92]. Among the different dopants tested, Ta [93], Al [94] and Ga [95] are to be highlighted, showing conductivities close or higher than 1 mS cm^{-1} [96,97]. Using a dual substitution strategy, the ionic conductivity at room temperature could be enhanced up to 1.8 mS cm^{-1} with the composition $\text{Li}_{6.65}\text{Ga}_{0.15}\text{La}_3\text{Zr}_{1.90}\text{Sc}_{0.10}\text{O}_{12}$ [98]. The average value of elastic modulus for the garnet family has been estimated to be 150 GPa [79]. A wide electrochemical stability window of 0–6 V against metallic lithium, low electronic conductivity and negligible grain boundary contribution of garnets are a very appealing for their use as electrolyte material [20,99]. However, issues related to a poor wettability with Li metal typically lead to high contact resistance at the Li metal-electrolyte interface, requiring certain interfacial modification [100] (see section 4). Also, garnets present some limitations in terms of structural stability when exposed to ambient conditions as they are particularly reacting with moisture [101,102]. The formation of unwanted Li_2CO_3 at the surface leads to detrimental side reactions with Li metal, for which the application of different surface cleaning strategies becomes important [51]. A recent study indicates that, without any surface modification, Li_2CO_3 -free LLZO shows intrinsic lithiophilicity [103].

Finally, one of the most studied and even commercially used solid-state materials is the lithium phosphorus oxynitride (LiPON) [104]. With a low Li-ion conductivity of $\sim 10^{-6} \text{ S cm}^{-1}$ at room temperature, the use of LiPON has been limited to thin film-based batteries, where the reduced electrolyte thickness drastically diminishes the associated ohmic resistance allowing its practical use [105]. The synthesis of thin film LiPON is generally carried out by reactive magnetron sputtering (see section 3.4), starting from a Li_3PO_4 target source and using N_2 as background gas. Amorphous films are obtained where N atoms are incorporated in the phosphate structure, forming doubly coordinated and triply coordinated N–P bonds that favor Li-ion mobility [106]. An elastic modulus of 77 GPa has been reported for a LiPON thin film in a thickness range of 1–10 μm [107]. LiPON proposes a large electrochemical stability (0–5 V against Li/Li⁺) [108], although the reason behind the stability against metallic lithium seems most likely to be associated to the formation of a stable SEI composed by small units of Li_3PO_4 , Li_3P , Li_3N and Li_2O [109]. Additionally, LiPON is compatible with a wide range of electrode materials, thus enabling the development of high voltage microbatteries. Recently, single phase LiPON was synthesized via mechano-synthesis [110], which opens the door to new advances for this material in the field of bulk-type solid-state batteries.

Many new solid electrolytes are expected to be discovered within the next years thanks to the power of computational tools to accelerate designing new materials. This is the case for Zr-doped LiTaSiO_5 ($\text{Li}_{1.1}\text{Ta}_{0.9}\text{Zr}_{0.1}\text{SiO}_5$) that achieves a conductivity of $2.97 \times 10^{-5} \text{ S cm}^{-1}$ at 25°C , two orders of magnitude higher than undoped LiTaSiO_5 [111]. This was made possible by the quasi 1D-pathway formed when enriching the structure with lithium by acceptor dopants such as Zr.

2.1.1.2. Sulfides. Glassy sulfides were the first sulfide conductors to be developed and are mainly represented by the binary systems Li_2S – SiS_2 , Li_2S – P_2S_5 and Li_2S – GeS_2 , often also combined in ternary systems with other compounds such as Li_3N or LiI [112–114]. Heat treatments above the crystallization temperature (T_c) give rise to the so-called glass-ceramic sulfides, with increased conduction properties due to the stabilization of highly conducting crystalline phases precipitated from

mother glasses [115]. Typical conductivity values in this family of materials are in the range of 10^{-4} to $10^{-3} \text{ S cm}^{-1}$ at room temperature [39], being $\text{Li}_7\text{P}_3\text{S}_{11-x}$ the composition with the highest reported conductivity reaching $5.4 \cdot 10^{-3} \text{ S cm}^{-1}$ at 25°C [116]. Glassy sulfides have low elastic moduli (10–30 GPa) and excellent formability, allowing them to be highly densified by pressing even at room temperature [117,118]. Notably, a recent report has shown that thermal treatment optimization of $\text{Li}_7\text{P}_3\text{S}_{11-x}$ can lead to a further densification that allows reaching even superior conduction properties ($1.7 \cdot 10^{-2} \text{ S cm}^{-1}$) was reported at room temperature by Seino et al. [119], see Fig. 1).

Crystalline sulfides, derived from the LISICON $\gamma\text{-Li}_3\text{PO}_4$ parent structure, have emerged in the last decade as a very promising alternative to glassy and glass-ceramic sulfide conductors. Thio-LISICON-like materials exhibit an orthorhombic structure responding to the general formula $\text{Li}_{3+x}(\text{P}_{1-x}\text{M}_x)\text{S}_4$ ($\text{M} = \text{Si}, \text{Ge}, \text{Sn}$) [120,121]. In these compounds, the aliovalent substitution of P^{5+} by Si^{4+} or Ge^{4+} is compensated by a Li-ion excess occupying interstitial sites, which generates shorter Li–Li hopping distances that results in higher Li mobility. Moreover, compared to its oxide counterpart, exchanging O^{2-} by the bigger S^{2-} anions helps enlarging the Li-ion conducting channels [30], thus resulting in high ionic conductivities, $> 10^{-4} \text{ S cm}^{-1}$ at room temperature [121]. Some of the most relevant materials within this group are $\text{Li}_{4-x}\text{Ge}_{1-x}\text{P}_x\text{S}_4$ or $\text{Li}_{4-x}\text{Sn}_{1-x}\text{As}_x\text{S}_4$, with conductivities up to $2.2 \cdot 10^{-3} \text{ S cm}^{-1}$ [122,123].

Moreover, a new group of materials derived from the thio-LISICON family has lately attracted enormous attention due to its extraordinary conductive properties. Responding to the general formula $\text{Li}_{10}\text{MP}_2\text{S}_{12}$ (being $\text{M} = \text{Si}, \text{Ge}, \text{Sn}$) and primarily represented by $\text{Li}_{10}\text{GeP}_2\text{S}_{12}$ (LGPS), this family is characterized by a tetragonal unit cell in which Li-ions are distributed in four different crystallographic sites [48]. According to theoretical calculations and NMR experiments, Li conduction primarily occurs through hopping on tetrahedrally coordinated sites that form ultra-fast one-dimensional tunnels with enhanced Li mobility [125]. This results in a certain anisotropy on the ionic conduction, with *ca.* 40 times higher conductivity on the *c*-axis than on the *ab* plane [126]. Overall conductivity of the parent LGPS compound was reported to be $1.2 \cdot 10^{-2} \text{ S cm}^{-1}$ at room temperature (Fig. 1), although the highest conductivity was found in the related $\text{Li}_{9.54}\text{Si}_{1.74}\text{P}_{1.44}\text{S}_{11.7}\text{Cl}_{0.3}$ material, which reaches the unprecedented value of $2.5 \cdot 10^{-2} \text{ S cm}^{-1}$ at 25°C [127]. LGPS exhibits soft mechanical properties and the reported elastic modulus value is about 20 GPa [128].

Finally, the sulfide-based lithium argyrodite family, with general formula $\text{Li}_6\text{PS}_5\text{X}$ ($\text{X} = \text{Cl}, \text{Br}$), is lately gaining increasing attention. Derived from the mineral argyrodite (Ag_8GeS_6), the crystal structure is based on a tetrahedral close packing of S^{2-}/X^- anions, in which the P^{5+} cations are distributed in ordered PS_4^{3-} tetrahedra, leaving the rest of unoccupied tetrahedral holes filled with dynamically disordered Li-ions [129]. This random distribution of the univalent cations is believed to play a key role on the high Li mobility, reaching high ionic conductivities close to $10^{-3} \text{ S cm}^{-1}$ for *e.g.* the $\text{Li}_7\text{P}_2\text{S}_8\text{I}$ structure [129]. The highest conductivity value within this family was recently achieved in the related thioantimonate iodine argyrodite $\text{Li}_{6.6}\text{Si}_{0.6}\text{Sb}_{0.4}\text{S}_5\text{I}$, reaching $2.4 \cdot 10^{-2} \text{ S cm}^{-1}$ at room temperature [130].

The main limitation of sulfides (glassy, glass-ceramic and/or crystalline) relates to their limited chemical (H_2S generation in contact with moisture) [131] and electrochemical stability [132]. Theoretical calculations of Han et al. [133] concluded that the electrochemical stability in a selection of sulfide electrolytes (including LGPS, Li_3PS_4 or $\text{Li}_7\text{P}_2\text{S}_8\text{I}$) was very similar, with narrow thermodynamic electrochemical stability windows between 1.6 V (reduction of Ge or P) and 2.3 V (oxidation of S). In the particular case of LGPS, recent reports have experimentally confirmed the narrow kinetic electrochemical stability window [133, 134]. Reduction (at $\sim 1.7 \text{ V}$) and oxidation (at $\sim 2.1 \text{ V}$) of LGPS leads to the decomposition of the electrolyte into Li_2S , $\text{Li}_{15}\text{Ge}_4$ and Li_3P at 0 V and S, P_2S_5 and GeS_2 at 2.31 V [126,135]. In contact with metallic Li, LGPS was also reported to decompose forming an interphase containing

Li_3P , Li_2S , and Li-Ge alloy [136]. In this sense, interface engineering and the addition of protective coatings become crucial for the practical application of these materials (see section 4).

2.1.1.3. Lithium phosphides. In recent years, a new family of Li superionic conductors has emerged and requires attention as possible electrolyte alternatives for SSBs in the future: lithium phosphides [137–139]. Among this family, the most promising materials in terms of conductivity are Li_9AlP_4 and $\text{Li}_{14}\text{SiP}_6$, with values of $3 \cdot 10^{-3} \text{ S cm}^{-1}$ and $1 \cdot 10^{-3} \text{ S cm}^{-1}$ respectively [138,139]. However, further work is still required in order to assess the electrochemical stability of these materials, as well as their compatibility with different electrodes.

2.1.2. Polymer and hybrid solid electrolytes

Solid polymer electrolytes (SPEs) generally consist of ionically-conducting solutions of a lithium salt in a polymer host matrix [148]. Apart from the inherent advantages of SEs in terms of safety, the use of SPEs brings additional benefits related to the possibility of using plastic processing techniques (e.g. co-extrusion and 3D-printing) [149–151] and to the higher flexibility of polymer-type cells [152]. SPEs have been thoroughly studied for the last forty years, and for a detailed account the reader is referred to any of the most recent reviews on the topic [57–65]. In this section, only a brief overview of the main classes and characteristics of SPEs will be provided.

The most important family of SPEs is based on polyethylene oxide (PEO) as host matrix. The ion transport in amorphous polyether-based polymer electrolytes is modulated by the polyether chains dynamics (segmental motion) [153]. PEO complexes at room temperature are usually semi-crystalline, and show low conductivity values, below $10^{-5} \text{ S cm}^{-1}$, thus well below the target conductivity for practical applications (Fig. 1) [143,145]. Consequently, lithium batteries with polymer electrolytes are generally operating at temperatures equal or higher than 60°C .

Polymer electrolytes based on non-polyether matrices have also been proposed, e.g. with polyacrylonitrile (PAN), polymethylmethacrylate (PMMA), polyvinylidene fluoride (PVDF), polyesters, etc. Among the non-PEO based matrices, high values of ionic conductivity and lithium transference number, resulting in the possibility of room-temperature operation, have been reported for some polyester and polycarbonate-based SPEs [144,154–158]. In addition, polycarbonate SPEs have higher electrochemical stability at high voltages than polyether SPEs, which may allow their use up to 4.2–4.3 V [159]. On the other hand, polymer-in-salt polycarbonate SPEs have poor mechanical properties and need therefore a mechanical support (e.g. a cellulosic or polyimide porous separator) [157,158]. Furthermore, polycarbonates degrade in contact with lithium metal, which lead the formation of liquid cyclic carbonates, particularly observed in the case of PEC and PPC-based electrolytes [160,161]. The high conductivity reported for these materials is thus possibly due to a collateral effect of the degradation, resulting from the presence of carbonate monomers acting as plasticizers.

The most straightforward ways to increase the conductivity of SPEs at lower temperatures are to hinder the polymer crystallization (in the case of semicrystalline polymers, such as PEO) and decrease the glass transition temperature (T_g). Crystallization can be hindered by increasing the disorder of the polymer matrix, e.g. by increasing the salt concentration, adding cross-linkers, using co-polymers, or comb-type polymer matrices [162–169]. Fully amorphous, polyether-based SPEs reach room-temperature conductivities between 10^{-5} and $10^{-4} \text{ S cm}^{-1}$. On the other hand, a decrease of the T_g implies an increase of the polymer chains mobility and a decrease of the matrix viscosity, which can be achieved, for example, by adding plasticizers [169–174]. Plasticized SPEs can easily reach conductivities higher than $10^{-4} \text{ S cm}^{-1}$ [174]. In general, amorphous and plasticized SPEs have worse mechanical properties than semi-crystalline, all-solid, SPEs, but a

compromise between transport and mechanical properties can be reached by an appropriate combination of cross-linkers and plasticizers [175].

To date, the decoupling of mechanical and transport properties in SPEs (i.e. increasing both mechanical and transport properties) remains a great challenge [176,177]. SPEs with good mechanical properties are obtained by using block-copolymer electrolytes, in which hard blocks (e.g. polystyrene) have structural functionality, whereas lithium-coordinating blocks ensure the conductivity [178]. Due to the enhanced mechanical properties, block-copolymer electrolytes may have higher resistance against lithium dendrite growth [179]. On the other hand, the presence of insulating structural blocks may result in a decrease of the conductivity.

Classical polymer electrolytes, prepared by dissolving a salt in a polymer matrix, are binary ion conductors, i.e. both anions and cations are mobile charge carriers [64]. This causes additional polarization phenomena (concentration polarization) and inhomogeneous lithium plating at high current densities, which eventually intensifies the growth of lithium dendrites [180]. In order to tackle this issue, single-ion conducting polymer electrolytes (SIC-PEs) have been proposed [181]. SIC-PEs can be prepared by grafting the anions on the polymer matrix [168,182,183], or by using bulky polyanions with negligible mobility [184–186]. SIC-PEs have in general lower conductivity than binary conductors, which is partially compensated by the higher lithium transference number. In terms of battery performance, SIC-PEs allow operation in the same range of temperature as binary SPEs ($60\text{--}80^\circ\text{C}$). Nonetheless, the use of SIC-PEs may result in a more stable lithium metal plating stripping process, due to the absence of concentration polarization phenomena. Promising performances have been obtained, in particular, by preparing block-copolymer SIC-PEs [187], which combine good mechanical properties and high transference numbers.

Another strategy to increase the ionic conductivity of SPEs consists in mixing inorganic particles (SiO_2 , Al_2O_3 , TiO_2 , ZrO_2 , etc.) within the polymer matrix to form a composite polymer electrolyte (CPE). The inorganic particles hinder the polymer crystallization and lower the T_g [145], thus increasing the ionic conductivity (Fig. 1). Furthermore, depending on the particle surface chemistry, the filler may interact with the polymer chains, resulting in an increase of the cation mobility [188,189]. Finally, the addition of inorganic fillers enhances the mechanical properties and the temperature stability range of the polymer matrix [190].

In recent years, promising results have been demonstrated by CPEs containing Li-ion conductive fillers (hybrid solid-state electrolytes, HSEs) [61,63]. Charge migration is aimed to occur through the inorganic phase, which is more conductive than the organic phase [191]. Increased conductivity has been reported for HSEs, with respect to filler-free polymer electrolytes [192–194], and also with respect to CPEs containing inactive fillers (Fig. 1) [146,195]. Ideally, the mixing of a highly conductive inorganic phase with an organic phase, less conductive, would result on a neat increase of the ionic conductivity, and the increase would be proportional to the content of the inorganic particles, approaching the ionic conductivity of inorganic electrolytes in ceramic-rich HSEs. Nonetheless, the lithium transport process across the heterogeneous medium is limited by the high interface resistance between the two phases, therefore the achievable conductivity is much lower than that of pure inorganic conductors [196]. However, a powerful feature of HSEs is that it is possible to obtain highly conductive composites with high concentration of inorganic particles, whereas the polymer mainly acts as binder [193,197,198]. In particular, by using “active” fillers with particular morphology, e.g. nanowires or nanofibers, it is possible to obtain fast Li-ion conduction paths through the inorganic phase, avoiding the charge transfer through the insulating polymer phase [147,199–201]. These systems show very high ionic conductivity, coupled with excellent mechanical properties, and have shown good cyclability even at room temperature and with high voltage cathodes, such as NMC and NCA [202–205]. High voltage, solid-state batteries can

be prepared also by using a bi-layer configuration, in which a polymer electrolyte layer is coupled with an inorganic electrolyte that, in turn, is in contact with the positive electrode (see Section 4) [206–210]. In general, the use of a soft polymer interlayer between lithium anode and an inorganic electrolyte reduces the interface resistance at the anode and improves the cyclability [206].

To date, the combination of polymer and inorganic conductors, either in layered or composite configurations (or the combination of both), represents the most promising approach for the development of safe and high-performing solid-state batteries. Altogether, there has been a considerable improvement in the application of polymer electrolytes with high voltage cathodes, testified by the increasing number of publications featuring cyclability tests with 4 V-class cathodes. This was prompted by the increased focus on high voltage applications, and was made possible, in particular, by the development of alternative polymer hosts, with higher oxidative stability than PEO. Whether it is possible to stabilize PEO-based electrolytes at high voltages is still a matter of debate, but the path towards high voltage polymer batteries is clearly open.

The race for developing new materials has intensively monopolized the scientific community and major results have been obtained in the last decades. There won't be a single solid electrolyte material, but most probably different chemistries will coexist depending on the cost, the performance, processing, sustainability and recycling potential. Even though, much research has been realized on solid electrolyte materials, it is most likely that new material discovery will happen in the near future.

2.2. Positive and negative electroactive materials

Overall, the most studied cathode active materials (CAMs) for SSBs are the same as those currently used in commercial LIBs, since they are the most promising to reach high energy and power densities. They include layered oxides LiCoO_2 (LCO), $\text{LiNi}_{1-x-y}\text{Co}_x\text{Al}_y\text{O}_2$ (NCA) and $\text{LiNi}_{1-x-y}\text{Co}_x\text{Mn}_y\text{O}_2$ (NMC); spinel LiMn_2O_4 (LMO) and polyanionic LiFePO_4 (LFP) [211].

Layered oxides crystallize in a hexagonal layered structure (αNaFeO_2 -type structure) where transition metal atoms and lithium alternate between oxygen layers, resulting in a 2-D diffusion path for lithium atoms. LCO still remains the best cathode material for portable electronic domain owing to its superior packing density ($\sim 4.3 \text{ g cm}^{-3}$), high initial coulombic efficiency, excellent cycle stability, high-voltage plateau and stable charge/discharge voltage. The upper cutoff voltage of LCO has been gradually increased from 4.2 to 4.45 V since 1991 via surface modification, with a concomitant increase in capacity from 137 to 180 mAh g^{-1} [212], still being far from the theoretical capacity (274 mAh g^{-1}). Poor structural stability and interface issues have prevented the use of LCO at higher voltages.

The high cost and supply risks of cobalt, coupled with the high voltage required by LCO, make $\text{LiNi}_{1-x-y}\text{Co}_x\text{Al}_y\text{O}_2$ (NCA) and $\text{LiNi}_{1-x-y}\text{Co}_x\text{Mn}_y\text{O}_2$ (NMC) better options for commercial Li-ion batteries. Both were developed from LiNiO_2 by partially substituting Ni by Co, Mn and Al, and both have been successfully commercialized. In $\text{LiNi}_{1-x-y}\text{Co}_x\text{Al}_y\text{O}_2$ (NCA, with typically $x = 0.15$ and $y = 0.05$) [213], Ni is partially replaced by Co to suppress phase transitions driven by lithium ordering [214] (considered detrimental for capacity retention) and eliminate Ni/Li cation mixing [215] (which limits the capacity of the material); while Al improves thermal stability of Ni-rich oxides [216, 217]. Indeed, delithiated Ni-rich layered oxides undergo thermally-induced phase transitions to spinel and rock-salt structures, which are accompanied by oxygen release. Such transformations are highly exothermic and can lead to thermal runaway of the battery [213]. NCA electrodes yield capacities of $\sim 200 \text{ mAh g}^{-1}$ in the range of 3.0–4.2 V [218].

Several NMC compositions starting from NMC111 ($x = y = 1/3$, with better safety properties compared to LCO and NCA) have been

commercialized. In these, increasing the Co content substantially reduces the capacity loss during cycling, while electrochemically inactive Mn dominates the thermal stability [219]. In delithiated NMC, the more Ni, the lower the onset temperature of the phase transitions and the larger the amount of oxygen release [220]. Efforts have been directed towards increasing Ni content to reach higher capacities without compromising safety, with compositional gradient strategies as most promising technical solutions (i.e. a Mn-rich shell region to reduce the amount of highly reactive Ni^{4+} at the surface and/or impede the reactivity towards the electrolyte) [221,222]. Following such approaches, prospects of NMC811 commercialization ($\sim 200 \text{ mAh g}^{-1}$ in the range 3.0–4.3 V) [219] have been announced [223].

LiFePO_4 (LFP) and LiMn_2O_4 (LMO), with 1D and 3D lithium diffusion processes respectively, represent safer alternatives to layered oxides at the expense of limited energy density. LFP crystallizes in the olivine structure from which Li-ions can be reversibly extracted yielding a capacity of 170 mAh g^{-1} and exhibit a potential plateau at 3.5 V vs. Li^+/Li^0 [224]. Despite the intrinsic advantages of such a low cell voltage in terms of safety, it limits the energy density and is considered the main drawback of LFP together with its low electronic conductivity. To surmount the kinetic limitations arising from such low intrinsic conductivity, LFP particles are typically covered with a nm-thick carbon layer resulting from the pyrolysis of a carbon organic or polymeric precursor in an inert or reducing atmosphere [225]. Partial or total replacement of Fe by another transition metal like Mn or Co is an effective strategy to increase the redox reaction voltage [226–228], although owing to cost, conductivity or stability issues, only the first have reached the market.

LiMn_2O_4 (LMO) spinel is another well-established cathode. Removal of lithium to form $\text{Li}_{1-x}\text{Mn}_2\text{O}_4$ occurs at $\approx 4 \text{ V}$ vs. Li^+/Li^0 with a capacity of about 120 mAh g^{-1} considering the extraction/insertion of 0.8 Li^+ per formula unit. This material exhibits an excellent power capability thanks to the 3D diffusion of Li-ions within the structure and better thermal stability compared to layered oxides. Additionally, manganese is inexpensive and environmentally benign. However, this material is prone to Mn^{2+} dissolution (resulting from Mn^{3+} disproportionation into Mn^{2+} and Mn^{4+}) in liquid electrolyte cells [229]. Manganese dissolution might be mitigated with SEs, possibly enabling the use of LMO in SSBs [105, 230–232]. Moreover, surface coatings with inert oxides such as Al_2O_3 have been proven effective to minimize this effect by avoiding direct contact with the electrolyte [233].

The Ni-substituted $\text{LiMn}_{1.5}\text{Ni}_{0.5}\text{O}_4$ (LNMO) spinel represents an interesting Co-free high energy alternative to current commercial cathodes [234,235]. In this material, Ni^{2+} is oxidized to Ni^{4+} at 4.70–4.75 V vs. Li^+/Li^0 , delivering 147 mAh g^{-1} . In its favor, the parasitic effects of Mn^{3+} are avoided, it can be completely delithiated without oxygen release and allows a reduction in raw material costs of 50% compared to NMC or NCA. Its high operating voltage has historically conflicted with the oxidation stability limit of most liquid electrolytes [236,237], therefore the use of SEs with wider electrochemical stability windows represents an important advantage.

Similarly to CAMs, the options for negative electrode materials for SSBs can be directly extrapolated from those already developed (and commercialized) for LIBs [238]. Metallic lithium combines a very negative redox potential (-3.04 V vs standard hydrogen electrode) with a low density (0.534 g cm^{-3}), which results in the highest theoretical capacity (3860 mAh g^{-1}). These appealing qualities resulted in a first commercialization attempt in the late 80s by Moli Energy, although all the commercialized cells (in which Li was paired to a MoS_2 cathode) were recalled owing to frequent accidents caused by Li-dendrite formation [239]. Cyclability is also a key issue as low coulombic efficiency leads to capacity fading. The low coulombic efficiency stems partially from the continuous loss of active Li in the SEI (solid electrolyte interface), but mostly from the fact that the SEI wraps plated lithium deposits, isolating them from the conductive network (inactive Li) [240].

The stringent demand for higher energy densities have motivated a revival of Li metal anodes, as are critical to overcome the energy-density

limit of Li-ion cells [212]. Still, graphite is the anode found in most Li-ion batteries since the first LCO/C rocking-chair cells were first commercialized in 1991 [241]. Graphite intercalates Li-ions at about 0.15 V vs Li^+/Li up to a final nominal composition LiC_6 (resulting from avoiding lithium occupation in the nearest neighbor positions, leading to a hexagonal ring) delivering a capacity of $372 \text{ mAh}\cdot\text{g}^{-1}$ [242].

Replacement of graphite anodes by silicon has been an active field of research. Pure silicon-based anode materials can theoretically deliver capacity of an order of magnitude higher ($3600 \text{ mAh}\cdot\text{g}^{-1}$) than the currently applied graphite anode. However, the large volume changes that alloy-type anodes undergo ($\sim 400\%$ for Si, compared to 10% for graphite) represents a major obstacle to their commercialization, and therefore must be contained in a composite design [243]. Current developments are oriented towards the use of high capacity Si/C composites as additives to graphite anodes, so that the best trade-off between capacity and volume changes is found without the need to change current processing technologies.

Opposite to silicon, $\text{Li}_4\text{Ti}_5\text{O}_{12}$ defect spinel (also written as $\text{Li}[\text{Li}_{1/3}\text{Ti}_{5/3}]\text{O}_4$, LTO) can reversibly intercalate lithium to yield the rock-salt type phase $\text{Li}_2[\text{Li}_{1/3}\text{Ti}_{5/3}]\text{O}_4$, with nearly no volume change [244]. This makes it a competitive commercial alternative to graphite for high rate designs despite limited capacity ($175 \text{ mAh}\cdot\text{g}^{-1}$) and voltage (1.55 V vs. Li/Li^+). Although Li-ion intercalation occurs above the HOMO of the electrolyte, continuous interfacial reactions with the electrolyte still occur, leading to gas evolution, which can be mitigated via surface modification [245].

Most research dealing with SSBs deals with the combination of the intercalation-type cathodes mentioned above with metallic lithium, although reports using graphite, silicon or LTO are also found [246–252]. Indeed, one of the primary drivers for SSBs is to enable the use of metallic lithium, although the use of commercial Li-ion anodes obviously benefits from mature materials solutions, sometimes with less stringent interfacial challenges, but also at the expense of energy density. However, SSBs bring also opportunities in terms of expanding the available cathode chemistries either towards more compatible materials (particularly when using sulfide-based electrolytes), either towards materials whose use was prevented in conventional Li-ion cells, i.e. materials prepared in the charged state or Li-less materials (enabled now by metallic Li at the anode), or high voltage materials [175,253–258].

The development of new active materials has been mainly limited by the liquid electrolyte stability at high voltage and only a limited number of materials has seen a real application. The development of solid electrolytes stable at high voltages is foreseen as a hope for finding new materials and/or revising previously discarded ones.

3. Processing techniques for solid-state batteries

The development of high performing materials is also associated to the optimization of scalable processing techniques allowing production at a high speed. Depending on the material and the targeted application, different processing techniques can be selected. In this section, generic processing techniques available for SSB technology at laboratory and industrial scale are detailed; they can be combined depending on the final selection of materials and components forming the solid-state cell.

3.1. Wet coating processing techniques

Wet coating processing techniques are typically used for the production of LIBs electrode at an industrial scale. The material to be deposited is dissolved or dispersed by different methods, in a liquid solvent, and coated on a substrate. The coated wet film (green sheet) is then dried and processed, e.g. by hot pressing, calendaring, laminating, etc.

Organic solvents are normally used as liquid media to dissolve polymer electrolytes or electrode binders, or to disperse ceramic or carbon-based materials. Due to environmental and safety concerns, the

importance of aqueous processing is constantly increasing [259–262]. Nevertheless, the replacement of organic solvents by water is hindered by the difficulty in controlling the rheological and drying behaviour of water-based slurries [263,264] and, in SSB-processing, by the reactivity of many SSEs with water [265].

Doctor blade (Fig. 2a–i), also known as knife coating or tape casting, is one of the most common wet coating techniques used for batteries [266], and allows achieving coating thicknesses lower than $50 \mu\text{m}$ [267]. Based on the tape casting technique, several coating methods have been developed for large-scale continuous processing, such as comma bar, reverse roll, gravure, Knife-over-roll-coating.

Slot-die coating (Fig. 2a–ii) represents another interesting option for industrial wet electrodes processing [268]. In this method, the solution/slurry is fed into a slot-die head, which is positioned above the moving substrate. The slurry distribution is controlled by the dimensions of the slot-die internal cavity and head opening. The thickness of the green sheet is determined by the substrate speed and by the speed at which the slurry is dispensed. Appropriate design of the slot die apparatus allows also deposition of multi-layered films.

Other wet coating techniques commonly used by the industry present more limitations for solid-state batteries or are still at an early stage. Dip-coating is widely used in LIBs processing, especially for the coating of separators [269,270]. More rarely, this technique has been applied for the preparation of electrodes [271] and solid-state electrolytes [272–274]. Dip-coating films have typical thicknesses in the nanometer range, which makes this technique particularly useful for the surface modification of pre-formed electrode or electrolyte layers. Thin solid-state films of electrolytes can also be prepared by spin coating [275–277], but the scalability of this technique is limited. Today wet coating is mostly used for processing the solid-state batteries, in particular for the formation of composite electrodes and SEs [24]. Polymer electrolytes, at least at a laboratory scale, are usually processed by tape casting. The polymer and salt are dissolved in a suitable solvent and electrolyte membranes are obtained by coating on a non-porous substrate, which is removed after drying [203,205,280–282]. Once processed, electrolyte and electrode layers can be merged by hot pressing. This method allows a better control over the thickness and facilitates the handling of the membrane [283]. In case of mechanically weak polymer electrolyte layers, the polymer electrolyte may be loaded on a supporting porous separator [25,158].

Lamination of separate electrode and electrolyte layers may lead to poor contact between electrolyte and electrodes and to poor battery performances. To avoid this issue, the electrolyte is often casted onto one of the electrodes (usually the cathode if lithium metal is used as anode). In this case, binder dissolution may result in the delamination of the electrode. This can be hindered by choosing a solvent which not dissolves the electrode binder, or by inducing partial crosslinking of electrode and electrolyte layer [284].

During the cathode preparation, one needs to pay attention to permit a sufficient ionic conduction. It is obviously possible to infiltrate the electrolyte slurry in a pre-formed porous electrode [285], or by solution processing followed by solvent evaporation. Nonetheless, the most common procedure is to add the electrolyte directly in the electrode formulation, prior to the electrode layer formation [286]. This further complicates the electrode processing. The solvent needs to dissolve both polymer electrolyte and binder and, as noted previously, this could result in possible delamination during subsequent coating of the polymer electrolyte separator, if the solvent of the electrolyte slurry dissolves or swells the binder. A related issue regards the CAM loading and cell energy density. The SE needs to be added in relatively high amounts to ensure high ionic transport across the electrode. For example, the polymer electrolyte content in the electrode reaches close to 30% of the electrode dry mass [287,288]. This translates in a decrease of the CAM/solvent ratio, as the slurry viscosity needs to be kept fairly constant, and thus complicates the preparation of high loading electrodes. At a laboratory scale, very low cathode loadings (below 1 mAh cm^{-2})

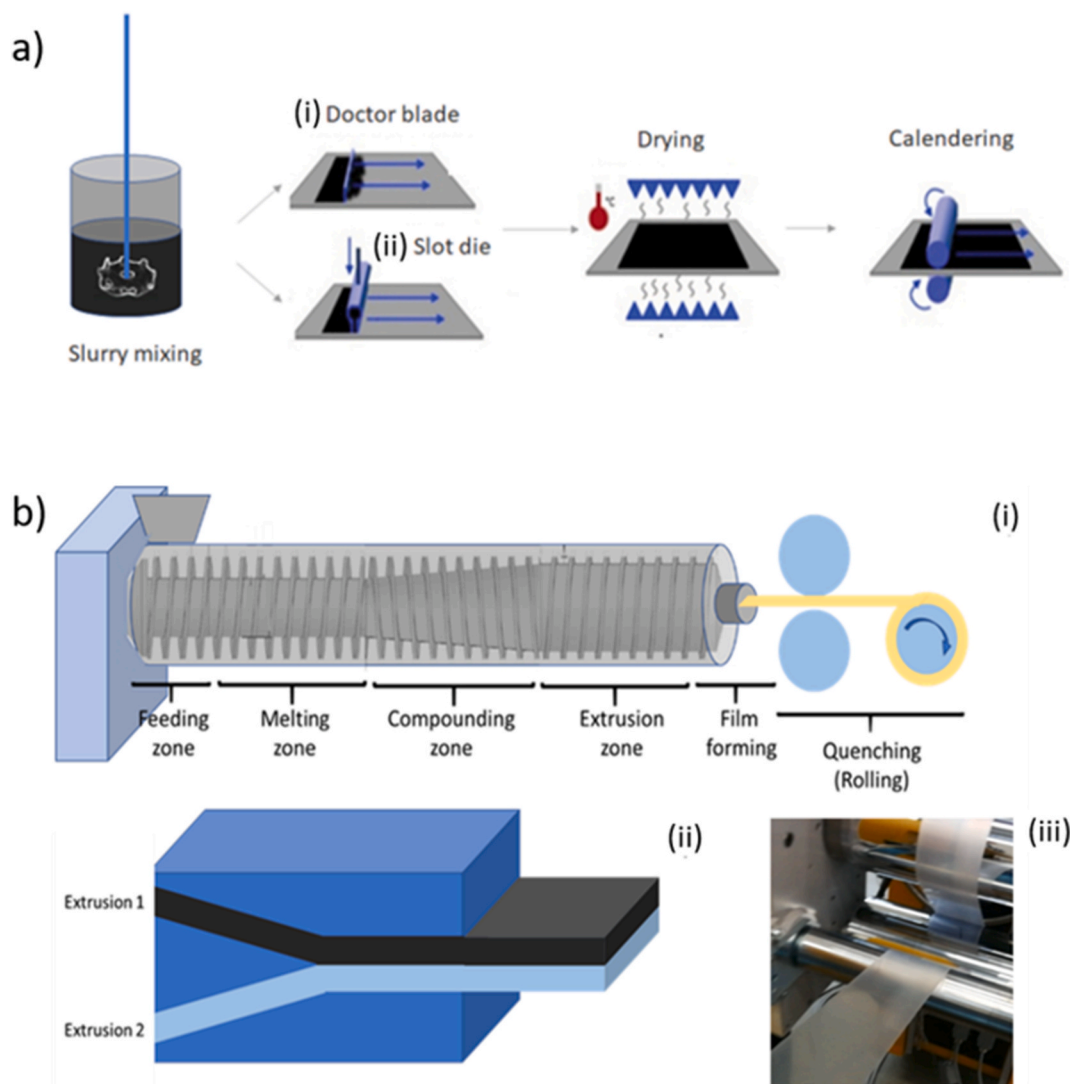


Fig. 2. a) Examples of wet coating techniques. First a slurry is formed by mixing the SE, CAM, electronic conductor additive and solvent and then the wet film is coated by i) tape casting or doctor blading, or ii) by slot-die coating. The deposited slurry is then dried and calendered. b) Sketch of i) a melt extruder, and ii) the co-extrusion process, in which two melts, deriving from distinct extruders, are fed into a single nozzle, iii) Photograph of an extruded polymer electrolyte after calendering.

are commonly used [289]. For comparison, commercial electrodes have loading between 1 and 3 mAh cm⁻², although loadings up to 4 mAh cm⁻² may also be required for high energy-density batteries [290]. Another possibility is the infiltration of a liquid polymer precursor in a porous cathode and subsequent in-situ polymerization. This approach has been recently used, for example, to prepare poly (1,3-dioxolane) by ring-opening polymerization of 1,3-dioxolane, catalysed by aluminium triflate (Al(OTf)₃) [291].

Besides processing of polymer electrolytes, wet coating techniques are interesting for the assembling of solid-state batteries with inorganic electrolytes, and in particular with sulfide-based electrolytes. At a laboratory scale, solid-state batteries based on these materials are usually prepared by compression of the solid-state electrolyte on the composite cathode, either by cold-sintering or hot sintering (see section 3.3), resulting in pellet-type cells. Sheet-type cells, in which the electrolyte powder is mixed with a polymer binder, can be prepared by wet-coating and by subsequent pressing [247]. Examples of sulfide slurries include thio-LISICON (Li_{3.25}Ge_{0.25}P_{0.75}S₄) with heptane as solvent and a cross-linkable polysiloxane as binder [292], Li₂S–P₂S₅ in hydrocarbon binder/xylene solution [248], or Li₃PS₄ in toluene [293]. A systematic study on binders and solvents for sulfide-based batteries processed in

solution was carried out by Lee et al. [294], which indicated acrylonitrile butadiene rubber and para-xylene as a suitable binder and solvent, respectively. A comparative study on binders for thiostannate (Li₁₀SnP₂S₁₂), was carried out by Riphaut et al. [295]. In this case, hydrogenated nitrile butadiene rubber (HNBR), polyisobutene (PIB) and poly(ethylene vinyl acetate) (PEVA) were indicated as suitable binders, whereas styrene butadiene rubber (SBR) and poly(methyl methacrylate) (PMMA) were rated as unsuitable.

Alternatively, sulfide solutions can be infiltrated in porous electrodes, prepared by conventional slurry processing, and the composite electrodes are then obtained by subsequent solvent evaporation, heat treatment, and cold pressing [296]. In a recent report, this method has been used to prepare argyrodite electrolytes supported on electrospun polyimide porous separators [297]. Polyimide membranes enhance the separator mechanical properties and can stand heat treatments at high temperatures, which are essential to obtain high crystallinity and conductivity with argyrodite electrolytes. The same method was later used to infiltrate an argyrodite solution in a complete cell assembly (LCO/LTO), similarly to the liquid electrolyte infiltration method in standard lithium-ion batteries.

Wet coating techniques can also be used with oxide type electrolytes,

although the need of high sintering temperatures to compact the casted green sheets may be a limiting factor for its application [298]. In laboratory scale, LLZO films with thicknesses between 20 and 30 μm were prepared by cast-sintering in the work of Yi et al. [299] LLZO powders were dispersed in acetone/ethanol slurry, and casted by wire wound rod coating (i.e. doctor blading with a spiral film applicator). Thin LLZO films were also obtained by sol-gel process [274,275]. Another interesting and easily scalable process involves the preparation of multilayered porous-dense ceramic films, through the addition of porogens (such as crosslinked PMMA particles) [301–303] or through template casting, for example on nonwoven fabrics [304]. Thick cast porogen- or template-containing layers are laminated on the top of a dense ceramic layer, which serves as separator, and the porogens and templates are finally eliminated during a subsequent sintering step. The resulting porous layers can be finally infiltrated with the electrode materials. A recent analysis from Schnell et al. considers that oxide-based SEs processing by wet coating techniques outstands other processing options due to a higher maturity (derived from their use in other sectors like solid oxide fuel cell production) and high throughput at industrial scale. But the impossibility of co-firing SE and CAMs requires the development of other processing options such as vapor deposition or aerosol deposition [289]. Despite all these recent progresses the most common procedure for oxide-type SEs still involves the formation of the cathode layer by wet coating and pressing on the top of an oxide pellet [305, 306].

Finally, electrospinning has to be mentioned due to its increasing importance in the field of hybrid solid electrolytes. In this technique, polymer fibers are spun by ejecting a charged polymer solution through a high-voltage electric field, resulting in the formation of porous nonwoven membranes on a metallic collector. Electrospinning has been widely used for the production of separators and porous membranes for gel-polymer electrolytes [307] but, more recently, it has been applied for the preparation of nanowires or nanofibers of conducting ceramics, which are spun from a polymer solution, usually poly(vinyl pyrrolidone). The polymer is then eliminated through calcination and the ceramic fibers are then incorporated in hybrid solid electrolytes [147, 201]. As noted in the previous section, these materials display particularly high ionic conductivity, making this technique highly interesting for solid-state battery applications. Despite these interesting results, the scalability of this technique needs to be demonstrated.

Altogether, wet coating is a versatile method that allows the processing of a wide variety of materials (from polymers to ceramic) obtaining thin and controlled films. This method is particularly promising for sulfide-based cells, and for lithium polymer cells. Nonetheless, wet coating is affected by a major drawback, which regards the use of toxic volatile organic solvents. Besides the obvious processing issues (need of adding an additional drying step, a densification step, solvent recovery, etc.), the use of solvents could lead to several other issues such as the risk of side reactions (e.g. between the residual solvent and the metallic lithium), and inhomogeneities in the membrane (by the concentration gradient of the dissolved material during the drying process).

3.2. Solvent-free extrusion processing

In order to avoid the use of toxic organic volatile solvents, solvent-free melt processing of SEs (Fig. 2b) is attracting attention as more economical and environmentally friendly alternative [308,309]. Furthermore, solvent-free processing is a good option for large and fast scale cell assembly production.

The extrusion process consists in three steps, namely i) the compounding, i.e. the preparation of viscous formulations by mixing and/or blending materials in a molten state; ii) the film forming process, by passing the melt through a flat film die; and finally, iii) the cooling or quenching, usually performed by rolling the extruded film through a pair of chilled rolls (Fig. 2b–i). During the extrusion, processing temperature and shear parameters have to be taken into account. The latter,

in turn, depends on the degradation mechanism and physical properties of the melted material, i.e. the glass transition temperature, the softening and melting temperatures, and rheological properties.

With melt extrusion, post-processing steps are not strictly necessary, although it is highly recommendable to accommodate thickness and increase homogeneity, especially in the case of polymer electrolytes. For inorganic electrolytes, with the exception of sulfides which can be extruded directly, a post-annealing step at high temperature is needed [119]. Furthermore, co-extrusion could be used to co-extrude directly the electrolyte onto the electrodes or to extrude multi-layered electrolytes or electrodes (Fig. 2b–ii) [310,311].

Due to these advantages, melt extrusion is considered as the most promising option for the processing of polymer electrolytes. Nonetheless, scientific literature on melt extrusion of polymer electrolytes is rather scarce, as the standard procedure for polymer electrolyte production at a laboratory scale remains the slurry-based process. On the other hand, patents concerning the processing of polymer electrolyte by melt extrusion appear already in the late eighties [312–314]. In these first applications, only the polymer electrolyte was extruded, whereas the electrode was prepared by a slurry processing. Later on, melt extrusion was applied on the preparation of electrodes [315]. In the co-extrusion processing, the electrode and electrolyte slurries are fed through two separate flow channels, and then co-extruded through a single slot-die. [316].

However, there are a few publications related to the extrusion of polymer electrolytes. In an early report, Baudry et al. reported the performances of co-extruded lithium polymer batteries [149]. More recently, Gonzales et al. described the properties of various types of composite polymer electrolytes prepared by melt extrusion [309,317, 318]. In a typical procedure, the compounding is performed at 160 °C, 80 rpm, for 20 min, and the resulting membranes are further hot pressed at 75 °C.

Huang et al. described the solvent-free processing of Ta-doped LLZO/PEO/LiTFSI composite polymer electrolytes [319]. The process conditions are similar to the previous case (blending at 150 °C, 60 rpm for 30 min, and final hot pressing). The authors also compared the performances of cast and extruded membranes, finding better performances for this latter one. This was ascribed to a reduction of Li_2CO_3 formation on LLZO surface, higher electrochemical stability and interfacial compatibility with lithium metal due to the absence of residual solvent traces, and higher conductivity due to more homogeneous dispersion of filler particles.

Melt extrusion and co-extrusion have also been used with ceramic-rich composite electrolytes. Herle and Gordon described the processing of Ta-doped LLZO-based SSBs by melt extrusion and subsequent sintering and lamination [320]. Electrodes and electrolyte (Ta-doped LLZO plus a polymeric binder) are firstly moulded or extruded to make a green tape. It is then laminated and sintered to obtain the final assembly. Kuppam and Subbaraman also describe the production of SSBs by co-extrusion [321]. By feeding a co-extrusion die with multiple melt-extruded thin films, it is possible to produce multi-layered assemblies in a single step, or even to extrude a complete cell assembly from one co-extrusion die.

The abundance of patent literature on melt-extrusion confirms the interest of industrial actors in the melt extrusion process. Due to the scalability and absence of toxic solvents, melt extrusion processing is likely to be the preferred option for mass production of polymer-type solid-state batteries.

3.3. Printing techniques

Printing techniques are gaining interest for battery processing, allowing a wider variety of geometries with respect to standard processing techniques [322]. The fabrication of battery components with complex architectures may be used to increase the surface contact between the battery layers, and thus to decrease the corresponding

interface resistances. Furthermore, printing allows production of batteries with alternative shapes and the direct integration of the battery in the electronic device to be powered, which may be important, for example, for wearable electronics. The most common printing techniques for batteries applications are classical 2D-printing techniques, such as screen-printing and stencil-printing, due to their simplicity and scalability [323]. In these techniques, the ink is pressed through a mesh, a patterned mask, or a stencil on a substrate while the excess ink is removed from the top of the mask. Other 2D-printing techniques such as flexography could be also appropriate for continuous roll-to-roll processing. It must be noted that the application of printing processing in solid-state electrolytes fabrication is at an early stage, but the field is developing rapidly. For example, stencil printing has been used to print UV-curable polymer electrolytes and electrodes with various shapes on different objects with arbitrary geometries [324,325]. In another report [326], screen printing was used to coat $\text{LiTi}_2(\text{PO}_4)_3$ and $\text{Li}_3\text{V}_2(\text{PO}_4)_3$ electrodes on the two sides of a LATP pellet, resulting in a monolithic all-phosphate cell by processing at a lower temperature compared to other techniques such as spark-plasma sintering. With respect to tape casting, screen printing allows a better attachment of the electrode layers onto the LATP pellet, due to the application of pressure during the process. Furthermore, repeated screen printing results in more dense electrode layers.

Besides 2D printing techniques, the next frontier is additive manufacturing or 3D printing, which allows obtaining more complex geometries, with a control of thicknesses down to a micrometric scale, and possibly a wider material choice with respect to 2D techniques. 3D printing techniques which have been applied to the processing of solid-state batteries include stereolithography, in which a photopolymerizable polymer precursor is locally cured through a light source, material-jetting techniques such as ink-jet printing and aerosol jet-printing, in which the material (ink or aerosol) is ejected through a nozzle, and material extrusion techniques, *i.e.* direct writing and fused deposition modelling, in which an ink or polymer melt is directly deposited on the target. As this field is expanding fast, other 3D-printing techniques may soon join the list. There are few examples in the literature of solid-state electrolytes processed by additive manufacturing. Stereolithography was used to prepare 3D polymer templates with complex geometries, which were then impregnated with LAGP powder [327]. After sintering/calcination, the negative LAGP 3D structure was obtained, and was finally filled with polypropylene or with an epoxy resin. In a more direct manner, stereolithography could be used to process photocurable polymer electrolytes. In a recent example, SPEs with 3D-spiral geometry were prepared, which were then impregnated with the electrode slurry [328]. The resulting assembly presented increased contact surface area between electrode and electrolyte, higher structural stability and higher adhesion strength between the various layers. Solid polymer electrolytes were also prepared by aerosol jet printing [329], and by fused deposition modelling [330,331], exploiting thus the thermoplastic properties of PEO. Co-extrusion, coupled with 3D printing, was used by Ragonès et al. to prepare solid-state batteries with exotic geometries [331]. In this preliminary study, a new design for a LFP/LTO coaxial battery is described with poly(lactic acid)/PEO-based polymer electrolyte. Anode, cathode and electrolyte are crushed and extruded in the form of filaments. These could be then used as feedstock for a fused-deposition 3D printer to form a coaxial cell around a central current collector.

As manufacturing perspectives, additive manufacturing is more suitable for the processing of polymer electrolytes. Contradicting this conclusion, McOwen et al. demonstrated microstructured LLZO electrolytes by direct writing of LLZO inks [332]. In this case, two different inks with different rheological properties were used: a “conformal” ink for the preparation of plane LLZO films, and a “self-supporting” ink for the drawing of microstructures such as columns, lines and grids, on top of LLZO films.

Altogether, printing process of solid-state-batteries, and in particular

additive manufacturing, is a promising and rapidly expanding field, although still at an early stage. Promising applications for additive manufacturing could be the production of microbatteries, cables- or fiber-type batteries, for wearable applications. On the other hand, with regard to large-scale battery production, 2D printing process may have an advantage towards additive manufacturing, thanks to its low throughput.

3.4. Pressing techniques

The assembling of SSBs by means of pressing techniques considers mainly three aspects: i) the densification of the SE, that should ensure good ionic conductivity, ii) the compactness and chemical stability of the composite cathode (formed by the CAM, an ionic conductive filler and an electronic conductive filler) and iii) the good physical contact between electrode and electrolyte, necessary to reduce the interfacial resistance. Materials are generally placed in form of powder in specific molds and pressed uniaxially, isostatically or pseudo-isostatically to form green pellets. The control of the pressure and the application time are relevant parameters that will depend on the material properties and required density. Process may or may not be followed by a sintering step at elevated temperatures.

The process of uniaxial pressing leads to the compaction of the powder in the shape of dies using a rigid punch or piston in a single axial direction. The presses can be mechanic or hydraulic. The method is not expensive and suitable for bulk production, but the uniformity of compaction is a major challenge. This technique is used for green densification of ceramics prior to sintering with a pressure of less than 200 MPa. Isostatic pressing helps to attain uniform densification since the compaction is achieved by isostatic pressure imposed by liquid or gaseous medium. The process offers flexibility in shape and dimensions that can be controlled by the pressing medium. However, scalability is a limiting factor by means of processing time and tooling cost. Pseudo isostatic pressing is also utilized to trap the powder within a die so that axial compression produces lateral pressure as well [333]. This process helps to achieve fast and uniform densification [333].

Generally, the total ionic conductivity in a SE is ruled by grain and grain boundary contributions, the latter being greatly influenced by the efficiency of densification (apart from other factors like material property, grain size, misorientation angle, etc). Depending on the thermo-mechanical properties of the chosen material, the densification process can be temperature-assisted; which involves annealing the pressed green pellets in a controlled atmosphere. This generally implies a limitation for processing certain composite cathodes, or cathode/SE bilayers, since temperature can induce chemical reactivity among the elements. Separate densification processes should be followed for electrode and electrolyte, although later cell assembly will generally end-up in a significantly high contact resistance at the interface. There have been several advancements in pressing techniques to face these challenges, mainly aiming to reduce the maximum processing temperature. Depending on the mechanical properties of materials, densification processes can be classified mainly into two: cold pressing, a pressure-driven process; and sintering, which is temperature-driven with or without pressure. A schematic summary of the densification of electrode-electrolyte stack with different co-sintering techniques is shown in Fig. 3a.

3.4.1. Cold/low temperature pressing

Firstly reported by Hans et al. in 1966, cold pressing is a pressure-driven densification process at room temperature (Fig. 3a–i), initially used for metal densification [334]. Later on, this technique was improved in aspects like the mode of pressing and assistance of temperature, and is widely used for a wide variety of materials processing, including commercial manufacturing of batteries. Indeed, calendaring, a crucial step in current commercial battery technologies, is a form of (low) temperature-assisted pressing for continuous processing. It

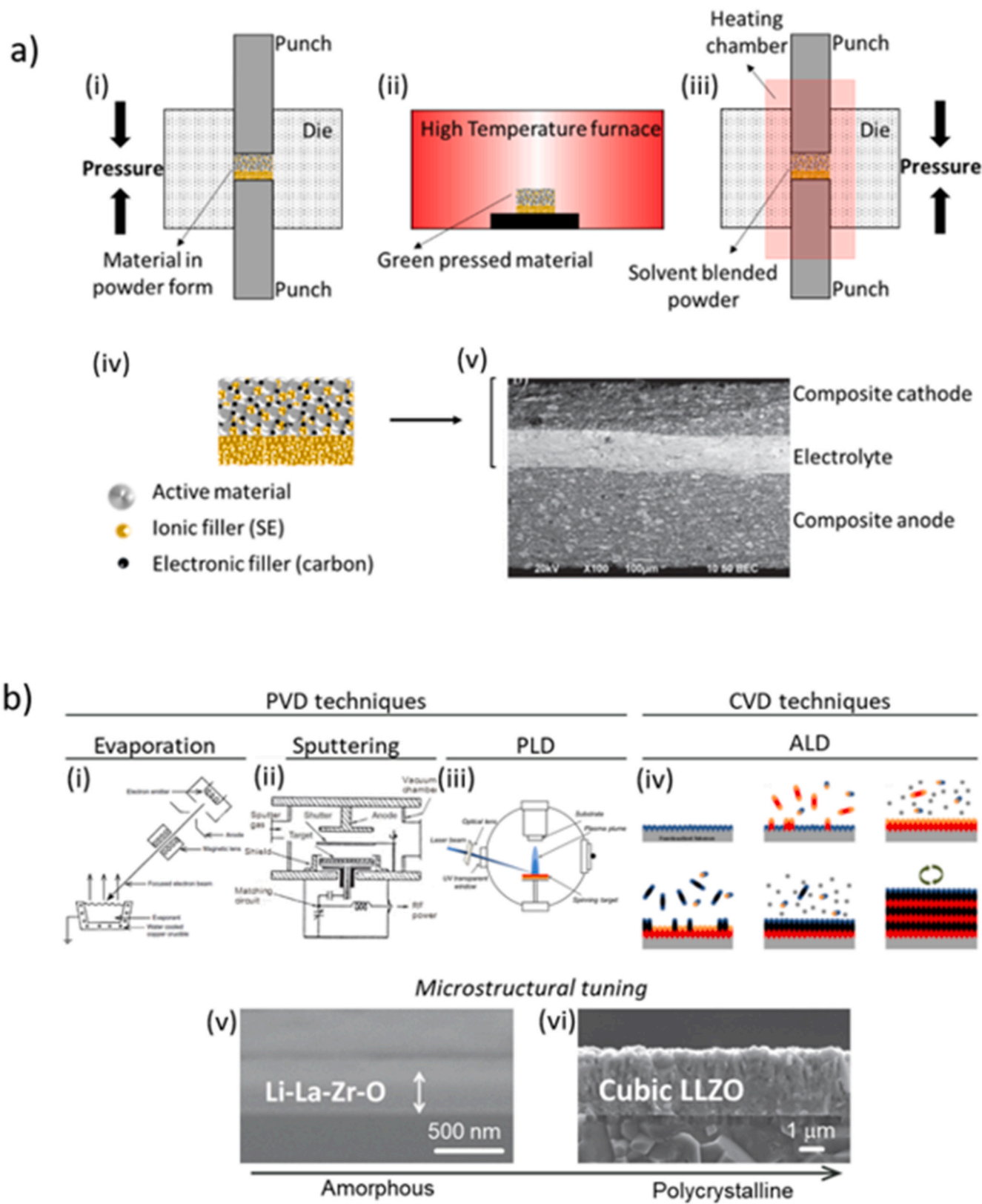


Fig. 3. a) Schematic illustration for densification of composite electrode-electrolyte stack by means of i) Cold pressing, ii) High temperature sintering, and iii) Cold sintering iv) Scheme illustrating the composite electrode-electrolyte stack. v) Cross section scanning electron microscopy image in backscattering mode corresponding to a $\text{Li}_3\text{V}_2(\text{PO}_4)_3$ | LAGP | $\text{Li}_3\text{V}_2(\text{PO}_4)_3$ solid-state battery prepared by one step spark plasma sintering (100 MPa, 680 °C) [350]. b) Schematic representation of the four most relevant vapor deposition techniques used in SSB: i) Evaporation [364], ii) sputtering [365], iii) PLD and iv) ALD [366]. Different thin film microstructures obtained in literature for the exemplifying material garnet LLZO: v) an amorphous Li-La-Zr-O film [367] and vi) a polycrystalline cubic $\text{Li}_7\text{La}_3\text{Zr}_2\text{O}_{12}$ film [368]. (Figures are reproduced with permission).

consists of smoothing and compressing a material (generally laminates) by passing a single continuous sheet through a number of pairs of heated rolls, also called calenders. Calendering is a step that commonly follows tape casting [335] as well as extrusion [20], in order to ensure the compactness of the laminates and assemblies. The main advantage of this processing is the easy low temperature densification and hence it is recognized for large scale fabrication. But is limited to either laminates or free-standing membranes, with soft mechanical properties of materials or with the addition of polymeric binders, not in case of purely inorganic batteries that have hard materials such as ceramic oxides. This process can be used for densification of cathode laminates, free standing electrolytes or even electrode-electrolyte multilayers.

Cold pressing at temperatures lower than 100 °C has also been adopted for polymer or composite SE compaction in SSB fabrication [336]. The polymer or polymer-blended ceramic composite is pressed uniaxially in a die for a few minutes, with a temperature in the range of 50–100 °C, depending on the thermal stability of the polymer and the desired density. Even though this process allows better battery performance for polymer-based batteries compared to conventional solution casting [337] the ceramic oxide based inorganic solid-state batteries are still beyond the scope because of their high temperature requirements for densification.

Additionally, cold pressing is often used for the preparation of sulfide-based soft-SEs, since their mechanical properties allow them to achieve strong compactness at grain boundaries and effective solid-solid interfaces with simple pressure [118]. The process has attracted much interest and R&D progress in the direction of scaling-up for sulfide-based SSBs since it does not need any heat treatment, which can cause reactivity with cathode materials or conductive additive. Nevertheless, remaining challenges associated to the ability of reaching high enough density, ionic and electronic conductivity requirements at the electrolyte and/or the cathode, along with general mechanical, chemical and electrochemical compatibility issues at cathode-electrolyte interface are still to be solved [118,132]. Again, it should be noted that cold pressing is generally incompatible with the processing of ceramic oxide electrolytes because of their hardness, and hence typically need of high temperature sintering to achieve high density and required conductivity. As an exception, a recent report has shown the implementation of a cold-pressed LISICON-based amorphous oxide as SE in SSB fabrication [339].

3.4.2. High temperature sintering

Densification by sintering involves the grain growth and atomic diffusion that leads to particle fusion by means of mass transport, which normally needs a thermodynamic driving force. Conventional sintering process of ceramics is driven by long duration firing at high temperatures typically above 1000 °C which depend on several factors such as nature of material, particle size, sintering atmosphere, etc. [340] In battery technology, high temperature sintering (Fig. 3a–ii) is typically used at the lab scale for the preparation of ceramic oxide electrolytes in all categories mentioned under section 2.1.1.1. However, the needed processing steps at high temperatures generally make this process incompatible with the vast majority of electrode formulations, since the high temperatures needed generally cause chemical reactivity between the components [341]. In this sense, there are several advancements in sintering techniques in order to reduce the temperature, involving hot pressing [93,342], hot isostatic pressing [343], field assisted sintering [344], flash sintering [345], microwave sintering [346–348] or spark plasma sintering [349]. Among these, spark plasma sintering (Fig. 3a–iv and v) [339,350,351,353] and high-pressure field assisted sintering [354] are already reported with the initial trials for SSB fabrication. However, it is still necessary to bring down the temperature and duration of the process even further in order to enable their application for a vast range of potential materials.

3.4.3. Cold sintering

Cold sintering was introduced by Gutamanas and co-workers in 1978, applied in powder metallurgy to compact metal/ceramic with high pressure (in the order of GPa) and low temperature [355]. A hydrothermal assisted isostatic hot pressing was introduced in 1986 and was well established for a broad type of ceramics [356]. Later, the cold sintering technique was modified by Randall et al. in 2016 by combining the previous technologies to densify ceramic oxides [357]. The process involves the densification with assistance of temperature and pressure (Fig. 3a–iii) in the presence of a transient liquid phase that acts as medium for mass transport by dissolution, precipitation and nucleation [358]. Unlike the conventional techniques, cold sintering is a multistep process involving i) particle compaction, enhanced by fluid flow via mechanical-chemical effect at solid-solid, solid-liquid and liquid-liquid interfaces and leading to grain boundary creep; ii) particle surface dissolution, evaporation of solvent and precipitation of solute; and iii) crystal growth or nucleation at the grain boundaries. Depending on the nature of the material, the type of solvent, temperature, pressure and duration, the process can have two different mechanisms; the first one involves grain growth and leads to grain fusion whereas the second occurs through the formation of kinetically hindering glassy interfaces. In this case a post-heat treatment is needed to catch up the conductivity limits. The glassy phase can be formed either by pressure induced crystal destruction at the grain boundaries or by partial dissolution of smaller particles in a solvent under pressing conditions [56,357]. The solvent can be aqueous, an alcohol, an acid or a salt solution, depending on the nature of the material, and densification can be achieved in a duration of less than 1 h with a pressure in the range of hundreds of MPa. The temperature values depend on the material, but the method ensures a reduction of 100–300 °C from the conventional sintering temperature. The technique has achieved major developments towards solid-state battery fabrication for SEs like LAGP ($\text{Li}_{1.5}\text{Al}_{0.5}\text{Ge}_{1.5}\text{P}_3\text{O}_{12}$) [360], LSZG ($\text{Li}_{13.9}\text{Sr}_{0.1}\text{ZnGe}_4\text{O}_{16}$) [361], cathode- LFP (LiFePO_4) [362], as well as anode- LTO ($\text{Li}_4\text{Ti}_5\text{O}_{12}$) [363].

3.5. Thin film vapor deposition

Thin film growth by vapor deposition techniques encompasses all deposition processes that involve the transfer of atoms from a certain source (which may be for example a thick pellet of the corresponding stoichiometry, but also a flow of reactants in the right ratio) to the desired substrate, all occurring through a gas phase. The process always takes place under controlled vacuum, helping for the effective material transfer towards the substrate and drastically limiting the cross-contamination. This way, film stoichiometry and microstructure can be perfectly controlled and tuned, allowing the *in-situ* growth of high-quality films, from amorphous to polycrystalline or epitaxial (Fig. 3b). The deposition process and subsequent film characteristics are controlled by a series of parameters, which may include the background pressure, applied power, reactants flow and/or substrate temperature. Importantly, the typical high power utilized during the processes usually allows the crystallization of the material in thin film form at temperatures considerably lower than the crystallization temperatures needed for bulky pellets (particularly important in the case of oxide SEs). However, deep understanding of the selected deposition process is always required for obtaining functional films, since deviations from target stoichiometry or different types of structural defects are common.

Vapor deposition techniques are frequently found in SSB technology, either for the deposition of thin film metallic layers, e.g. Li thin film anodes [369], or ceramic films for two main applications: the growth of thin film inorganic electrolytes for microbatteries [105,370,371] or the deposition of protective coatings in different instable interfaces [372]. In the former case, most common examples are the growth of amorphous LiPON [373], or lately other crystalline ceramic materials such as LLZO or LLTO [374,375]. The growth of ceramic protective layers is also a very important application in SSBs and thus can be widely found in

literature for coating of the upmost surface of all different cell components (SE, anode, cathode or current collector; more details in section 4). This way, electrochemically stable interfaces can be fabricated, often with significantly reduced associated resistance (e.g. improved wetting properties of lithium in bulk inorganic electrolyte) [258,376]. Additionally, these coatings can be also effectively used as impermeable layers preventing the diffusion of unwanted species through the battery [377].

3.5.1. Physical Vapor Deposition

Physical Vapor Deposition (PVD) techniques refer to deposition processes that are not mediated by a chemical reaction. In SSBs, the most relevant and widely applied are sputtering, Pulsed Laser Deposition (PLD) and evaporation (Fig. 3b). In particular, evaporation is the most common technique for the deposition of metals, whereas the deposition of ceramic thin films is mainly done by either sputtering or PLD, due to their high versatility that allows the growth of complex materials with great stoichiometry and microstructure control. As drawbacks, PVD techniques are often criticized for their high costs, greater than other industrialized battery processing techniques. Other important limitations are the low deposition rates, typically in the order of few nm per minute and limiting the maximum practical thickness achievable to a few μm , and the still relatively high temperatures (usually $> 200^\circ\text{C}$) often needed for the deposition of crystalline ceramic films, which may compromise the integrity of other battery components.

Evaporation: This technique relies on the direct evaporation of the material (a metal), placed on a heated container, towards the desired substrate (Fig. 3b-i). Two main types of evaporation can be distinguished, depending on the heating source utilized: thermal evaporation, when the material is heated through a series of resistors; and e-beam evaporation, where an energetic electron gun is used to heat the target material. This technique is particularly relevant for Li metal-based batteries, since evaporation is often applied for the direct deposition of thin Li metal film as anode, see e.g. Bates et al. [369]. Moreover, it has been utilized for depositing other metals (In, Al, etc.) as coating layer of thicker Li foils, as it improves the wetting properties of Li in certain ceramic electrolytes by the formation of lithium alloys [378,379].

Sputtering: The principle of sputtering consists of the bombardment of a dense target material with positively charged ions, accelerated by means of a high voltage applied between the target material (acting as cathode) and the substrate (Fig. 3b-ii). The charged ions, typically Ar^+ , transfer their kinetic energy to the target material, ablating and ejecting it towards the substrate. The simplest configuration uses a direct current to generate the voltage (DC sputtering). This fact limits the application of the technique to only electronic conducting materials, thus it is mainly used for the deposition of metals. However, simple dielectric ceramics can also be deposited if certain reactive species are introduced in the deposition chamber during the process. The so-called reactive DC sputtering relies on the reaction between the ablated material and the reactive species (most typically O_2), for the in-situ formation of the desired compound (a metal oxide, in the case of O_2). Nevertheless, the sputtering of dielectric materials is most commonly done by radio-frequency (RF) sputtering, where plasma is generated by applying power at a certain radio frequency, which in turn reduces the associated impedance allowing plasma ignition. In SSBs, sputtering is often used as an alternative to evaporation (DC sputtering), for the deposition of Li or other metallic films such as Mg [380] or Au [381,382]. Also, ceramic protective layers are commonly deposited by RF sputtering or reactive DC sputtering. Examples of that are the protection of Li anode foils with Al_2O_3 [383] or SnO_2 [384], or the deposition of thin film electrolytes for all solid-state microbatteries (e.g. LiPON [108] or LLZO [385]).

Pulsed Laser Deposition: PLD technique also relies on the ablation of a dense pellet of the desired material, in this case by means of a high energy pulsed laser. The ablation generates a plasma that is directed towards the substrate where the film is subsequently grown (Fig. 3b-iii). The PLD process depends on a series of influencing parameters that

affect the growth rate, film crystallinity and microstructure, which includes the background gas and partial pressure, laser fluence and substrate temperature. Particularly relevant is the background pressure, since it plays the double role of controlling the kinetics of the plasma (which in turn results on great microstructural tuning capabilities) and, if needed, compensating the partial reduction of oxide materials during the deposition process under vacuum (through the introduction of an O_2 flow). A great flexibility and control of the deposition process is making PLD very popular lately, especially for the growth of complex ceramics such as most of the SoA oxide ceramic electrolytes for SSBs (LLZO, LLTO, LiPON, etc.) [370]. Still, special care must be taken when depositing Li-containing films, since recent reports have shown significant off-stoichiometries due to substantial Li loss during the material transfer from the pellet to the substrate. In order to compensate this, several strategies have been proven to be effective, such as the overlithiation of the ablated target [375] or the addition of thin film Li reservoirs in the substrate by means of multilayer deposition [374]. Important efforts are being done nowadays on the scaling up of PLD process to industrial scale, mainly associated to the development of large area deposition systems. Advanced equipment from different companies have recently shown the ability to coat big substrates (even up to 150 mm in diameter), thus being able to integrate it in batch production lines.

3.5.2. Chemical vapor deposition

In opposition to PVD techniques, Chemical Vapor Deposition (CVD) requires a chemical reaction between two or more components for the growth of the desired material. At the present time, the Atomic Layer Deposition (ALD) is particularly relevant for SSB technology, especially for the growth of thin film protective layers [386]. In ALD, monolayers of the desired material are sequentially grown on top of a substrate, when exposed to a gas flow of reactants under controlled atmosphere (Fig. 3b-iv). Careful selection of the chemical precursors permits a self-limiting and conformal growth, allowing the coating of 3D-shaped substrates. This way, fully stoichiometric and uniform thicknesses can be achieved in large surface area substrates (ca. 150 mm in diameter). Similar to other vapor deposition techniques, the main drawbacks are the low deposition rates and cost, that includes gas precursors. Multiple materials for SSBs have been deposited by ALD, including cathodes (LiFePO_4 [387], LiCoO_2 [388]), anodes ($\text{Li}_4\text{Ti}_5\text{O}_{12}$ [389] and ceramic electrolytes (LiPON [390,391], LLZO [392]). Moreover, as mentioned before, the use of ALD to grow conformal protective layers between chemically or electrochemically incompatible materials has been explored successfully (see e.g. the use of ALD-deposited Al_2O_3 layers to reduce interfacial resistance between Li and a garnet ceramic electrolyte in Ref. [258]). For more details about this technique the reader may refer to recently published extensive reviews by Lu et al. [393] and Liu et al. [394].

In conclusion, several different processing techniques are available and can be applied to different sets of materials and technological applications (see Table 1). With regard to the prospect of large-scale production, tape casting and extrusion are probably the most suited techniques, due to the simplicity of the process, maturity of these technologies and easy scalability, in particular concerning the possibility of application to a continuous roll-to-roll process (R2R). Between the two classes of processes, melt extrusion has the decisive advantage of being a solvent-free process, thus avoiding the corresponding costs and issues related to toxicity and increased process complexity. However, this technique has stringent materials requirements, specifically it is suited for thermoplastic materials, such as PEO-based polymer electrolytes and possibly mixtures of polymer and ceramic electrolytes (composite and hybrid solid electrolytes). Inorganic electrolytes can be processed by wet coating (in particular tape casting) although solvent compatibility needs to be considered, in particular with sulfide electrolytes. Printing techniques are gaining increasing interest, but their application in the field of solid-state batteries is relatively new, and their use will probably be limited to particular applications, such as wearable

Table 1
Comparison of different processing techniques for SSB fabrication.

Process	Candidate materials	Advantages	Disadvantages
Tape casting	SPEs, oxides, sulfides, cathodes	- Easily scalable - Simple process - Mature technology	- Use of solvents - Needs drying process - Needs post-process (calendering, sintering, etc.)
Dip coating	SPEs, oxides, cathodes	- Easily scalable - Simple process - Mature technology	- Use of solvents - Needs drying process - Needs post-process - Low thickness
Extrusion	SPEs, HSEs, cathodes, Li anode	- Easily scalable - Simple process - Mature technology - No solvents	- Demanding in terms of material requirements (temperature, melt viscosity)
2D-Printing	SPEs, cathodes	- Versatile process - Multiple technologies - Form-factor-free batteries	- Novel application - Use of solvents - Use of masks - Needs post-process
3D-Printing	SPEs, oxides, cathodes, Li anode scaffolds	- Easily scalable - Versatile process - Multiple technologies - Wide variety of geometries and architectures	- Novel application - Scalability - Low throughput
Cold/low temperature pressing	SPEs, HSEs, sulfides, cathodes, Li metal anode	- Easily scalable - Simple process - Wide variety of geometries and architectures	- Limited to mechanically soft materials
High temperature sintering	Oxides	- High density, strong mechanical properties and high Li-ion conductivity	- Cost - Scalability - Thermal stability issues
Cold sintering	HSEs, oxides, sulfides, cathodes, anodes	- Low temperature - Fast process - Suitable for hard and soft materials - Simple process - Easily scalable	- Selection of compatible solvent - Solubility of particles limited - Needs post treatment
Thin Film Vapor Deposition	Oxides and polyanionic compounds, cathodes, Li metal anode, interface processing	- High purity with controlled stoichiometry and microstructure - Apt for microbatteries - Conformal coating - Intimate contact between layers	- Cost - Scalability - Deposition time

electronics. Cold pressing techniques are generally coupled to tape casting and extrusion processes for the lamination and densification of electrode and electrolyte layers. But it has been explored with soft materials such as sulfides for the solvent free fabrication of SSBs in R&D scale. Low processing temperatures are favourable in this case since the thermal induced interface reactivity is negligible between the elements. At the same time high temperature densification requirement for oxides makes them incompatible with cold pressing and needs sintering. There are several promising developments in sintering techniques to reduce the processing temperature but still the method is challenging for SSB fabrication due to thermal induced interface reactivity between electrolyte and active material. But the newly emerging cold sintering technique is bridging this gap by reducing the densification temperature of oxides to a limit at which the interface remains unaffected. Thin film

vapor deposition techniques seek attention due to its applicability in a wide range of materials which include cathodes, anodes and electrolytes. The materials can be processed with high purity and controlled stoichiometry. But low throughput limits its scalability and at the same time makes it suitable for interface processing and microbattery fabrication.

4. Interfacial challenges for full cell development

Contrary to current LIBs, in which the liquid electrolyte is wetting the cathode and anode so that it ensures the transfer of Li-ions, SSBs require well-controlled physical contact between the individual components and materials. The requirements for the interfaces can be summarized as follows: i) intimate contact presenting low resistance to Li transfer, ii) stable interfaces to promote long battery lifetime. In this section, the importance of integrating the interface layers during the cell processing together with challenges related to materials interfaces will be discussed in detail, suggesting industrially-viable solutions (Fig. 4). In SSB, several solid-solid interfaces can be found between the different components and materials. At the anode, the major interface is between the Li metal and the SE; at the SE, interfaces emerge if the SE is a composite material; at the cathode, several interfaces coexist such as between the CAM and the SE, between the conductive additive and the CAM (and/or the SE); and finally, the interface between the current collector and the cathode is also of importance. It is of paramount importance to redesign and adapt the production chain of batteries to the solid-state technology, taking into account the coexistence of the different interfaces and their corresponding physical properties. Possible processing techniques for each component are presented in Fig. 4 and discussed hereafter.

4.1. Interfaces at composite solid cathodes

Cell integration leads to many interfaces at cell component level (electrode/electrolyte) as well as at the composite electrode level (CAM/electrolyte, current collector/electrolyte material), and interfacial problems account for much of the difficulties encountered in the course of realizing a SSB. Poor contact is a major source of charge accumulation and mass transfer resistance between electrode materials, SE and current collector. In some cases, performance can be enhanced by maximizing the contact area between CAM, ion-conductive phase and electron-conductive phase.

However, volume changes of the electroactive cathode particles during electrochemical cycling (mechanical challenges) and the thermal and electrochemical stability of electrode and electrolyte materials (chemical challenges) are also major causes of cell impedance growth and cell failure. These are described below in more detail together with technical approaches to overcome them.

4.1.1. Mechanical interfacial challenges

All electrode materials experience mechanical stress during electrochemical cycling. This stress is caused by the volumetric and structural changes during reversible Li-ion insertion and extraction. The anisotropic cell parameter variation of typical Li-ion cathode materials ranges between 2% (e.g. between LiCoO_2 and $\text{Li}_{0.5}\text{CoO}_2$ in the *c* direction) to >5% (between LiFePO_4 and FePO_4 in the *a* direction) as described in section 2.2, leading to cracks and loss of contact at the interfaces between CAM, electronic conducting material and SE in the cathode (see Fig. 5a). Such mechanical fatigue is a barrier for electronic and ionic transport and has been associated to capacity fading and battery failure [395–397].

The mechanical properties of the interface between CAM and SE differ strongly depending on the choice of electrolyte. Rigid ceramics like oxides (*i.e.* with a high Young modulus, over 100 GPa, see section 2.1.1.1) will accumulate important local stresses that could lead to fracture of the ceramic cathode, whereas ductile ceramics, like sulfides

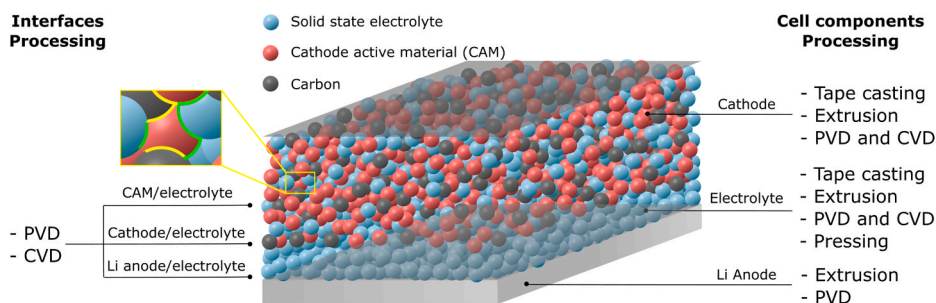


Fig. 4. Schematic of the battery components present in a solid-state battery containing a Li metal negative electrode (grey bottom), the SE (blue balls), the CAM (composed of CAM -red balls-, conductive carbon additive -black balls-, and SE). The grey upper plane represents the current collector. The processes that could be applied for each component are listed in the column on the right-hand side whereas the processes for the interfaces are listed in the left-hand side column. The inset shows the different interfaces present in the cathode (green and yellow lines represent the CAM-SE and CAM-conductive additive interfaces, respectively). (For interpretation of the references to colour in this

figure legend, the reader is referred to the Web version of this article.)

(~20 GPa [398]), thiophosphates or polymers (<1 GPa) will support mechanically the volume expansion more effectively. The physical contact between the solid electrolyte and the CAM will be affected (Fig. 5a). This enables keeping good interfacial contact during lithiation/delithiation. Nonetheless, although mechanical issues caused by volume changes during cycling are less severe using polymer electrolytes, electrochemical and mechanical modelling indicates that electrode and electrolyte undergo opposite deformation during lithiation/delithiation, which can still result in stress build-up or in the detachment of the polymer electrolyte [399].

Several solutions have been proposed to mitigate the impact of the mechanical degradation of the interfaces between the electrolyte and the CAM:

Use of conductive additives: In order to avoid any electronic contact loss compulsory for electron collection and for power density, conductive additives are key to maintain electronic conductivity within the electrode despite the volume changes, although this solution does not solve ionic transport losses. In particular, high aspect-ratio conducting additives, e.g. carbon fibers, allow mitigating the loss of electronic conduction between CAM particles and current collector with the progress of cell cycling [403].

AM morphology: Particle size and morphology play a critical role not only on the packing density of the material but as well on the contact surface between the materials composing a solid electrode. In this sense, decreasing the size of the CAM particles increase the surface area of exchange of the CAM with the SE and conductive additive [404]. With smaller particle size, the mechanical stress and effective volume expansion per particle is less important.

External conditions: Mechanical integrity of the electrode and the complete cell can also be achieved by maintaining external forces such as pressure on the cell. This has been particularly proven for polymer-based SSB and sulfide electrolyte-containing cells [405,406]. Thanks to the soft properties of these two materials (as mentioned in section 2.1), the constant pressure facilitates the SE reorganization and provides constant intimate contact with the CAM and conductive additive.

4.1.2. Chemical and electrochemical challenges

Interfacial side reactions resulting in the diffusion of elements and possibly the formation of an interphase between a SE and a CAM are generally thermally-induced processes. The temperatures required in certain processing techniques (which in turn will depend on the selected electrolyte, *vide supra*) will thus have a strong impact on the chemical stability between the two materials. As previously mentioned, some processing techniques require high temperatures in order to densify the materials together and to decrease the interfacial resistance, particularly for oxide-based electrolytes (high temperature sintering, section 3.4.2). Thermal degradation of positive electrode materials in contact with SEs often leads to new phases, most often unwanted products, which cause high interfacial resistance leading to severe degradation on the electrochemical performances [351,407]. Such chemical reactivity between the SE and the CAM has also been observed after operation at room

temperature [401], since oxidation of the anion by reduction of the transition metal is often favourable for many cathode/conductor couples [408–410]. On the other hand, the reactivity between impurities adsorbed at the cathode surface and the SE is also to be taken into account, e.g. carbonates and other species are detrimental, as reported for sulfide solid-state cells [411]. A better understanding of the kinetic and thermodynamic reactivity pathways between the CAM at different states of charge, surface species and the electrolyte is thus key for determining electrochemical performance of such systems.

On another hand, many SEs will be oxidized forming phases with lower lithium content when subjected to the cathode potential. PEO-based polymer electrolytes have limited oxidative stability, up to about 4 V [412]. Furthermore, it has been suggested that some cathode materials with high oxidizing ability (in particular LiCoO_2) facilitate PEO degradation [410]. The presence of -OH groups may be one of the causes of low oxidative stability in PEO-based electrolytes [413]. The oxidation potential of polymer chains in polymer electrolytes is possibly lowered with respect to the pristine polymers by coordination with the lithium salt, due to a screening of the positive charge in the oxidized state by the salt anion [414]. Altogether, the applicability of polyether electrolytes is practically limited to 3 V-class cathodes, such as LFP. This problem can however be mitigated by using coated CAMs, such as $\text{Li}_{1.4}\text{Al}_{0.4}\text{Ti}_{1.6}(\text{PO}_4)_3$ -coated LiCoO_2 , which stabilize PEO towards oxidation [415]. Higher stability (>4 V) was claimed also for composite polymer electrolytes with respect to filler-free polymer electrolytes, specifically with LLZO [416], and with $\text{LiZr}_2(\text{PO}_4)_3$ [417] as fillers. This was attributed to the Lewis acid-base interaction between filler and salt, which hinders anion decomposition. This issue may be tackled also through the use of alternative polymer hosts with improved electrochemical stability. For example, polymer electrolytes based on poly(ethylene ether carbonate) demonstrated good cyclability (at room temperature) with NMC622 as cathode material and with a cut-off voltage of 4.3 V [418].

In the case of inorganic compounds, the oxidation limit is primarily determined by the anion chemistry, with fluorides having the highest oxidation limits, followed by chlorides, polyanionic oxides and non-polyanionic oxides [31,401]. As mentioned in section 2.1, sulfides exhibit the narrowest electrochemical stability window, and get oxidized above 2–2.5 V; while LATP and LAGP exhibit the highest theoretical oxidation stability (>4 V) [35]. Such electrochemical processes will occur wherever the SE reaches the electron path (current collector, conductive additive). LiPON represents a rare exception, as the electrochemical decomposition products at both high and low voltage are electronic insulators, resulting in stable passivating layers with ionic conductivity [35].

Therefore, to overcome the above-mentioned challenges, the approaches listed below should be taken into consideration in order to obtain a SSB with adequate cell performance.

Stable electrolyte-active materials combinations: When designing a solid-state cell, appropriate combinations of materials and adequate processing techniques must be identified to ensure the

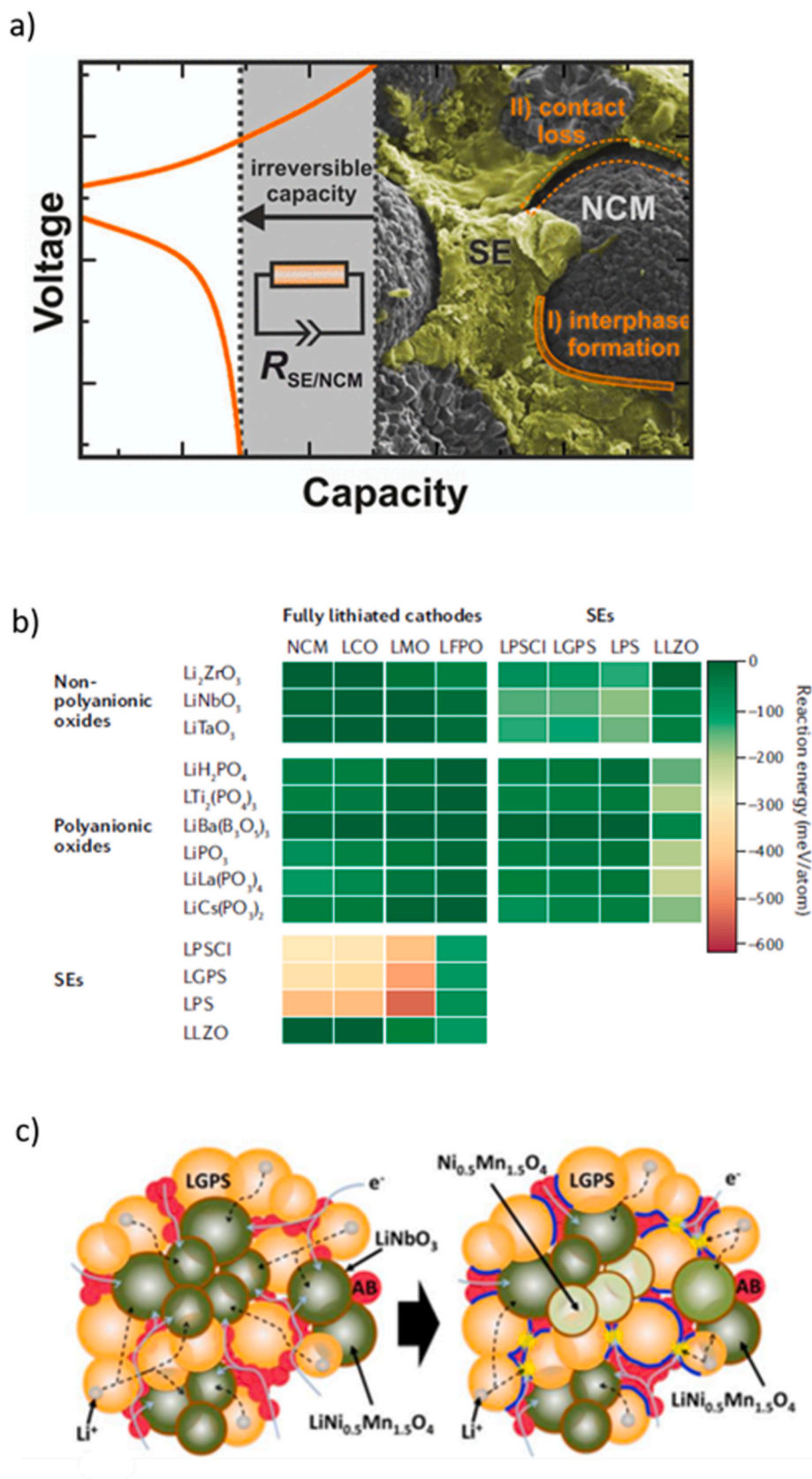


Fig. 5. a) Capacity fading caused by the contraction of the CAM upon delithiation resulting in contact loss between the SE (β - Li_3PS_4) and CAM particles (NCM, referred as NMC in this review) observed by ex-situ SEM [400] b) DFT-computed chemical mixing reaction energies of fully lithiated cathode/SE, fully lithiated cathode/coating, and coating/SE interfaces in meV/atom [401]. c) Schematics of the interfacial reactions in a composite solid cathode under charge/discharge operation. The cathode contains LNMO as CAM (green particles) coated with LiNbO_3 , LGPS SE (orange particles) and acetylene black (AB) as electron conducting additive (pink particles). Reversible Li intercalation occurs between the LNMO cathode and the LGPS electrolyte. The LiNbO_3 coating layer acts as a buffer to facilitate Li diffusion at high voltages. In contrast, oxidative decomposition of LGPS occurs at the LGPS/AB interface during the charging process, which causes irreversible capacity loss. The decomposition layer could isolate the delithiated LNMO phase from ion and/or electron percolative pathways resulting in capacity fading upon cycling [402]. (Figures are reproduced with permission). (For interpretation of the references to colour in this figure legend, the reader is referred to the Web version of this article.)

chemical and electrochemical stability of the material, and decomposition interfacial products must be equally considered in the design of composite cathodes. It is essential that the decomposition products exhibit poor electronic transport, otherwise continuous decomposition will occur.

Fig. 5b summarizes DFT-computed chemical mixing reaction energies between fully lithiated CAM and electrolytes. Sulfide and thiophosphate are less stable when combined with oxide cathodes than with LiFePO_4 , as predicted from chemical mixing calculations [401] and in explicit interface calculations [35]. On the other hand, oxides and phosphate SEs exhibit improved chemical stability with oxide cathodes compared to sulfide SEs. They are also predicted to be compatible with LFP, though [401]. These calculations represent a powerful tool to identify appropriate matching of materials, however further research is needed to understand the impact of the presence of third species such as conducting additives, or the reaction atmosphere. Additionally, a much higher reactivity is expected for (partially) delithiated CAMs and the results might be chemistry-dependent within a same family of materials.

Multi-layer configurations: in which the catholyte and the SE are of different nature, represent a related strategy that has been successfully demonstrated. Several examples can be found in literature, where combinations of different inorganic and polymeric electrolytes are complementarily used.

As an example of a full inorganic cell, LATP has been used as catholyte when using an NMC cathode and a $\beta\text{-Li}_3\text{PS}_4$ separator, allowing to employ LATP in a bulk-type SSB without a sintering step of the full cell, which would result in undesired decomposition interfacial products at the cathode [419].

Combinations of different polymer electrolytes have also been reported. Bilayer polymer electrolytes, with PEO/LiTFSI at the anode side, and Poly(N-methyl-malonic amide) (PMA) as polymer host at the cathode side have shown good cyclability in LCO/Li cells [281]. PAN-based electrolytes are often used in multi-layered electrolytes as catholytes and cathode buffer layers. Examples include PEO/LATP/PAN sandwich electrolytes, with NMC622 as cathode material [420], PEGDA/PAN-LATP/PAN tri-layered electrolyte (again with NMC622) [208], and bilayer PEO-SN/PAN-LATP, with NMC811 [421]. High conductivity values with PAN-based electrolytes may be due to the residual presence of solvent traces (such as DMF or DMAc) [60], but this apparently does not affect negatively the cell performance, at least if these solvents do not get in contact with the anode. Polycarbonates are supposedly more stable against oxidation than polyethers [60], and are often used with 4 V-class cathodes. Examples include poly(triethylene glycol carbonate) (PTEC)/LiTFSI, cycled in LFMP/Li cells [159], poly(vinyl carbonate) (PVCA)/ $\text{Li}_{10}\text{SnP}_2\text{S}_{12}$ (LSnPS) composites, also with LFMP as cathode material [422], and poly(fluoroethylene carbonate) (PFEC)/LiDFOB, cycled with LCO, and even with the 5 V-class cathode material LNMO [423].

Artificial coating layers: The use of protective layers between the cathode material and the SE is a demonstrated method to extend the experimentally-measured electrochemical stability window at the cathode/SE interface and avoid electrolyte decomposition when subjected to high voltage. The coating material must be an ionic conductor and electronic insulator, following the same operating principle of the SE in liquid cells. Moreover, the potential drop will be sufficient only if the electronic conductivity of the coating is lower than that of the SE. Finding suitable artificial coating layers for polymer electrolytes is particularly challenging, since these already exhibit very low electronic conductivities [424]. Nonetheless, there are several examples reporting improved stability when inorganic or organic coatings are combined with SPEs, although further improvements are still needed to reach competitive cyclability values. This is the case of LCO coated with Li_3PO_4 , LAGP or Al_2O_3 [425–427] coupled to cross-linked polyether based polymer electrolytes, even with a high cut-off voltage of 4.4 V. The feasibility of this approach was confirmed by a more recent study, which reported improved cycle stability with PEO-based electrolyte and

LATP-coated LCO as cathode material, with a cut-off voltage of 4.2 V [415]. NMC111 carboxymethylcellulose (CMC) coatings have also been explored [428]. CMC presents lower oxidative stability than the polymer electrolyte itself, but the degradation results in a stable passivation layer, practically forming a stable cathode-electrolyte interphase. Li et al. developed LATP-coated LCO and NMC532, obtaining good cyclability with a PEO-based electrolyte (200 cycles with capacity retention higher than 80%), even with a cut-off potential of 4.3 V [429]. Nonetheless, complete and homogeneous coating cannot be achieved by mechanical milling alone. Defects in the coating possibly impair the stabilization effect of the passivating layer [430].

The materials choices for cathode/inorganic SE interfaces are larger, also because the requirements for ionic conductivity are less stringent than the bulk electrolyte as coatings must be thin uniform layers [408]. Therefore, oxides like LiNbO_3 or LTO [401,431,432] or phosphates like Li_3PO_4 [326] can successfully stabilize cathode/inorganic SE interfaces leading to improved cycling stability. These materials exhibit thermodynamic stability limits close to 4 V, which might be further extended by slow oxidation kinetics [73]. However, careful assessment with respect to specific cathode/SE combinations is still needed. As discussed previously, a recent computational screening study of chemical reactivity between pairs recommends phosphate coatings for sulfide SEs and oxide coatings for oxide SEs as general guidelines (see Fig. 5b) [401].

The coating techniques for cathode active material particles and electrode sheets have been recently reviewed by Du et al. [36] The most common coating techniques include magnetron sputtering (MS), spark plasma sintering, pulsed laser deposition (PLD), sol-gel synthesis, chemical vapor deposition (CVD), atomic layer deposition (ALD) and wet coating techniques such as spray coating, spin coating, and solvent casting.

More recently, sol-gel synthesis has been used to prepare various types of core-shell active material particles, such as NCA particles with an Al-rich shell and outer LiNbO_3 layer [413], LATP-coated LCO and LFP particles [414], and LLZO-coated LMO particles [416]. Alternatively, microwave-assisted synthesis was used to prepare core-shell structures with NCA surrounded with NiAl_2O_4 [420], whereas ALD was used to coat a dual layer of LGPS and LiNbO_3 on LCO [417], and on NMC811 particles [415]. Oxidative chemical vapor deposition (oCVD) was used to deposit a conformal layer of the electronically conductive poly(3,4-ethylenedioxythiophene) (PEDOT) on both secondary and primary NMC particles [419].

Some of these coating techniques may be utilized to apply interlayers on pre-assembled electrode sheets. For example, NMC622/LLZO cathodes were coated with graphite interlayer by doctor blade [412], and ALD was used to coat LCO electrode sheets with a lithium tantalate film [418]. The coating of the electrode sheets, compared to coating of the active material particles, may result in improved stabilization of the electrolyte at high voltages, due to simultaneous protection of the active material and conductive particle interfaces.

In situ formation of cathodic-SEI (CEI): Interface stabilization in polyether electrolytes could be achieved also through specific electrolyte additives. Similar to the role of ethylene carbonate in the anodic-SEI formation mechanism (see section 4.2), these additives decompose at the cathode and form a stable lithium-conducting interlayer, thus avoiding further electrolyte decomposition. As illustrated in Fig. 5c, the formation of a cathodic SEI (CEI) could help enhancing the SSB performances and maintain long cycle life. A possible candidate as cathodic-SEI (CEI) former is the salt lithium bis(oxalato)borate (LiBOB). PEO electrolyte containing the salt cocktail LiTFSI-LiBOB- LiNO_3 showed electrochemical stability up to 4.6 V (by floating test) and good cyclability in NMC111/Li cells [434]. Another candidate as CEI former is AlF_3 . This Lewis acid was recently proposed as additive, with the double function of current collector passivating agent and CEI former [291]. Its use as additive in poly-DOL (poly-dioxolane) electrolyte allowed cycling with NMC622 as cathode material with a cut-off voltage of 4.2 V. Additionally, the formation of the CEI should be tuned to enhance the

SSB performances and maintain long cycle life. As previously noted, Li et al. demonstrated that it is possible to obtain good cyclability through the combined use of cathode material coating and electrolyte additives [429]. In this specific case, LiBOB and LiPF₆ were used as salt additives (together with LiTFSI as main salt), the first one as CEI former and the second as passivating agent for the current collector.

Interfaces with current collector: Current collectors are a fundamental part of the battery since they ensure the transport of electrons to and from an external circuit and, often, they are used as mechanical support for casting of the composite cathode on top of them. A low resistive interface is important to limit localized high current densities and consequently a higher internal resistance and decreased round-trip efficiency. Often overlooked in literature, these interfaces might present chemical and electrochemical instability issues that need to be addressed [436]. In general, aluminium current collectors are the preferred choice for the cathode side, widely used with lithium transition metal oxides up to 5 V vs. Li/Li⁺ [437]. It is well accepted that the native Al₂O₃ passivation layer growing on the surface of Al plays a major role on the protection of the current collector towards corrosion, although this native protective layer may not be sufficient in the presence of certain salts. It has been reported in liquid-based systems that LiPF₆ promotes further protection of the Al through the formation of a stronger AlF–Al₂O₃ passivation layer [438,439], whereas aluminium is corroded at about 3.8 V vs Li/Li⁺ in the presence of LiTFSI, the most common salt used in SPEs [440–442]. Yang et al. associated the Al instability with LiTFSI to the reaction between this salt and the Al₂O₃ passivation layer of the current collector, forming Al[N(CF₃SO₂)₂]₃ and exposing the metallic Al to degradation [443]. Anti-corrosion strategies such as increasing the salt concentration in the electrolyte [444,445], using additives such as Pyr₄TFSI [446] or fumed silica [447], or adding artificial coatings like carbon [448] or polymeric layers [449] have been proposed.

The electrochemical stability of the current collector also needs to be considered. Koerver et al. investigated the effect of upper voltage limit in SSBs with NMC-LPS composite cathodes [450]. Surprisingly, they found out that the main degradation occurs on the current collector surface rather than on the cathode particles, presumably associated to the potential drop at the interface between the current collector and the solid electrolyte. The resistive interlayer formed has a negative impact into the cell performance and highlights the necessity of a thorough design and passivation of current collectors when building SSBs.

Alternative materials have also been explored aiming for a better contact with the CAM and/or gain flexibility in the cells. For example, Choi et al. successfully implemented a carbon nanotubes (CNT) sheet as current collector in sulfide-based SSBs [451]. A great flexibility of the CNT sheets allowed an improved adherence with the composite electrode and a reduced interfacial resistance. De et al. developed a flexible current collector by preparing an electronically conductor nanocomposite with PEO polymer and Cu-coated carbon fibers [452]. The use of PEO in the current collector helped to improve the mechanical strength while maintaining flexibility, as well as allowing a strong attachment with the cathode material. A similar strategy of building elastic but robust current collectors was developed by Chen et al., by depositing Ag microflakes as a conductive layer on a stretchable carbon–polymer composite [453].

Finally, Cr₂N and Ni–Al–Cr current collectors have been suggested for oxide-based SSBs, when high temperature sintering steps are required [454,455]. This is the case of thin film batteries built on a layer-by-layer fabrication mode, where post-deposition annealing is typically required to obtain the high performing crystalline phase of the active materials. In order to avoid element diffusion and/or formation of secondary phases, oxidation resistant current collectors are needed (*viz.* Cr₂N or the Ni–Al–Cr superalloy, in the reported cases).

In summary, a cathode electrode composed of at least three materials (cathode active material, catholyte and conductive additive) leads undoubtedly to many challenges at the interfaces. These are electrochemical,

chemical and mechanical challenges.

The nature of the active material and its restless volume expansion and contraction throughout cycling is naturally affecting the physical contact between the three materials. To overcome this challenge, it is recommended to focus on adapting active material particles so they have a limited volume expansion at the outer particle level or adapt the solid electrolyte so it can follow the volume changes with deformable properties.

Chemical and electrochemical issues, that can be tackled as a single problem, is a major challenge for long cycle life cathode components. Research efforts should be concentrated on finding the best combination of materials to avoid premature degradation, and trying innovative configurations such as multilayer or thin coatings to block the direct contact between the electroactive material and the solid electrolyte. It is not to forget that the cathode-electrolyte interface is still overlooked, mainly due to technical challenges for its study. Understanding such interface layer would shed some light on developing new composite solid cathodes.

4.2. Li metal/electrolyte interface

In solid-state batteries, Li metal is the mostly used anode material (see section 2.2), independently of the solid electrolyte. However, severe issues need to be overcome to achieve good cyclability and enhance cycle life and high power: i) accommodate the volume change produced during the plating/stripping process, while maintaining the interfacial contact between anode and electrolyte; ii) hinder the formation of lithium dendrites, which could lead to short-circuit; iii) protect the electrolyte from degradation due to contact with lithium metal [456].

4.2.1. Mechanical stability and lithium dendrites formation

During battery cycling, lithium metal is constantly electrodeposited and stripped on/from the anode surface. Consequently, the interface between the SE and the Li metal is in constant evolution, which affects the mechanical stability of the electrolyte-electrode ensemble. Indeed, the thickness of the Li metal electrodeposited at the interface can reach up to 15 µm for a cathode loading of 3 mAh·cm^{−2}. Such considerable thickness change alters both the mechanical and electrochemical properties of the interface. The accommodation of this extra layer is therefore extremely dependent on the mechanical properties of the electrolyte, and on the ability of accommodating additional stress. Furthermore, inhomogeneous lithium plating/stripping leads to low coulombic efficiency, continuous electrolyte degradation, and to the risk of short circuit. Additionally, local accumulation of lithium metal deposits results in inhomogeneous pressure distribution, thus contributing to further decrease the mechanical stability of the cell. The effect of non-homogeneous deposition is less important for low CAM loadings but becomes crucial for high loadings and high current densities. Finally, the formation of Li dendrites is still an important issue in SSBs.

Dendrite formation mechanism has been correlated to the mechanical properties of the SE (*i.e.* shear modulus, density and presence of pores), physicochemical properties of the SE (*e.g.* electronic conductivity) or interfacial issues (composition and instability) [457]. In general, it is assumed that SEs with high shear modulus can somehow hinder dendritic growth. However, dendrites growth has been demonstrated even with dense and hard ceramic electrolytes such as LLZO, in which lithium dendrites can grow along the grain boundaries (Fig. 6a) [458, 459]. Recent studies also suggest that the use of ceramic SEs can promote, in fact, fast dendrite formation. This is partly attributed to the large curvature of dendrite tips in confined space (such as grain boundaries in ceramic SEs). Counterintuitively, good chemical compatibility between the SE and lithium metal can further promote dendritic growth due to a low Li consumption by side reactions [460].

In the following sections, different strategies to enhance the electrodeposition process and prevent dendrite formation are discussed, including the use of external pressure, use of 3D lithium metal anodes, increase of Li metal wettability, electrolyte nanostructuration, and stabilization of the interface through interlayers.

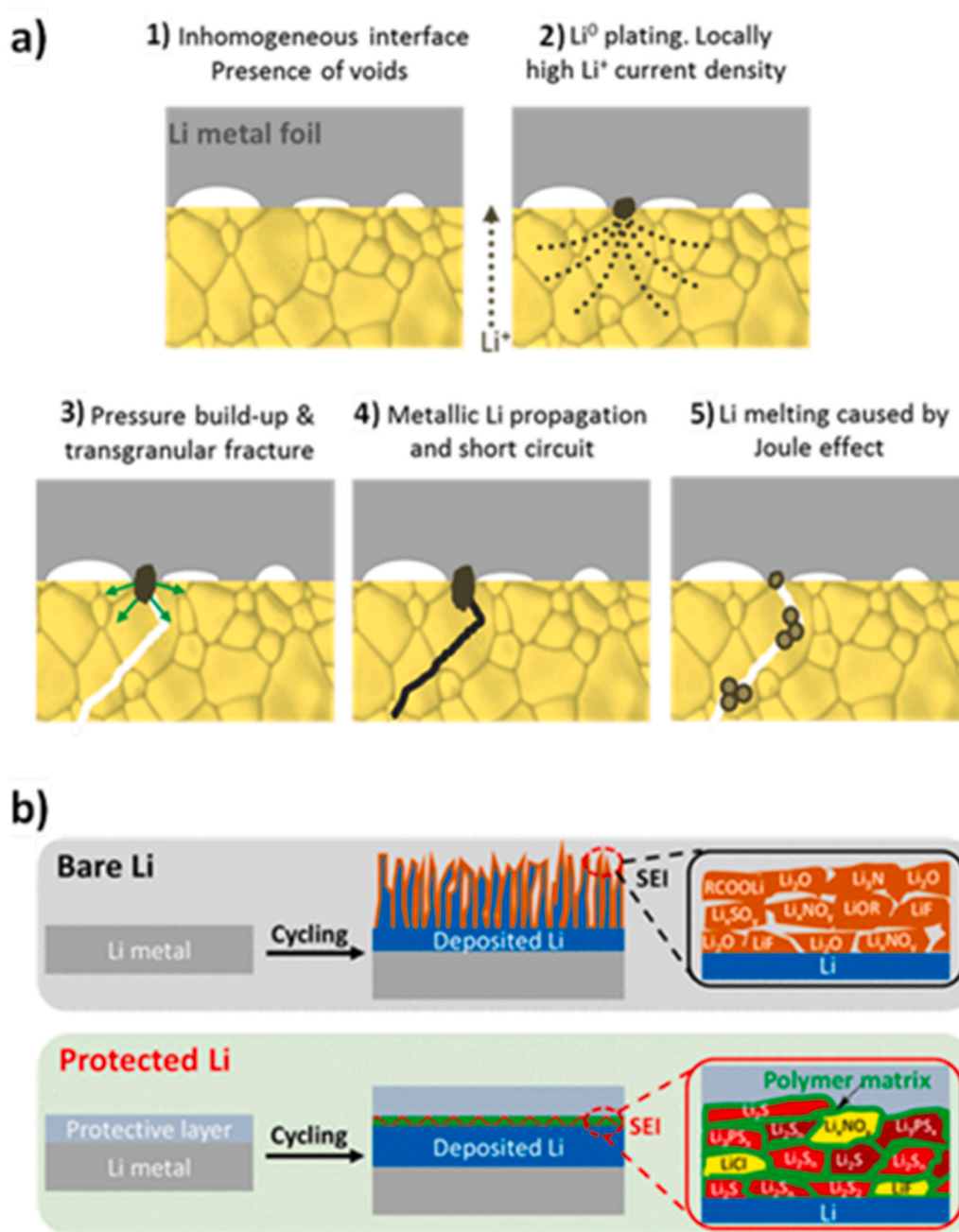


Fig. 6. a) Mechanical failure via Li filament formation in a Ga-doped LLZO garnet ceramic electrolyte during Li electrodeposition [458]. b) Li stripping and plating at the Li metal – polymer electrolyte protecting inter-layer [475]. (Figures are reproduced with permission).

Role of pressure: To maintain a constant contact between the Li metal anode and the SE an external pressure is required [461]. This enables keeping a physical contact at the anode interface during stripping, when the extra layer is removed, while also improving the contact at the cathode side. However, a constant, well-balanced, and uniform pressure is required to avoid crack formation in ceramic electrolytes or electrolyte spreading with polymer electrolytes, the latter possibly leading to short circuit. It is worth pointing out that large external pressures may favor the growth of lithium dendrites into the grain boundaries of the SE [462]. Therefore, an optimum range of external pressure can be defined, with the minimum value located above the Li yield stress (2.2 MPa), whereas the upper limit depends on the mechanical properties of the SE (<1 GPa for sulfides, > 1 GPa for oxides).

SE/Li surface treatment: A homogeneous and constant contact at the interface is required to enhance the interfacial exchange (ionic and

electronic). The influence of surface roughness in the ceramic electrolyte on the plated Li metal layer was studied by Basappa et al. [463]. It was reported that the interfacial resistance is reduced when the contact surface area is high. Therefore, a rough surface should be preferred to a mirror flat surface. This approach was recently implemented by Zang et al., which showed higher cyclability in Li/Li symmetric cells and Li/LFP cells, by using patterned lithium metal anodes, due to selective lithium deposition in the grooves of the anode [464]. Nevertheless, a rough surface creates peaks of current which could lead to localized current spikes and formation of local voids and Li metal aggregates [464]. Similarly, nanostructuring of the SEs can help obtaining a more uniform electrodeposition morphology, even with relatively weak SEs [465–467]. Nanostructured SEs can be obtained by using template materials such as cellulose [468] or surface modification [376]. Additionally, thermal treatment at temperatures close to the melting point of

Li metal favours homogeneous deposition of Li [379,469]. Such treatment significantly lowers the ASR value creating an intimate contact between Li metal and SE. The stability and kinetics of the Li-LLZO interface were characterized by Sharafi et al. as a function of temperature and current density [470]. Polycrystalline LLZO was densified using a rapid hot-pressing technique achieving $97 \pm 1\%$ relative density, and $<10\%$ grain boundary resistance, effectively consisting of an ensemble of single LLZO crystals. It was determined that by heating to 175°C , the room temperature Li-LLZO interface resistance decreases dramatically from 5822 (as-assembled) to $514\ \Omega\ \text{cm}^2$; a >10 -fold decrease. In characterizing the maximum sustainable current density (or critical current density - CCD) of the Li-LLZO interface, several signs of degradation were observed. In DC cycling tests, significant deviation from Ohmic behavior was observed. In post-cycling tests, regions of metallic Li were detected, propagating parallel to the ionic current. The relationships and phenomena observed in this work can be used to better understand the Li-LLZO interface stability, enabling the use of batteries employing Li metal anodes [463,470].

Another strategy to stabilize the Li metal-garnet interface presented in the literature consists in limiting the formation of Li_2CO_3 on the surface of garnet ceramic sheets during the process. Thus, the lithiophilicity of the surface is increased, which permits accessing higher current densities, as high as $900\ \mu\text{A}\ \text{cm}^{-2}$ at 60°C [103].

3D lithium anodes: Another strategy to improve the lithium/SE interface implies the use of three-dimensional (3D) lithium anodes. In this approach, lithium is mixed most frequently with a carbonaceous material resulting in a composite anode. The electrolyte-electrode contact area is greatly increased, which reduces the interfacial resistance and distributes the ion flux more uniformly, thus improving the cyclability. However, the use of 3D Li anodes requires the construction of a continuous Li-ion percolation path from the anode pores to the electrolyte bulk, which is technically challenging due to the reactivity and the low melting point of lithium. A possible solution is the use of polymer electrolyte interlayers. Liu et al. developed 3D Li anodes using host liquid-like (flowable) PEG/LiTFSI interlayers and LLZO/PEO CPE middle layer [471]. LFP/Li cells with this configuration could be cycled for 700 cycles at 60°C , with relatively high cathode loading ($6\ \text{mg}\ \text{cm}^{-2}$), and current density of $1\ \text{mA}\ \text{cm}^{-2}$. Similar experiments using Ni foam [209] or well-aligned channels of Li/C-wood [472] were also conducted, showing promising cycling performances at different temperatures. It is worth mentioning that the use of 3D Li anode, although effective in suppressing dendrites growth, brings about a reduction of the cell energy density due to the presence of an additional passive element. This effect, especially with regards to the volumetric energy density, must be carefully considered if strict energy density targets are set. Amongst all the strategies proposed, the lack of maturity of the 3D lithium anode development is limiting its industrial integration in SSBs [473]. Recent advanced on lithium-free anodes have also shown encouraging results using argyrodite SE and Ag-C composite anode [474].

Interlayers: Another approach consists in the engineering of the lithium surface by the deposition of a thin buffer layer, with the aim of stabilizing the electrodeposition process through the accommodation of volume changes and dendrite growth obstruction (Fig. 6b). The coating processing routes for lithium metal anodes have been reviewed by Du et al. [36] and more recently by Tong et al. [476]. The most common processing techniques include vacuum-coating (e.g. ALD, MS), wet coating (such as tape casting and spin coating), and solvent-free, *in situ* polymerization of cross-linkable polymer or organic ionic plastic crystal [477] coatings. The processing routes for the fabrication of interlayers at the anode are similar to those employed for the cathodic interlayers, with stricter constraints due to the reactivity of metallic lithium. The application of wet-coating techniques, in particular, is limited by the reactivity of most solvents with lithium, except ether-based solvents and hydrocarbons. Sol-gel techniques are not applicable as lithium metal is not stable in hydrolytic conditions. Alternatively, *in-situ* formation of a buffer layer (or *in-situ* SEI) can be prompted through the introduction of

functional additives in the electrolyte. This strategy is commonly used with liquid electrolytes but it has been employed in some cases also with polymer and ceramic electrolytes [478–480].

A typical example of lithium anode protection is the deposition of a LiPON interlayer between the lithium anode and the polymer electrolyte separator [481]. LiPON has an estimated shear modulus of 31 GPa, and could therefore hinder completely lithium dendrite growth. The deposition of a ZnO layer, by ALD, was proven to increase the lithiophilicity of the Cu current collector, and thus the efficiency of the lithium plating/stripping process [46]. Au buffer layers [382] and ALD-deposited Al_2O_3 layers [258] are also found to reduce the ASR and therefore enhance the contact.

Lithium nitride (Li_3N) is particularly promising as buffer layer, due to its high lithium conductivity, stability and wettability versus lithium metal. Li_3N buffer layers have been used especially in garnet-based SSBs, where they can also act as additional lithium sources, compensating lithium loss due to electrolyte decomposition [374,482]. Li_3N interlayers can be also formed *in-situ*, by decomposition of precursor layers, e.g. tin nitride [480] or carbon nitride [484]. Similarly, Li_3N can be useful also as interlayer with polymer electrolytes. In a recent example, Mg_3N_2 was used in combination with a PEO-based electrolyte. Mg_3N_2 decomposes into Li_3N and Mg upon cycling, the former being a fast Li-ion conductor whereas the second helps redistributing the current density on the electrode surface [485].

Polymer and/or composite coatings of lithium metal anodes are also useful strategies in modulating the electrodeposition process in order to suppress Li dendrite formation, in both liquid and SEs. Lopez et al. [486] studied the lithium deposition with various polymer coatings, finding that the use of polymers with high dielectric constant, low surface energy, and low reactivity towards lithium induce more homogeneous lithium deposition. This strategy is effective to reduce the formation of Li dendrites (Fig. 6b). More recently, Kong et al. reported a 3D coarse-grained molecular simulation study on the deposition of lithium in the presence of polymer coatings [487]. The study confirms that polymers with high dielectric permittivity favor a more homogeneous lithium deposition. Interestingly, the authors also indicate that viscoelastic polymers, with intermediate stiffness and short relaxation times, outperform the most rigid polymers in terms of resistance to lithium dendrite growth.

Polymer electrolyte interlayers can help reducing the interface resistance, enhance the plating/stripping process and protect the ceramic separator from degradation. Besides the obvious improvement of the mechanical contact, it is found that buffer layers with lower conductivity than the main SE (this is usually the case when comparing polymer electrolytes with inorganic electrolytes) can dampen the inhomogeneous current during electrodeposition [462]. Indeed, polymer electrolyte interlayers have been used extensively and quite successfully. Zhou et al. reported sandwich electrolytes with cross-linked polymer electrolyte layers coated on both side of ceramic pellets (LATP and LLZO) [489]. A higher electrochemical stability for the SPE towards reduction was observed, which was attributed to the formation of electrical double layers at the polymer-ceramic interfaces, reducing the magnitude of the electric field across the Li/polymer interface. In addition, the improved contact between lithium and polymer layer (in comparison to a ceramic electrolyte) reduces the transfer resistance and provides uniform Li-ion flux across the interface, thus hindering dendrite formation. Wang et al. used a bilayer electrolyte composed of a PEO/LiTFSI layer (on the anode side) and a ceramic-rich PEO/LAGP/LiTFSI main separator layer [490]. Again, the combined use of a polymer interlayer and a composite separator suppressed dendrite formation. The effect of the PEO molecular weight on cyclability was also tested. Interestingly, PEO, with the highest elongation at rupture and intermediate tensile strength, provided the best results, whereas the PEO interlayer with the highest tensile strength was easily pierced by dendrites. These results suggest that the interlayer toughness should be maximized in order to hinder the dendrite growth.

Single-ion conducting polymer electrolytes (SIC-PEs) are not affected by concentration polarization, therefore they are supposedly the most effective solution against lithium dendrites growth. However, the low conductivity (lower than $10^{-6} \text{ S cm}^{-1}$ in this case) may affect negatively the cell performance. This strategy was adopted by Zhou et al., who coated garnet pellets with SIC-PEs interlayers, which resulted in dendrites suppression and reduction of the interface resistance [206].

Other recent examples of the application of polymer electrolyte interlayers include PEO/LiTFSI/LLTO-nanofiber composite electrolyte coated with PEO/LiTFSI interlayers [207], gel polymer interlayers (PVDF-HFP + carbonate based electrolyte) coated on garnet separators [491], and the protection of a LAGP separator through a photopolymerizable polyethylene glycol diacrylate (PEGDA) layer applied directly on the lithium surface [208].

4.2.2. Chemical and electrochemical stability

The extremely reactive nature of Li metal favours electrolyte decomposition on its surface. The electrochemical stability of the electrolyte-anode assembly depends on the nature of the SE and, more particularly, on the specific composition of the surface. If the electrolyte is degraded, or if a stable interlayer is not formed, application of an artificial interlayer may be necessary. In the following subsections, the stability of the most common SE classes towards lithium metal and the different solutions applied in the various cases are examined.

Oxide-based and polyanionic solid electrolytes: Oxide-based SE are usually stable with Li metal thanks to the low reduction potential of this category of materials (see section 2.1). Chemical and electrochemical reactions occur for materials containing certain elements that oxidize and reduce at the operation potential of the battery. This behaviour has been observed in LLTO, containing Ti^{4+} that reduces to Ti^{3+} at around 1.8 V. In practice, direct contact with Li metal already reduces Ti^{4+} to Ti^{3+} leading to the degradation of the SE as revealed by its colour change [375]. Some garnet SEs present similar drawbacks as this family of electrolytes requires substitution on the Li, Zr or La site to stabilize the cubic phase. When using elements such as Nb [492,493] or Ta [492], an electrochemical reaction is observed when the material is in contact with Li metal. It is therefore recommended to select Al^{3+} [91, 494] and Ga^{3+} [95] substitution to avoid spontaneous reduction of the SE, which could lead to the appearance of electronic conductivity on the ceramic electrolyte. Still, chemical inhomogeneities at the surface of garnet SEs could lead to instabilities against Li metal, in particular at the grain boundaries [495]. Similarly, Ge reduction in LAGP electrolyte with Li metal negatively affects the SE properties [496]. In this case, the addition of protective interlayers is necessary, e.g. metallic Ge [497], conductive polymer coatings [498,499], glass ceramics [276] or composite films [81].

LiPON electrolytes, widely used for microbatteries, have been reported to be thermodynamically unstable against Li metal. Its degradation results in the formation of Li_2O , Li_3N , Li_3PO_4 and Li_3P [109]. As commented in section 2.1.1, these side products are however stable against metallic lithium and show a positive effect on the Li metal/-electrolyte interface as it passivates the SE forming a thin layer at the interface that acts as SEI and inhibits further side reactions [73,109, 501]. Therefore LiPON electrolyte does not require any protecting interlayer and can be even used as protective coating for other types of SE.

Sulfide-based solid electrolytes: Sulfide materials show strong reducing properties when in contact with Li metal. The solid electrolyte interface (SEI) layer formed at the interface can be tailored by tuning the sulfide material composition. For instance, the presence of Ge in $\text{Li}_{10}\text{GeP}_2\text{S}_{12}$ leads to a thinner SEI layer upon cycling of symmetric cells [251], compared to samples prepared with Si, such as $\text{Li}_{10}\text{SiP}_2\text{S}_{12}$ [502]. Other strategies used to stabilize the sulfide electrolyte with Li metal include the use of a Li metal alloy as a protective layer on top of Li metal. For example, Li-In alloys are often used with sulfide electrolytes [246, 503]. However, the use of indium is not feasible for large-scale

production as it decreases the cell voltage and increases the cost. Several processing techniques could be applied to form protective coatings such as vapor deposition processes (for example ALD) [504,505] or reactive etching. Another possibility is to adsorb a thin layer of a reactive molecule, e.g. N_2 , SO_2 , or halogens, on the sulfide surface. During lamination, this reactive layer reacts with the lithium metal forming a protective interlayer [506]. Alternatively, a polymer electrolyte interlayer can be used [210].

Polymer-based electrolytes: The chemical stability of polymer electrolytes with lithium metal varies according to the polymer chemistry. Among the most common polymer matrices for polymer electrolytes, PEO and polyethers show the highest stability towards lithium metal. In the case of PEO, electrolyte degradation can be inhibited by the formation of a stable SEI, although this appears to depend on the purity of the materials and on the cell assembly procedure, as well as the salts and additives used in the electrolytes [507]. On the contrary, some polycarbonates, e.g. polypropylene carbonate, and poly(trimethylene carbonate) (PTMC), show signs of degradation with lithium metal [160, 508]. In some cases, this can lead to an increase of the ionic conductivity due to the formation of liquid carbonate monomers [161]. Among the other most common polymer hosts for SPEs, poly(acrylonitrile) (PAN), poly(methylmethacrylate) (PMMA), and poly(vinylidene fluoride) (PVDF), show poor or insufficient compatibility with lithium metal [511–513]. On the other hand, poly(vinylidene-co hexafluoropropylene) (PVDF-HFP), although in theory is not stable, is routinely used as matrix for the gel-polymer electrolytes with lithium metal anodes [514], in which the chemical stability of the interface and SEI formation are highly dependent on the chemistry of liquid electrolyte introduced in the gel-polymer electrolyte [514].

The anode interface is probably the most critical element in the whole SSB cell. The use of Li as anode is accompanied by seemingly insurmountable issues, the most important being dendrites growth, which have hindered insofar the development of Li-metal rechargeable batteries. The whole development of SSEs has been indeed prompted, among other reasons, by the hope of enabling the use of Li metal, that is, the hope towards higher energy densities. However, to date, SSEs have struggled to demonstrate safe and prolonged cycling with Li metal anode.

In the last years, many progresses have been reported through the application of several strategies, such as application of pressure, nano-structuration, application of interlayers, etc. This last approach, in particular, is a promising, versatile, and easily scalable tool to improve cyclability, and is effective with both ceramic and polymer electrolytes. The application of interlayers is also necessary to address the chemical and electrochemical instability of some SSEs, such as sulfides, NASICON-type SSEs, and some types of polymer electrolytes. Most probably, the use of Li metal anodes with SEs will rely on the application of this kind of solution.

Nevertheless, it is important to stress that SSBs will not be deployed at a large scale if safe and long cycling is not demonstrated also in realistic conditions, i.e. at “large” current densities ($>1 \text{ mA cm}^{-2}$), and with charge/discharge capacities higher than 1 mAh cm^{-2} .

4.3. Interface between polymer and inorganic electrolytes

By coupling polymer and inorganic electrolytes, non-negligible interface resistance across the two phases is usually observed. This effect is particularly important in hybrid SEs (HSEs), which show lower ionic conductivity than predicted by the rule of mixture. In polymer rich hybrid electrolytes, charge migration occurs mostly through the polymer phase, indicating that the interphases charge transfer is hindered or sluggish [196]. Ceramic-rich hybrid electrolytes show even lower conductivity due to the increase of the tortuosity in the polymer phase [515]. High conductivity values are obtained mostly with nanofiber or nanowire fillers [147], which offer continuous conduction pathways through the ceramic phase. The issue is critical, obviously, also for multilayered electrolytes. As a matter of fact, the interface between ceramic and polymer electrolytes is studied preferentially in model

systems with layered configuration. The results of these studies are also applicable to composite hybrid electrolytes.

Charge transport across inorganic-polymer electrolyte interfaces is characterized by i) high interface resistance, and ii) higher activation energy for the ion transfer across the interface than for ion transport in the bulk phases [516]. Glass electrolytes, which are grain boundary-free, also demonstrate the presence of high interfacial resistance, such as between LiPON and a SPE [481]. The resistance is however dependent on the electrolyte processing, and can be reduced by optimizing the contact between the two phases (namely by depositing LiPON on the SPE). Langer et al. revealed that the transport across the interface has higher activation energy than the bulk conductivity for SPE/LLZO/SPE multilayer electrolytes [517]. From these studies, it can be concluded that the transport across the two phases is a thermally activated process, intrinsically hindered by the high activation energy. The problem is further enhanced in case of a poor interface contact.

The origin of this high interface resistance is not obvious. Gupta and Sakamoto tried to answer this question for sandwich PEO-LiTFSI/LLZO/PEO-LiTFSI electrolytes [518]. The observed high interface resistance ascribed to the presence of insulating impurities on the surface of LLZO, in particular Li_2CO_3 . Indeed, removal of interface impurities by high-temperature treatment greatly decreased the interface resistance. Other studies confirm that, at least with garnet-type fillers, the presence of surface insulating impurities like LiOH or Li_2CO_3 is an obstacle to the interface charge transfer. Huo et al. reported overall improved electrochemical performances, in garnet-rich HSEs, by using Li_2CO_3 -free particles purified by thermal treatment at 600 °C [519]. Li et al. tackled the issue by doping LLZO with LiF [520]. The latter accumulates on the surface and grain boundaries, increasing the resistance against corrosion from CO_2 and humidity, thus hindering the formation of LiOH and Li_2CO_3 . Concurrently, the interface resistance between SPE and LiF-doped LLZO pellets was reduced by half with respect to pristine LLZO.

Another possible factor influencing the interface resistance is the formation of an electrical double layer, *i.e.* the occurrence of space-charge phenomena at the interface. The presence of a space charge region may provide an additional conduction pathway for Li-ion motion, along the particle surface, if the particle concentration exceeds the percolation threshold value [521]. One issue in this sense is represented by particle agglomeration, which has been shown to occur already at low concentration [522]. Particle agglomeration reduces the contact area between inorganic particles and the polymer matrix, thus disrupting the surface percolation network. Below the percolation threshold, space charge effect may inhibit the charge exchange between particles and matrix, thus contributing positively to the interface resistance. Brogioli et al. developed a model for the interface double layer between LLZO and a SPE, also taking into account space-charge effects [523]. Following this model, the authors conclude that space charge effects are only partly responsible for the interface resistance. The latter is again attributed to the high activation energy for lithium-ion transfer between the two phases.

Chemical compatibility between inorganic and polymer electrolyte is another important aspect to be considered in the design of hybrid SEs, particularly in those with highly reactive ceramic electrolytes such as sulfides and garnet-type oxides. Garnet-complexation of amide-type solvent molecules was found to trigger dehydrofluorination of PVDF in LLZO/PVDF/ LiClO_4 CPEs [524]. However, in this case, the reaction did not affect negatively mechanical properties and cell performances. Altogether, further studies are needed to confirm the compatibility between PVDF-based polymers and garnet-type electrolytes.

The stability of sulfide electrolytes with PEO-based SPEs is also subject of study, as the latter are possible candidates as interlayers between lithium and sulfides. Ripphaus et al. examined the stability between thiostannate $\text{Li}_{10}\text{SnP}_2\text{S}_{12}$ (LSPS) and a PEO-based SPE, finding evidence for chemical reactivity, leading to increasing impedance between the two phases [525]. Simon et al. investigated the interface

between argyrodite-type $\text{Li}_6\text{PS}_5\text{Cl}$ and PEO/LiTFSI [526]. As in the previous report, they also observed degradation at the interface, with formation of polysulfides, LiF, and other argyrodite decomposition products. However, in this case the authors claimed that the overall effect could be positive, as the newly formed interfaces were characterized by low impedance and low activation energy.

To conclude, the interface resistance is an obstacle to the development of layered, composite and hybrid solid electrolytes (HSEs). With regards to the latter, it appears that the conductivity can be maximized by i) avoiding the formation of insulating species on the inorganic particles surface, ii) maximizing the contact area between the organic and inorganic phases, *e.g.* by avoiding particle agglomeration, and iii) creating percolation pathways through the inorganic phase, *e.g.* by using ceramic nanowires or nanofibers. This last approach is particularly promising, as the inorganic phase is usually more conductive than the polymer phase. In the case of layered electrolytes, control and engineering of the interface are critical to enhance cell performances. Finally, attention needs to be paid also to the chemical compatibility of the various components, in particular with highly reactive materials such as garnet-type electrolytes and sulfides.

5. Conclusions and perspectives

Materials development: From a materials perspective, a critical issue is the development of a robust solid-state electrolyte, especially in terms of mechanical and chemical stability, high Li-ion conductivity and processability (Fig. 7). Unfortunately, it is not possible to highlight one material (not even one family) over others, since those outperforming in one critical aspect lack of other fundamental characteristics. Inorganic solid electrolytes, mainly represented by complex oxides such as $\text{Li}_7\text{La}_3\text{Zr}_2\text{O}_{12}$ and sulfide materials like $\text{Li}_{10}\text{GeP}_2\text{S}_{12}$, stand out for their high Li-ion conductivity but mainly fail in terms of rigidity (oxides) and low electrochemical stability (sulfides), see Fig. 7 – Oxides & Sulfides. Meanwhile, organic electrolytes, mostly formed by polymeric matrices (the most common being PEO) in which a Li-salt is dissolved, are easily processable but exhibit lower Li-ion conductivity and thermal stability (Fig. 7 – Polymers). An interesting alternative is represented by composite hybrid solid electrolytes (HSEs), formed by the combination of the two classes of materials. A HSE, able to combine the benefits of both inorganic and organic components (Fig. 7 – Composites), might be the key for overcoming current limitations of solid-state electrolytes. However, understanding the formation of interfaces between the two components is crucial to maximize the transport properties. Eventually, the fabrication of hybrid electrolytes with single ceramic conduction pathways (3D network) in flexible polymeric matrices could eliminate the interfacial resistance, thus optimizing this approach.

For electrode materials, cathode materials such as LCO, NMC or LFP have already been used commercially in LIBs. The main challenge nowadays relates to the effective combination of materials in full cells, with special attention to the understanding and control of the multiple degradation issues in the CAM/electrolyte interfaces. In this sense, the use of polymer electrolytes as catholytes seems to be less problematic than the use of inorganic electrolytes, in terms of interface resistance and mechanical stability. Nonetheless, the feasibility of polymer electrolyte-containing cathodes with low temperature operation, higher electrochemical stability, high-rate capability and practical loading, needs to be fully demonstrated. On the anode side, the beneficial effect of solid-state electrolytes on reducing the Li dendrite propagation has motivated an important resurgence of metallic Li as the most promising anode material for high-energy SSBs. However, important limitations arise from the chemical incompatibility between Li and most common SEs. In this context, the strategies described in section 4 of this review (and summarized below) will be crucial for the achievement of high performance, long lasting SSBs.

Processing techniques: Heavily dependent on the selection of materials, a wide variety of techniques can be adapted for the processing of



Fig. 7. Radar chart presenting the most relevant properties of the polymer, composite, oxide and sulfide families of solid-state electrolytes. The considered properties include chemical stability and electrochemical performance (Ionic conductivity and transference number (t^+), stability against Li metal, stability against high voltage cathode, interfacial resistance), thermal and mechanical stability and cell integration towards manufacturing (described as processability and cost).

all individual SSB components. The important background coming from the mature LIBs production technology and the possibility of a drop-in solution (i.e. manufactured in similar production lines as LIBs) has motivated wet coating techniques to continue being one of the prominent options for the production of SSBs. Wet coating techniques are currently used in both laboratory and industrial scale for the production of CAMs and electrolytes, mainly polymer-based. Still, the quest for cheaper and more environmentally friendly options is lately favouring the development of alternative solvent-free techniques such as melt extrusion. It is important to note that this is efficiently applied to both polymer-based electrolytes and inorganic sulfides. Cold and hot pressing are generally employed to densify different kinds of solid-state electrolytes, although in many cases (particularly for complex oxide electrolytes) high temperature ($>800\text{ }^{\circ}\text{C}$) sintering steps are also required. The sintering step has important implications in the SSB fabrication flow, since most common CAMs do not stand the required sintering temperatures. In this sense, the development of alternative processing tools such as cold sintering represents a promising route, allowing the densification of oxide electrolytes at temperatures compatible with other cell components.

Significant advances are also taking place in the optimization of thin film processing for SSBs. Cutting-edge vapor deposition techniques such as sputtering, PLD or ALD are being used for multiple purposes, including the direct fabrication of solid-state electrolytes in thin film form (e.g. thin film LiPON-based batteries) or the protection of different cell components with thin coating layers, to avoid chemical degradation or to reduce the interfacial resistance. The layer-by-layer and subsequent conformal growing characteristics of ALD make this technique especially suited for the coating of the typical 3D-shaped electrodes and/or rough surfaces found in SSBs. Therefore a prominent role of ALD on the development of advanced SSBs in the future is foreseen.

Alternative techniques such as spray coating, screen printing or dip

coating techniques, definitely require attention and might have an impact in battery production due to their scalability, especially for obtaining thin films with inorganic components. Finally, the explosive development of 3D printing might promote new routes for easy processing of SSBs with complex structures and alternative geometries.

Full cell integration: Clearly, one of the most important limitations of SSBs nowadays relates to the presence of multiple, highly-resistive, solid-solid interfaces and to possible interfacial degradation events in the course of battery operation. These are either associated to internal mechanical processes (volume change of the CAM, formation of voids and subsequent loss of electronic/ionic percolation) or (electro)chemical processes (formation of new interphases, dendrite growth) upon cycling. The solution to these challenges lies in the understanding and control of the interfaces and their evolution during the whole battery life, for which the development of advanced *in-situ* monitoring techniques is crucial [527,528]. In order to avoid chemical degradation issues, the most trivial approach is the selection of compatible materials, although this option is intrinsically limited due to the relatively narrow electrochemical stability window of most electrolyte materials. Innovative strategies to mitigate this issue include building stable interlayers between chemically incompatible materials. This could be done either by adding thin protective coatings, using multilayer electrolyte solutions, or by forcing the formation of stable interlayers through the addition of reactive species to the electrolyte/AM formulation. Due to the extended use of metallic Li as anode material, the development of artificial interlayers between anode and electrolyte is one of the key aspects to be addressed in the future generation of SSBs.[529] In this sense, the application of advanced thin film deposition techniques such as ALD will be fundamental.

Mechanical degradation issues are also heavily affecting the long term cyclability of SSBs and great effort is placed in controlling the volume expansion and voids formation in the electrodes. On one side,

the loss of percolation in composite cathodes, derived from mechanical transformations during charge/discharge, is being tackled by the addition of thin conductive films between CAM and catholyte or, more simply, by the addition of conductive additives. On the other side, the development of 3D-shaped porous structures and engineered electrode/electrolyte interfaces has been shown to give promising results for the control of volume expansion and dendrite formation at the anode.

In conclusion, the success of SSBs as advanced electrochemical energy storage systems must involve necessarily a further development of the technology in terms of advanced materials (hybrid solid-state electrolytes with enhanced properties), processing techniques (for cell components manufacturing and protective coatings) and, most importantly, full cell integration. In this sense, a deep understanding of interfaces and interphase formation upon battery operation is critical for the achievement of high performing and long-lasting cells. The formation of artificial protective layers by either thin film coating or controlled chemical formation is a key parameter and the use of advanced interface characterization techniques will be fundamental.

Declaration of competing interest

The authors declare that they have no known competing financial interests or personal relationships that could have appeared to influence the work reported in this paper.

Acknowledgments

This work was carried out within the project framework EU-horizon 2020 project IMAGE, under the grant agreement N° 769929 and MINECO Spanish national grant 3D-ACCESS (reference number: PID2019-107106RB-C33). The authors thank Gene Nolis for his support during the manuscript revisions.

References

- [1] M. Sanders, *The Rechargeable Battery Market and Main Trends 2012-2025*, "Michigan, 2017.
- [2] M. Armand, J.M. Tarascon, Building better batteries, *Nature* 451 (7179) (07-Feb-2008) 652–657, <https://doi.org/10.1038/451652a>. Nature Publishing Group.
- [3] B. Scrosati, Recent advances in lithium ion battery materials, *Electrochim. Acta* 45 (15–16) (May 2000) 2461–2466, [https://doi.org/10.1016/S0013-4686\(00\)00333-9](https://doi.org/10.1016/S0013-4686(00)00333-9).
- [4] Y. S. Meng, "Lithium metal anode – advanced characterization, slides from the web seminar by Dr. Y. Shirley Meng," doi: 10.1149/OSF.IO/6FR7C.
- [5] X. Feng, M. Ouyang, X. Liu, L. Lu, Y. Xia, X. He, Thermal runaway mechanism of lithium ion battery for electric vehicles: a review, in: *Energy Storage Materials*, vol. 10, Elsevier B.V., 01-Jan-2018, pp. 246–267, <https://doi.org/10.1016/j.ensm.2017.05.013>.
- [6] Q. Wang, P. Ping, X. Zhao, G. Chu, J. Sun, C. Chen, Thermal runaway caused fire and explosion of lithium ion battery, *J. Power Sources* 208 (15 Jun 2012) 210–224, <https://doi.org/10.1016/j.jpowsour.2012.02.038>. Elsevier.
- [7] A. Iturrondobea, et al., Post-mortem analysis of calendar-aged 16 ah NMC/graphite pouch cells for EV application, *J. Phys. Chem. C* 121 (40) (Oct. 2017) 21865–21876, <https://doi.org/10.1021/acs.jpcc.7b05416>.
- [8] A. Perea, M. Dontigny, K. Zaghib, Safety of solid-state Li metal battery: solid polymer versus liquid electrolyte, *J. Power Sources* 359 (Aug. 2017) 182–185, <https://doi.org/10.1016/j.jpowsour.2017.05.061>.
- [9] W. Zhang, J. Nie, F. Li, Z.L. Wang, C. Sun, A durable and safe solid-state lithium battery with a hybrid electrolyte membrane, *Nanomater. Energy* 45 (Mar. 2018) 413–419, <https://doi.org/10.1016/j.nanoen.2018.01.028>.
- [10] J. Janek, W.G. Zeier, A solid future for battery development, *Nature Energy* 1 (9) (08-Sep-2016) 1–4, <https://doi.org/10.1038/nenergy.2016.141>. Nature Publishing Group, pp.
- [11] A. Gutiérrez-Pardo, et al., Will the competitive future of solid state Li metal batteries rely on a ceramic or a composite electrolyte? *Sustain. Energy Fuels* 2 (10) (Sep. 2018) 2325–2334, <https://doi.org/10.1039/c8se00273h>.
- [12] J.B. Goodenough, P. Singh, "Review—solid electrolytes in rechargeable electrochemical cells, *J. Electrochem. Soc.* 162 (14) (Oct. 2015) A2387–A2392, <https://doi.org/10.1149/2.0021514jes>.
- [13] A. Manthiram, X. Yu, S. Wang, Lithium battery chemistries enabled by solid-state electrolytes, *Nature Reviews Materials* 2 (4) (14-Feb-2017) 1–16, <https://doi.org/10.1038/natrevmats.2016.103>. Nature Publishing Group.
- [14] F. Zheng, M. Kotobuki, S. Song, M.O. Lai, L. Lu, Review on solid electrolytes for all-solid-state lithium-ion batteries, *J. Power Sources* 389 (Jun. 2018) 198–213, <https://doi.org/10.1016/j.jpowsour.2018.04.022>.
- [15] X. Zhang, J.-C. Daigle, K. Zaghib, Comprehensive review of polymer architecture for all-solid-state lithium rechargeable batteries, *Materials* 13 (11) (May 2020) 2488, <https://doi.org/10.3390/ma13112488>.
- [16] I. Gracia, M. Armand, D. Shanmukaraj, Li metal polymer batteries, in: *Solid Electrolytes For Advanced Applications*, Springer International Publishing, 2019, pp. 347–373.
- [17] P. Knauth, Inorganic solid Li ion conductors: an overview, *Solid State Ionics* 180 (14–16) (Jun. 2009) 911–916, <https://doi.org/10.1016/j.ssi.2009.03.022>.
- [18] Q. Liu, et al., Challenges and perspectives of garnet solid electrolytes for all solid-state lithium batteries, *J. Power Sources* 389 (Jun. 2018) 120–134, <https://doi.org/10.1016/j.jpowsour.2018.04.019>.
- [19] V. Thangadurai, D. Pinzaru, S. Narayanan, A.K. Baral, Fast solid-state Li ion conducting garnet-type structure metal oxides for energy storage, *J. Phys. Chem. Lett.* 6 (2) (15-Jan-2015) 292–299, <https://doi.org/10.1021/jz501828v>. American Chemical Society.
- [20] B. Kumar, L.G. Scanlon, Polymer-ceramic composite electrolytes, *J. Power Sources* 52 (2) (Dec. 1994) 261–268, [https://doi.org/10.1016/0378-7753\(94\)02147-3](https://doi.org/10.1016/0378-7753(94)02147-3).
- [21] S.-J. Tan, X.-X. Zeng, Q. Ma, X.-W. Wu, Y.-G. Guo, Recent advancements in polymer-based composite electrolytes for rechargeable lithium batteries, *Electrochem. Energy Rev.* 1 (2) (Jun. 2018) 113–138, <https://doi.org/10.1007/s41918-018-0011-2>.
- [22] A. Manuel Stephan, K.S. Nahm, Review on composite polymer electrolytes for lithium batteries, *Polymer* 47 (16) (26-Jul-2006) 5952–5964, <https://doi.org/10.1016/j.polymer.2006.05.069>. Elsevier BV.
- [23] J. Schnell, et al., "All-solid-state lithium-ion and lithium metal batteries – paving the way to large-scale production, *J. Power Sources* 382 (Apr. 2018) 160–175, <https://doi.org/10.1016/j.jpowsour.2018.02.062>.
- [24] J. Wu, Z. Rao, Z. Cheng, L. Yuan, Z. Li, Y. Huang, "Ultrathin, flexible polymer electrolyte for cost-effective fabrication of all-solid-state lithium metal batteries, *Adv. Energy Mater.* 9 (46) (Dec. 2019) 1902767, <https://doi.org/10.1002/aenm.201902767>.
- [25] K. Murata, S. Izuchi, Y. Yoshihisa, An overview of the research and development of solid polymer electrolyte batteries, *Electrochim. Acta* 45 (8) (2000) 1501–1508, [https://doi.org/10.1016/S0013-4686\(99\)00365-5](https://doi.org/10.1016/S0013-4686(99)00365-5).
- [26] R.C. Xu, X.H. Xia, S.Z. Zhang, D. Xie, X.L. Wang, J.P. Tu, Interfacial challenges and progress for inorganic all-solid-state lithium batteries, in: *Electrochimica Acta*, vol. 284, Elsevier Ltd, 10-Sep-2018, pp. 177–187, <https://doi.org/10.1016/j.electacta.2018.07.191>.
- [27] Z. Gao, et al., Promises, challenges, and recent progress of inorganic solid-state electrolytes for all-solid-state lithium batteries, *Adv. Mater.* 30 (17) (2018) 1–27, <https://doi.org/10.1002/adma.201705702>.
- [28] Y. Wang, et al., Design principles for solid-state lithium superionic conductors, *Nat. Mater.* 14 (10) (Oct. 2015) 1026–1031, <https://doi.org/10.1038/nmat4369>.
- [29] S. Xia, X. Wu, Z. Zhang, Y. Cui, W. Liu, Practical challenges and future perspectives of all-solid-state lithium-metal batteries, in: *Chem.*, vol. 5, Elsevier Inc, 11-Apr-2019, pp. 753–785, <https://doi.org/10.1016/j.chempr.2018.11.013>, 4.
- [30] W.D. Richards, L.J. Miara, Y. Wang, J.C. Kim, G. Ceder, Interface stability in solid-state batteries, *Chem. Mater.* 28 (1) (Jan. 2016) 266–273, <https://doi.org/10.1021/acs.chemmater.5b04082>.
- [31] B. Zheng, H. Wang, Z. Gong, Y. Yang, J. Ma, A review of inorganic solid electrolyte/electrode interface in all-solid-state lithium batteries, *Sci. Sin. Chim.* 47 (5) (May 2017) 579–593, <https://doi.org/10.1360/n032016-00239>.
- [32] D.H.S. Tan, A. Banerjee, Z. Chen, Y.S. Meng, From nanoscale interface characterization to sustainable energy storage using all-solid-state batteries, *Nat. Nanotechnol.* 15 (3) (01-Mar-2020) 170–180, <https://doi.org/10.1038/s41565-020-0657-x>. Nature Research.
- [33] X. Yu, A. Manthiram, Electrode-electrolyte interfaces in lithium-based batteries, *Energy Environ. Sci.* 11 (3) (01-Mar-2018) 527–543, <https://doi.org/10.1039/c7ee02555f>. Royal Society of Chemistry.
- [34] Y. Xiao, Y. Wang, S.H. Bo, J.C. Kim, L.J. Miara, G. Ceder, Understanding interface stability in solid-state batteries, *Nature Reviews Materials* 5 (2) (01-Feb-2020) 105–126, <https://doi.org/10.1038/s41578-019-0157-5>. Nature Research.
- [35] M. Du, K. Liao, Q. Lu, Z. Shao, Recent advances in the interface engineering of solid-state Li-ion batteries with artificial buffer layers: challenges, materials, construction, and characterization, *Energy Environ. Sci.* 12 (6) (Jun. 2019) 1780–1804, <https://doi.org/10.1039/c9ee00515c>.
- [36] W. Zhang, et al., Interfacial processes and influence of composite cathode microstructure controlling the performance of all-solid-state lithium batteries, *ACS Appl. Mater. Interfaces* 9 (21) (May 2017) 17835–17845, <https://doi.org/10.1021/acsami.7b01137>.
- [37] K. Nie, et al., Interfaces between cathode and electrolyte in solid state lithium batteries: challenges and perspectives, *Frontiers in Chemistry* 6 (12-Dec-2018) 616, <https://doi.org/10.3389/fchem.2018.00616>. DEC. Frontiers Media S.A.
- [38] M. Tatsumisago, M. Nagao, A. Hayashi, Recent development of sulfide solid electrolytes and interfacial modification for all-solid-state rechargeable lithium batteries, *Journal of Asian Ceramic Societies* 1 (1) (01-Mar-2013) 17–25, <https://doi.org/10.1016/j.jascers.2013.03.005>. Taylor and Francis Ltd.
- [39] V. Thangadurai, S. Narayanan, D. Pinzaru, Garnet-type solid-state fast Li ion conductors for Li batteries: critical review, *Chem. Soc. Rev.* 43 (13) (07-Jul-2014) 4714–4727, <https://doi.org/10.1039/c4cs00020j>. Royal Society of Chemistry.
- [40] J.C. Bachman, et al., Inorganic solid-state electrolytes for lithium batteries: mechanisms and properties governing ion conduction, *Chem. Rev.* 116 (1) (2016) 140–162, <https://doi.org/10.1021/acs.chemrev.5b00563>.

- [42] T. Famprikis, P. Canepa, J.A. Dawson, M.S. Islam, C. Masquelier, Fundamentals of inorganic solid-state electrolytes for batteries, *Nat. Mater.* (2019), <https://doi.org/10.1038/s41563-019-0431-3>.
- [43] Z. Zhang, et al., New horizons for inorganic solid state ion conductors, *Energy Environ. Sci.* 11 (8) (01-Aug-2018) 1945–1976, <https://doi.org/10.1039/c8ee01053f>. Royal Society of Chemistry.
- [44] Z. Wu, et al., Utmost limits of various solid electrolytes in all-solid-state lithium batteries: a critical review, in: *Renewable and Sustainable Energy Reviews*, vol. 109, Elsevier Ltd, 01-Jul-2019, pp. 367–385, <https://doi.org/10.1016/j.rser.2019.04.035>.
- [45] Y. Zhu, J.C. Gonzalez-Rosillo, M. Balaish, Z.D. Hood, K.J. Kim, J.L.M. Rupp, “Lithium-film ceramics for solid-state lithionic devices,” *Nature Reviews Materials*, Nature Research (26-Nov-2020) 1–19, <https://doi.org/10.1038/s41578-020-00261-0>.
- [46] M. Liu, et al., Controlling the lithium-metal growth to enable low-lithium-metal-excess all-solid-state lithium-metal batteries, *ACS Mater. Lett.* 22 (May 2020) 665–670, <https://doi.org/10.1021/acsmaterialslett.0c00152>.
- [47] Y. Guo, H. Li, T. Zhai, Reviving lithium-metal anodes for next-generation high-energy batteries, *Adv. Mater.* 29 (29) (Aug. 2017) 1700007, <https://doi.org/10.1002/adma.201700007>.
- [48] D. Lin, Y. Liu, Y. Cui, Reviving the lithium metal anode for high-energy batteries, *Nat. Nanotechnol.* 12 (3) (2017) 194–206, <https://doi.org/10.1038/nnano.2017.16>.
- [49] C. Yu, et al., Accessing the bottleneck in all-solid-state batteries, lithium-ion transport over the solid-electrolyte-electrode interface, *Nat. Commun.* 8 (1) (Dec. 2017) 1–9, <https://doi.org/10.1038/s41467-017-01187-y>.
- [50] Julien Mauger, Armand Paoletta, Zaghbi, Building better batteries in the solid state: a review, *Materials* 12 (23) (Nov. 2019) 3892, <https://doi.org/10.3390/ma12233892>.
- [51] D. Wang, C. Zhu, Y. Fu, X. Sun, Y. Yang, Interfaces in garnet-based all-solid-state lithium batteries, *Adv. Energy Mater.* 2001318 (2020) 1–23, <https://doi.org/10.1002/aenm.202001318>.
- [52] S. Lou, et al., “Interface issues and challenges in all-solid-state batteries: lithium, sodium, and beyond, *Adv. Mater.* (Jul. 2020) 2000721, <https://doi.org/10.1002/adma.202000721>.
- [53] K. Kerman, A. Luntz, V. Viswanathan, Y.-M. Chiang, Z. Chen, Review—Practical challenges hindering the development of solid state Li ion batteries, *J. Electrochem. Soc.* 164 (7) (2017) A1731–A1744, <https://doi.org/10.1149/2.1571707jes>.
- [54] K.-N. Jung, H.-S. Shin, M.-S. Park, J.-W. Lee, Solid-State lithium batteries: bipolar design, fabrication, and electrochemistry, *ChemElectroChem* 6 (15) (2019) 3842–3859, <https://doi.org/10.1002/celec.201900736>.
- [55] F. Hao, F. Han, Y. Liang, C. Wang, Y. Yao, Architectural design and fabrication approaches for solid-state batteries, *MRS Bull.* 43 (10) (2018) 775–781, <https://doi.org/10.1557/mrs.2018.211>.
- [56] Y. Liu, Q. Sun, D. Wang, K. Adair, J. Liang, X. Sun, Development of the cold sintering process and its application in solid-state lithium batteries, *J. Power Sources* 393 (Jul. 2018) 193–203, <https://doi.org/10.1016/j.jpowsour.2018.05.015>.
- [57] J. Nunes-Pereira, C.M. Costa, S. Lancers-Méndez, Polymer composites and blends for battery separators: state of the art, challenges and future trends, *J. Power Sources* 281 (2015) 378–398, <https://doi.org/10.1016/j.jpowsour.2015.02.010>.
- [58] J. Muldoon, C.B. Bucur, N. Boaretto, T. Gregory, V. Di Noto, Polymers: opening doors to future batteries, *Polym. Rev.* 55 (2) (2015) 208–246, <https://doi.org/10.1080/15583724.2015.1011966>.
- [59] J. Wan, J. Xie, D.G. Mackanic, W. Burke, Z. Bao, Y. Cui, Status, promises, and challenges of nanocomposite solid-state electrolytes for safe and high performance lithium batteries, *Mater. Today Nano* 4 (2018) 1–16, <https://doi.org/10.1016/j.mtnano.2018.12.003>.
- [60] J. Mindemark, M.J. Lacey, T. Bowden, D. Brandell, “Beyond PEO—alternative host materials for Li+-conducting solid polymer electrolytes, in: *Progress in Polymer Science*, vol. 81, Elsevier Ltd, 01-Jun-2018, pp. 114–143, <https://doi.org/10.1016/j.progpolymsci.2017.12.004>.
- [61] M. Keller, A. Varzi, S. Passerini, Hybrid electrolytes for lithium metal batteries, *J. Power Sources* 392 (Jul. 2018) 206–225, <https://doi.org/10.1016/j.jpowsour.2018.04.099>.
- [62] D.T. Hallinan, I. Villaluenga, N.P. Balsara, Polymer and composite electrolytes, *MRS Bull.* 43 (10) (2018) 759–767, <https://doi.org/10.1557/mrs.2018.212>.
- [63] B. Commarieu, A. Paoletta, J.C. Daigle, K. Zaghbi, “Toward high lithium conduction in solid polymer and polymer–ceramic batteries, in: *Current Opinion in Electrochemistry*, vol. 9, Elsevier B.V., 01-Jun-2018, pp. 56–63, <https://doi.org/10.1016/j.coelec.2018.03.033>.
- [64] F. Lv, et al., Challenges and development of composite solid-state electrolytes for high-performance lithium ion batteries, *J. Power Sources* 441 (2019) 227175, <https://doi.org/10.1016/j.jpowsour.2019.227175>.
- [65] J. Lopez, D.G. Mackanic, Y. Cui, Z. Bao, Designing polymers for advanced battery chemistries, *Nat. Rev. Mater.* 4 (5) (2019) 312–330, <https://doi.org/10.1038/s41578-019-0103-6>.
- [66] H.-P. Hong, Crystal structure and ionic conductivity of Li₁₄Zn(GeO₄)₄ and other new Li⁺ superionic conductors, *Mater. Res. Bull.* 13 (2) (Feb. 1978) 117–124, [https://doi.org/10.1016/0025-5408\(78\)90075-2](https://doi.org/10.1016/0025-5408(78)90075-2).
- [67] Y. A. Du and N. A. W. Holzwarth, “Li-ion diffusion mechanisms in crystalline Li₂S₂PO₈ 4S₂ electrolytes,” *Bull. Am. Phys. Soc.*, vol. Volume 52, Number 1, 2007.
- [68] Z. Zishan, Z. Zhongtai, T. Zilong, S. Wanci, Lithium inorganic solid electrolytes, *Prog. Chem.* 15 (2003) 101–106, <https://doi.org/10.3321/j.issn:1005-281X.2003.02.003>.
- [69] Y.A. Du, N.A. W. Holzwarth, Li Ion Diffusion Mechanisms in the Crystalline Electrolyte, 2007, <https://doi.org/10.1149/1.2772200>.
- [70] Y. Deng, et al., Structural and mechanistic insights into fast lithium-ion conduction in Li₄SiO₄-Li₃PO₄ solid electrolytes, *J. Am. Chem. Soc.* 137 (28) (Jul. 2015) 9136–9145, <https://doi.org/10.1021/jacs.5b04444>.
- [71] Y. Deng, et al., Enhancing the lithium ion conductivity in lithium superionic conductor (LISICON) solid electrolytes through a mixed polyanion effect, *ACS Appl. Mater. Interfaces* 9 (8) (Mar. 2017) 7050–7058, <https://doi.org/10.1021/acsami.6b14402>.
- [72] P.G. Bruce, A.R. West, Ion trapping and its effect on the conductivity of LISICON and other solid electrolytes, *J. Solid State Chem.* 53 (3) (Jul. 1984) 430–434, [https://doi.org/10.1016/0022-4596\(84\)90122-1](https://doi.org/10.1016/0022-4596(84)90122-1).
- [73] Y. Zhu, X. He, Y. Mo, Origin of outstanding stability in the lithium solid electrolyte materials: insights from thermodynamic analyses based on first-principles calculations, *ACS Appl. Mater. Interfaces* 7 (42) (Oct. 2015) 23685–23693, <https://doi.org/10.1021/acsami.5b07517>.
- [74] C. Mariappan, C. Yada, F. Rosciano, B. R.-J. of P. Sources, and undefined, Correlation between Micro-structural Properties and Ionic Conductivity of Li_{1.5}AlO_{1.5}Ge_{1.5}(PO₄)₃ Ceramics, “Elsevier, 2011.
- [75] B. Kumar, D. Thomas, J. Kumar, “Space-Charge-Mediated superionic transport in lithium ion conducting glass–ceramics, *J. Electrochem. Soc.* 156 (7) (2009) A506, <https://doi.org/10.1149/1.3122903>.
- [76] V. Thangadurai, W. Weppner, Recent progress in solid oxide and lithium ion conducting electrolytes research, *Ionics* 12 (1) (May 2006) 81–92, <https://doi.org/10.1007/s11581-006-0013-7>.
- [77] T. Takahashi, H. I.-E. Conversion, and undefined, Ionic Conduction in Perovskite-type Oxide Solid Solution and its Application to the Solid Electrolyte Fuel Cell, “Elsevier, 1971.
- [78] X. Xu, Z. Wen, X. Yang, J. Zhang, Z.G.-S.S. Ionics, undefined, “High Lithium Ion Conductivity Glass-Ceramics in Li₂O–Al₂O₃–TiO₂–P₂O₅ from Nanoscaled Glassy Powders by Mechanical Milling,” Elsevier, 2006.
- [79] J. Wolfenstine, J.L. Allen, J. Sakamoto, D.J. Siegel, H. Choe, Mechanical behavior of Li-ion-conducting crystalline oxide-based solid electrolytes: a brief review, *Ionics* 24 (5) (May 2018) 1271–1276, <https://doi.org/10.1007/s11581-017-2314-4>.
- [80] S. Xiong, et al., “Design of a multifunctional interlayer for NASICON-based solid-state Li metal batteries, *Adv. Funct. Mater.* 30 (22) (May 2020) 2001444, <https://doi.org/10.1002/adfm.202001444>.
- [81] P. Hartmann, et al., Degradation of NASICON-type materials in contact with lithium metal: formation of mixed conducting interphases (MCI) on solid electrolytes, *J. Phys. Chem. C* 117 (41) (Oct. 2013) 21064–21074, <https://doi.org/10.1021/jp4051275>.
- [82] Y. Inaguma, et al., High ionic conductivity in lithium lanthanum titanate, *Solid State Commun.* 86 (10) (Jun. 1993) 689–693, [https://doi.org/10.1016/0038-1098\(93\)90841-A](https://doi.org/10.1016/0038-1098(93)90841-A).
- [83] F. Aguesse, J.M. López Del Amo, V. Roddatis, A. Aguadero, J.A. Kilner, Enhancement of the grain boundary conductivity in ceramic Li_{0.34}La_{0.55}TiO₃ electrolytes in a moisture-free processing environment, *Adv. Mater. Interfaces* 1 (7) (Oct. 2014) 1300143, <https://doi.org/10.1002/admi.201300143>.
- [84] J.F. Wu, X. Guo, Origin of the low grain boundary conductivity in lithium ion conducting perovskites: Li₃xLa_{0.67-x}TiO₃, *Phys. Chem. Chem. Phys.* 19 (8) (Feb. 2017) 5880–5887, <https://doi.org/10.1039/c6cp07757a>.
- [85] J.F. Wu, X. Guo, Size effect in nanocrystalline lithium-ion conducting perovskite: Li_{0.30}La_{0.57}TiO₃, *Solid State Ionics* 310 (Nov. 2017) 38–43, <https://doi.org/10.1016/j.ssi.2017.08.003>.
- [86] V. Thangadurai, H. Kaack, W.J.F. Weppner, Novel fast lithium ion conduction in garnet-type Li₅La₃M₂O₁₂ (M = Nb, Ta), *J. Am. Ceram. Soc.* 86 (3) (2003) 437–440, <https://doi.org/10.1111/j.1151-2916.2003.tb03318.x>.
- [87] R. Murugan, V. Thangadurai, W. Weppner, Fast lithium ion conduction in garnet-type Li₇La₃Zr₂O₁₂, *Angew. Chem. Int. Ed.* 46 (41) (2007) 7778–7781, <https://doi.org/10.1002/anie.200701144>.
- [88] L. Xu, et al., “Garnet solid electrolyte for advanced all-solid-state Li batteries, *Adv. Energy Mater.* (May 2020) 2000648, <https://doi.org/10.1002/aenm.202000648>.
- [89] S. Adams, R. R.-J. of M. Chemistry, and undefined, Ion Transport and Phase Transition in Li_{7-x}La₃Zr_{2-x}M_xO₁₂ (M = Ta 5+, Nb 5+, X = 0, 0.25, 2012 *pubs.rsc.org*.
- [90] C.A. Geiger, et al., “Crystal chemistry and stability of ‘Li₇La₃Zr₂O₁₂’ garnet: a fast lithium-ion conductor, *Inorg. Chem.* 50 (3) (Feb. 2011) 1089–1097, <https://doi.org/10.1021/ic101914e>.
- [91] A. Paoletta, et al., Discovering the influence of lithium loss on garnet Li₇La₃Zr₂O₁₂ electrolyte phase stability, *ACS Appl. Energy Mater.* 3 (4) (Apr. 2020) 3415–3424, <https://doi.org/10.1021/acsaem.9b02401>.
- [92] J.L. Allen, J. Wolfenstine, E. Ranganamy, J. Sakamoto, Effect of substitution (Ta, Al, Ga) on the conductivity of Li₇La₃Zr₂O₁₂, *J. Power Sources* 206 (May 2012) 315–319, <https://doi.org/10.1016/j.jpowsour.2012.01.131>.
- [93] X.X. Pan, J.X. Wang, X.H. Chang, Y.D. Li, W.B. Guan, A novel solid-liquid route for synthesizing cubic garnet Al-substituted Li₇La₃Zr₂O₁₂, *Solid State Ionics* 317 (Apr 2018) 1–6, <https://doi.org/10.1016/j.ssi.2017.12.034>.
- [94] C. Bernuy-Lopez, W. Manalastas, J.M. Lopez Del Amo, A. Aguadero, F. Aguesse, J. A. Kilner, Atmosphere controlled processing of ga-substituted garnets for high lithium conductivity ceramics, *Chem. Mater.* 26 (12) (Jun. 2014) 3610–3617, <https://doi.org/10.1021/cm5008069>.

- [96] J.F. Wu, W.K. Pang, V.K. Peterson, L. Wei, X. Guo, Garnet-type fast Li-ion conductors with high ionic conductivities for all-solid-state batteries, *ACS Appl. Mater. Interfaces* 9 (14) (Apr. 2017) 12461–12468, <https://doi.org/10.1021/acsaami.7b00614>.
- [97] J.F. Wu, et al., Gallium-doped Li₇La₃Zr₂O₁₂ garnet-type electrolytes with high lithium-ion conductivity, *ACS Appl. Mater. Interfaces* 9 (2) (2017) 1542–1552, <https://doi.org/10.1021/acsaami.6b13902>.
- [98] L. Buannic, et al., Dual substitution strategy to enhance Li⁺ ionic conductivity in Li₇La₃Zr₂O₁₂ solid electrolyte, *Chem. Mater.* 29 (4) (Feb. 2017) 1769–1778, <https://doi.org/10.1021/acs.chemmater.6b05369>.
- [99] E.J. Cussen, Structure and ionic conductivity in lithium garnets, *J. Mater. Chem.* 20 (25) (Jun. 2010) 5167–5173, <https://doi.org/10.1039/b925553b>.
- [100] L. Cheng, et al., Effect of surface microstructure on electrochemical performance of garnet solid electrolytes, *ACS Appl. Mater. Interfaces* 7 (3) (Jan. 2015) 2073–2081, <https://doi.org/10.1021/am508111r>.
- [101] G. Larraz, A. Orera, M.L. Sanjuán, Cubic phases of garnet-type Li₇La₃Zr₂O₁₂: the role of hydration, *J. Mater. Chem.* 1 (37) (Oct. 2013) 11419–11428, <https://doi.org/10.1039/c3ta11996c>.
- [102] W. Xia, et al., Reaction mechanisms of lithium garnet pellets in ambient air: the effect of humidity and CO₂, *J. Am. Ceram. Soc.* 100 (7) (Jul. 2017) 2832–2839, <https://doi.org/10.1111/jace.14865>.
- [103] J.F. Wu, et al., In situ formed shields enabling Li₂CO₃-free solid electrolytes: a new route to uncover the intrinsic lithiophilicity of garnet electrolytes for dendrite-free Li-metal batteries, *ACS Appl. Mater. Interfaces* 11 (1) (Jan. 2019) 898–905, <https://doi.org/10.1021/acsaami.8b18356>.
- [104] J.B. Bates, et al., Fabrication and characterization of amorphous lithium electrolyte thin films and rechargeable thin-film batteries, *J. Power Sources* 43 (1–3) (Mar. 1993) 103–110, [https://doi.org/10.1016/0378-7753\(93\)80106-Y](https://doi.org/10.1016/0378-7753(93)80106-Y).
- [105] N.J. Dudney, Solid-state thin-film rechargeable batteries, *Mater. Sci. Eng. B: Solid State Materials for Advanced Technology* 116 (3) (2005) 245–249, <https://doi.org/10.1016/j.mseb.2004.05.045>.
- [106] B. Fleutot, B. Pecquenard, H. Martinez, M. Letellier, A. Levasseur, Investigation of the local structure of LiPON thin films to better understand the role of nitrogen on their performance, *Solid State Ionics* 186 (1) (Mar. 2011) 29–36, <https://doi.org/10.1016/j.ssi.2011.01.006>.
- [107] E.G. Herbert, W.E. Tenhaeff, N.J. Dudney, G.M. Pharr, Mechanical characterization of LiPON films using nanoindentation, *Thin Solid Films* 520 (1) (Oct. 2011) 413–418, <https://doi.org/10.1016/j.tsf.2011.07.068>.
- [108] X. Yu, J.B. Bates, G.E. Jellison, F.X. Hart, A stable thin-film lithium electrolyte: lithium phosphorus oxynitride, *J. Electrochem. Soc.* 144 (2) (1997) 524–532, <https://doi.org/10.1149/1.1837443>.
- [109] A. Schwöbel, R. Hausbrand, W. Jaegermann, Interface reactions between LiPON and lithium studied by in-situ X-ray photoemission, *Solid State Ionics* 273 (May 2015) 51–54, <https://doi.org/10.1016/j.ssi.2014.10.017>.
- [110] P. López-Aranguren, et al., Crystalline LiPON as a bulk-type solid electrolyte, *ACS Energy Lett.* (Jan. 2021) 445–450, <https://doi.org/10.1021/acseenergylett.0c02336>.
- [111] Q. Wang, J. Wu, Z. Lu, F. Ciucci, W.K. Pang, X. Guo, “Solid electrolytes: a new lithium-ion conductor LiTaSiO₅: theoretical prediction, materials synthesis, and ionic conductivity (adv. Funct. Mater. 37/2019, Adv. Funct. Mater. 29 (37) (Sep. 2019) 1970253, <https://doi.org/10.1002/adfm.201970253>.
- [112] R. Mercier, J.P. Malugani, B. Fahys, G. Robert, Superionic conduction in Li₂S-P₂S₅-LiI glasses, *Solid State Ionics* 5 (C) (1981) 663–666, [https://doi.org/10.1016/0167-2738\(81\)90341-6](https://doi.org/10.1016/0167-2738(81)90341-6).
- [113] M. Kbal, M. Makytá, A. Levasseur, P. Hagenmuller, Characterization and electrical behavior of new lithium chalcoborate thin films, *Solid State Ionics* 15 (2) (1985) 163–169, [https://doi.org/10.1016/0167-2738\(85\)90096-7](https://doi.org/10.1016/0167-2738(85)90096-7).
- [114] S. Kondo, K. Takada, Y. Yamamura, New lithium ion conductors based on Li₂S-Si₂S₃ system, *Solid State Ionics* 53–56 (1992) 1183–1186, [https://doi.org/10.1016/0167-2738\(92\)90310-L](https://doi.org/10.1016/0167-2738(92)90310-L). PART 2.
- [115] F. Mizuno, A. Hayashi, K. Tadanaga, M. Tatsumisago, New, highly ion-conductive crystals precipitated from Li₂S-P₂S₅ glasses, *Adv. Mater.* 17 (7) (Apr. 2005) 918–921, <https://doi.org/10.1002/adma.200401286>.
- [116] A. Hayashi, K. Minami, S. Ujiie, M. Tatsumisago, Preparation and ionic conductivity of Li₇P₃S₁₁-Z glass-ceramic electrolytes, *J. Non-Cryst. Solids* 356 (44–49) (2010) 2670–2673, <https://doi.org/10.1016/j.jnoncrsol.2010.04.048>.
- [117] A. Kato, M. Nose, M. Yamamoto, A. Sakuda, A. Hayashi, and M. Tatsumisago, “Mechanical properties of sulfide glasses in all-solid-state batteries,” doi: 10.2109/jcersj2.18022.
- [118] A. Sakuda, A. Hayashi, M. Tatsumisago, Recent progress on interface formation in all-solid-state batteries, *Current Opinion in Electrochemistry* 6 (1) (01-Dec-2017) 108–114, <https://doi.org/10.1016/j.coelec.2017.10.008>. Elsevier B.V.
- [119] Y. Seino, T. Ota, K. Takada, A. Hayashi, M. Tatsumisago, A sulphide lithium super ion conductor is superior to liquid ion conductors for use in rechargeable batteries, *Energy Environ. Sci.* 7 (2) (Jan. 2014) 627–631, <https://doi.org/10.1039/c3ee41655k>.
- [120] R. Kanno, T. Hata, Y. Kawamoto, M. Irie, Synthesis of a new lithium ionic conductor, thio-LISICON-lithium germanium sulfide system, *Solid State Ionics* 130 (1) (May 2000) 97–104, [https://doi.org/10.1016/S0167-2738\(00\)00277-0](https://doi.org/10.1016/S0167-2738(00)00277-0).
- [121] M. Murayama, et al., Synthesis of new lithium ionic conductor thio-LISICON - lithium silicon sulfides system, *J. Solid State Chem.* 168 (1) (2002) 140–148, <https://doi.org/10.1006/jssc.2002.9701>.
- [122] R. Kanno, M. Murayama, Lithium ionic conductor thio-LISICON: the Li₂S-GeS₂-P₂S₅ system, *J. Electrochem. Soc.* 148 (7) (Jul. 2001), <https://doi.org/10.1149/1.1379028>.
- [123] G. Sahu, Z. Lin, J. Li, Z. Liu, N. Dudney, C. Liang, Air-stable, high-conduction solid electrolytes of arsenic-substituted Li₄SnS₄, *Energy Environ. Sci.* 7 (3) (Mar. 2014) 1053–1058, <https://doi.org/10.1039/c3ee43357a>.
- [124] N. Kamaya, et al., A lithium superionic conductor, *Nat. Mater.* 10 (9) (2011) 682–686, <https://doi.org/10.1038/nmat3066>.
- [125] X. Liang, et al., In-Channel and in-plane Li ion diffusions in the superionic conductor Li₁₀GeP₂S₁₂ probed by solid-state NMR, *Chem. Mater.* 27 (16) (Aug. 2015) 5503–5510, <https://doi.org/10.1021/acs.chemmater.5b01384>.
- [126] Y. Mo, S.P. Ong, G. Ceder, First principles study of the Li₁₀GeP₂S₁₂ lithium super ionic conductor, *Material*, *Chem. Mater.* 24 (1) (Jan. 2012) 15–17, <https://doi.org/10.1021/cm203303y>.
- [127] Y. Kato, et al., High-power all-solid-state batteries using sulfide superionic conductors, *Nat. Energy* 1 (4) (Apr. 2016) 1–7, <https://doi.org/10.1038/nenergy.2016.30>.
- [128] Z.Q. Wang, M.S. Wu, G. Liu, X.L. Lei, B. Xu, C.Y. Ouyang, “Elastic Properties of New Solid State Electrolyte Material Li₁₀GeP₂S₁₂: A Study from First-Principles Calculations, 2014.
- [129] H.-J. Deiseroth, et al., Li₆PS₅X: A class of crystalline Li-rich solids with an unusually high Li⁺ mobility, *Angew. Chem. Int. Ed.* 47 (4) (Jan. 2008) 755–758, <https://doi.org/10.1002/anie.200703900>.
- [130] L. Zhou, A. Assoud, Q. Zhang, X. Wu, L.F. Nazar, New family of argyrodite thioantimonate lithium superionic conductors, *J. Am. Chem. Soc.* 141 (48) (Dec. 2019) 19002–19013, <https://doi.org/10.1021/jacs.9b08357>.
- [131] H. Muramatsu, A. Hayashi, T. Ohtomo, S. Hama, M. Tatsumisago, Structural change of Li₂S-P₂S₅ sulfide solid electrolytes in the atmosphere, *Solid State Ionics* 182 (1) (Feb. 2011) 116–119, <https://doi.org/10.1016/j.ssi.2010.10.013>.
- [132] Y.S. Jung, D.Y. Oh, Y.J. Nam, K.H. Park, Issues and challenges for bulk-type All-solid-state rechargeable lithium batteries using sulfide solid electrolytes, *Isr. J. Chem.* 55 (5) (May 2015) 472–485, <https://doi.org/10.1002/ijch.201400112>.
- [133] F. Han, Y. Zhu, X. He, Y. Mo, C. Wang, Electrochemical stability of Li₁₀GeP₂S₁₂ and Li₇La₃Zr₂O₁₂ solid electrolytes, *Adv. Energy Mater.* 6 (8) (Apr. 2016) 1501590, <https://doi.org/10.1002/aenm.201501590>.
- [134] B.R. Shin, Y.J. Nam, D.Y. Oh, D.H. Kim, J.W. Kim, Y.S. Jung, Comparative study of TiS₂/Li-In all-solid-state lithium batteries using glass-ceramic Li₃PS₄ and Li₁₀GeP₂S₁₂ solid electrolytes, *Electrochim. Acta* 146 (Nov. 2014) 395–402, <https://doi.org/10.1016/j.electacta.2014.08.139>.
- [135] F. Han, T. Gao, Y. Zhu, K.J. Gaskell, C. Wang, A battery made from a single material, *Adv. Mater.* 27 (23) (Jun. 2015) 3473–3483, <https://doi.org/10.1002/adma.201500180>.
- [136] S. Wenzel, et al., Direct observation of the interfacial instability of the fast ionic conductor Li₁₀GeP₂S₁₂ at the lithium metal anode, *Chem. Mater.* 28 (7) (Apr. 2016) 2400–2407, <https://doi.org/10.1021/acs.chemmater.6b00610>.
- [137] H. Eickhoff, et al., “Lithium phosphidogermanates α- and β-Li₈GeP₄—a novel compound class with mixed Li⁺ ionic and electronic conductivity, *Chem. Mater.* 30 (18) (Sep. 2018) 6440–6448, <https://doi.org/10.1021/acs.chemmater.8b02759>.
- [138] S. Strangmüller, et al., Fast ionic conductivity in the most lithium-rich phosphosilicate Li₁₄SiP₆, *J. Am. Chem. Soc.* 141 (36) (Sep. 2019) 14200–14209, <https://doi.org/10.1021/jacs.9b05301>.
- [139] T.M.F. Restle, et al., Fast lithium ion conduction in lithium phosphoaluminate, *Angew. Chem.* 59 (Dec. 2020) 2–11, <https://doi.org/10.1002/ange.201914613>.
- [140] H. Aono, Ionic conductivity of solid electrolytes based on lithium titanium phosphate, *J. Electrochem. Soc.* 137 (4) (1990) 1023, <https://doi.org/10.1149/1.2086597>.
- [141] M. Itoh, Y. Inaguma, W.-H. Jung, L. Chen, T. Nakamura, High lithium ion conductivity in the perovskite-type compounds Ln₁₂Li₂TiO₃ (Ln=La,Pr,Nd,Sm), *Solid State Ionics* 70–71 (May 1994) 203–207, [https://doi.org/10.1016/0167-2738\(94\)90310-7](https://doi.org/10.1016/0167-2738(94)90310-7).
- [142] E. Rangasamy, et al., An iodide-based Li₇P₂S₈I superionic conductor, *J. Am. Chem. Soc.* 137 (4) (Feb. 2015) 1384–1387, <https://doi.org/10.1021/ja508723m>.
- [143] H. Zhang, et al., Lithium bis(fluorosulfonyl)imide/poly(ethylene oxide) polymer electrolyte, *Electrochim. Acta* 133 (Jul. 2014) 529–538, <https://doi.org/10.1016/j.electacta.2014.04.099>.
- [144] J. Mindemark, B. Sun, E. Törmä, D. Brandell, High-performance solid polymer electrolytes for lithium batteries operational at ambient temperature, *J. Power Sources* 298 (Dec. 2015) 166–170, <https://doi.org/10.1016/j.jpowsour.2015.08.035>.
- [145] F. Croce, G.B. Appetecchi, L. Persi, B. Scrosati, Nanocomposite polymer electrolytes for lithium batteries, *Nature* 394 (6692) (Jul. 1998) 456–458, <https://doi.org/10.1038/28818>.
- [146] L. Chen, Y. Li, S.P. Li, L.Z. Fan, C.W. Nan, J.B. Goodenough, “PEO/garnet composite electrolytes for solid-state lithium batteries: from ‘ceramic-in-polymer’ to ‘polymer-in-ceramic,’ *Nanomater. Energy* 46 (Apr. 2018) 176–184, <https://doi.org/10.1016/j.nanoen.2017.12.037>.
- [147] K. Fu, et al., Flexible, solid-state, ion-conducting membrane with 3D garnet nanofiber networks for lithium batteries, *Proc. Natl. Acad. Sci. U.S.A.* 113 (26) (2016) 7094–7099, <https://doi.org/10.1073/pnas.1600422113>.
- [148] M. Armand, Polymers with ionic conductivity, *Adv. Mater.* 2 (6–7) (01-Jun-1990) 278–286, <https://doi.org/10.1002/adma.19900020603>. John Wiley & Sons, Ltd, pp.
- [149] P. Baudry, S. Lascaud, H. Majastre, D. Bloch, Lithium polymer battery development for electric vehicle application, *J. Power Sources* 68 (2) (Oct. 1997) 432–435, [https://doi.org/10.1016/S0378-7753\(97\)02646-3](https://doi.org/10.1016/S0378-7753(97)02646-3).

- [150] A.J. Blake, et al., 3D printable ceramic-polymer electrolytes for flexible high-performance Li-ion batteries with enhanced thermal stability, *Adv. Energy Mater.* 7 (14) (Jul. 2017) 1602920, <https://doi.org/10.1002/aenm.201602920>.
- [151] L.J. Deiner, C.A.G. Bezerra, T.G. Howell, A.S. Powell, "Digital printing of solid-state lithium-ion batteries, *Adv. Eng. Mater.* 21 (11) (Nov. 2019) 1900737, <https://doi.org/10.1002/adem.201900737>.
- [152] Z. Chen, et al., 4-V flexible all-solid-state lithium polymer batteries, *Nanomater. Energy* 64 (2019) 103986, <https://doi.org/10.1016/j.nanoen.2019.103986>.
- [153] M.C. Lonergan, A. Nitzan, M.A. Ratner, D.F. Shriver, Dynamically disordered hopping, glass transition, and polymer electrolytes, *J. Chem. Phys.* 103 (8) (Aug. 1995) 3253–3261, <https://doi.org/10.1063/1.470257>.
- [154] Y. Tominaga, K. Yamazaki, Fast Li-ion conduction in poly(ethylene carbonate)-based electrolytes and composites filled with TiO₂ nanoparticles, *Chem. Commun.* 50 (34) (May 2014) 4448–4450, <https://doi.org/10.1039/c3cc49588d>.
- [155] T. Okumura, S. Nishimura, Lithium ion conductive properties of aliphatic polycarbonate, *Solid State Ionics* 267 (Dec. 2014) 68–73, <https://doi.org/10.1016/j.ssi.2014.09.011>.
- [156] K. Kimura, J. Motomatsu, Y. Tominaga, Correlation between solvation structure and ion-conductive behavior of concentrated poly(ethylene carbonate)-based electrolytes, *J. Phys. Chem. C* 120 (23) (Jun. 2016) 12385–12391, <https://doi.org/10.1021/acs.jpcc.6b03277>.
- [157] J. Zhang, et al., Safety-reinforced poly(propylene carbonate)-based all-solid-state polymer electrolyte for ambient-temperature solid polymer lithium batteries, *Adv. Energy Mater.* 5 (24) (Dec. 2015) 1501082, <https://doi.org/10.1002/aenm.201501082>.
- [158] K. Kimura, M. Yajima, Y. Tominaga, A highly-concentrated poly(ethylene carbonate)-based electrolyte for all-solid-state Li battery working at room temperature, *Electrochem. Commun.* 66 (May 2016) 46–48, <https://doi.org/10.1016/j.elecom.2016.02.022>.
- [159] W. He, et al., Carbonate-linked poly(ethylene oxide) polymer electrolytes towards high performance solid state lithium batteries, *Electrochim. Acta* 225 (Jan. 2017) 151–159, <https://doi.org/10.1016/j.electacta.2016.12.113>.
- [160] C. Wang, H. Zhang, J. Li, J. Chai, S. Dong, G. Cui, The interfacial evolution between polycarbonate-based polymer electrolyte and Li-metal anode, *J. Power Sources* 397 (Sep. 2018) 157–161, <https://doi.org/10.1016/j.jpowsour.2018.07.008>.
- [161] B. Commarieu, et al., Solid-to-liquid transition of polycarbonate solid electrolytes in Li-metal batteries, *J. Power Sources* 436 (Oct. 2019) 226852, <https://doi.org/10.1016/j.jpowsour.2019.226852>.
- [162] R. Khurana, J.L. Schaefer, L.A. Archer, G.W. Coates, Suppression of lithium dendrite growth using cross-linked polyethylene/poly(ethylene oxide) electrolytes: a new approach for practical lithium-metal polymer batteries, *J. Am. Chem. Soc.* 136 (20) (May 2014) 7395–7402, <https://doi.org/10.1021/ja502133j>.
- [163] J. Li, Y. Lin, H. Yao, C. Yuan, J. Liu, Tuning thin-film electrolyte for lithium battery by grafting cyclic carbonate and combed poly(ethylene oxide) on polysiloxane, *ChemSusChem* 7 (7) (Jul. 2014) 1901–1908, <https://doi.org/10.1002/cssc.201400113>.
- [164] R. Rohan, et al., A high performance polysiloxane-based single ion conducting polymeric electrolyte membrane for application in lithium ion batteries, *J. Mater. Chem.* 3 (40) (2015) 20267–20276, <https://doi.org/10.1039/C5TA02628H>.
- [165] J.-C. Daigle, et al., Lithium battery with solid polymer electrolyte based on comb-like copolymers, *J. Power Sources* 279 (Apr. 2015) 372–383, <https://doi.org/10.1016/j.jpowsour.2014.12.061>.
- [166] N. Boaretto, C. Joost, M. Seyfried, K. Vezzù, V. Di Noto, Conductivity and properties of polysiloxane-polyether cluster-LiTFSI networks as hybrid polymer electrolytes, *J. Power Sources* 325 (Sep. 2016) 427–437, <https://doi.org/10.1016/j.jpowsour.2016.06.034>.
- [167] I. Aldalur, M. Martínez-Ibañez, A. Krztoń-Maziopa, M. Piszcz, M. Armand, H. Zhang, Flowable polymer electrolytes for lithium metal batteries, *J. Power Sources* 423 (May 2019) 218–226, <https://doi.org/10.1016/j.jpowsour.2019.03.057>.
- [168] S. Schmohl, X. He, H.-D. Wiemhöfer, Boron trifluoride anionic side groups in polyphosphazene based polymer electrolyte with enhanced interfacial stability in lithium batteries, *Polymers* 10 (12) (2018) 1350, <https://doi.org/10.3390/polym10121350>.
- [169] W. Wei, Z. Xu, L. Xu, X. Zhang, H. Xiong, J. Yang, Flexible ionic conducting elastomers for all-solid-state room-temperature lithium batteries, *ACS Appl. Energy Mater.* 1 (12) (Dec. 2018) 6769–6773, <https://doi.org/10.1021/acsaem.8b01796>.
- [170] M. Echeverri, N. Kim, T. Kyu, Ionic conductivity in relation to ternary phase diagram of poly(ethylene oxide), succinonitrile, and lithium bis(trifluoromethane)sulfonimide blends, *Macromolecules* 45 (15) (Aug. 2012) 6068–6077, <https://doi.org/10.1021/ma3008509>.
- [171] H. Zhao, et al., Plasticized polymer composite single-ion conductors for lithium batteries, *ACS Appl. Mater. Interfaces* 7 (34) (Sep. 2015) 19494–19499, <https://doi.org/10.1021/acsaami.5b06096>.
- [172] B. Chen, et al., A new composite solid electrolyte PEO/Li10GeP2S12/SN for all-solid-state lithium battery, *Electrochim. Acta* 210 (Aug. 2016) 905–914, <https://doi.org/10.1016/j.electacta.2016.06.025>.
- [173] J. Zheng, H. Dang, X. Feng, P.-H. Chien, Y.-Y. Hu, "Li-ion transport in a representative ceramic-polymer-plasticizer composite electrolyte: Li₇La₃Zr₂O₁₂-polyethylene oxide-tetraethylene glycol dimethyl ether, *J. Mater. Chem.* 5 (35) (2017) 18457–18463, <https://doi.org/10.1039/C7TA05832B>.
- [174] F. Chen, et al., All-solid-state lithium battery fitted with polymer electrolyte enhanced by solid plasticizer and conductive ceramic filler, *J. Electrochem. Soc.* 165 (14) (Nov. 2018) A3558–A3565, <https://doi.org/10.1149/2.1371814jes>.
- [175] L. Porcarelli, C. Gerbaldi, F. Bella, J.R. Nair, Super soft all-ethylene oxide polymer electrolyte for safe all-solid lithium batteries, *Sci. Rep.* 6 (1) (Jan. 2016) 1–14, <https://doi.org/10.1038/srep19892>.
- [176] D. Bresser, S. Lyonnard, C. Iojoiu, L. Picard, S. Passerini, Decoupling segmental relaxation and ionic conductivity for lithium-ion polymer electrolytes, *Mol. Syst. Des. Eng.* 4 (4) (2019) 779–792, <https://doi.org/10.1039/C9ME00038K>.
- [177] C. Austen Angell, Concepts and conflicts in polymer electrolytes: the search for ion mobility, *Electrochim. Acta* 313 (Aug. 2019) 205–210, <https://doi.org/10.1016/j.electacta.2019.03.193>.
- [178] G.M. Stone, et al., Resolution of the modulus versus adhesion dilemma in solid polymer electrolytes for rechargeable lithium metal batteries, *J. Electrochem. Soc.* 159 (3) (Jan. 2012) A222–A227, <https://doi.org/10.1149/2.030203jes>.
- [179] C. Monroe, J. Newman, The impact of elastic deformation on deposition kinetics at lithium/polymer interfaces, *J. Electrochem. Soc.* 152 (2) (2005) A396, <https://doi.org/10.1149/1.1850854>.
- [180] J.-N. Chazalviel, Electrochemical aspects of the generation of ramified metallic electrodeposits, *Phys. Rev.* 42 (12) (Dec. 1990) 7355–7367, <https://doi.org/10.1103/PhysRevA.42.7355>.
- [181] H. Zhang, et al., Single lithium-ion conducting solid polymer electrolytes: advances and perspectives, *Chem. Soc. Rev.* 46 (3) (2017) 797–815, <https://doi.org/10.1039/C6CS00491A>.
- [182] R. Mezziane, J.-P. Bonnet, M. Courty, K. Djellab, M. Armand, Single-ion polymer electrolytes based on a delocalized polyanion for lithium batteries, *Electrochim. Acta* 57 (Dec. 2011) 14–19, <https://doi.org/10.1016/j.electacta.2011.03.074>.
- [183] Q. Ma, et al., Single lithium-ion conducting polymer electrolytes based on a super-delocalized polyanion, *Angew. Chem. Int. Ed.* 55 (7) (Feb. 2016) 2521–2525, <https://doi.org/10.1002/anie.201509299>.
- [184] N. Lago, O. Garcia-Calvo, J.M. Lopez del Amo, T. Rojo, M. Armand, All-solid-state lithium-ion batteries with grafted ceramic nanoparticles dispersed in solid polymer electrolytes, *ChemSusChem* 8 (18) (Sep. 2015) 3039–3043, <https://doi.org/10.1002/cssc.201500783>.
- [185] I. Villaluenga, et al., Nanostructured single-ion-conducting hybrid electrolytes based on salty nanoparticles and block copolymers, *Macromolecules* 50 (5) (Mar. 2017) 1998–2005, <https://doi.org/10.1021/acs.macromol.6b02522>.
- [186] S. Chereddy, et al., An alternative route to single ion conductivity using multi-ionic salts, *Mater. Horizons* 5 (3) (2018) 461–473, <https://doi.org/10.1039/C7MH01130J>.
- [187] R. Bouchet, et al., Single-ion BAB triblock copolymers as highly efficient electrolytes for lithium-metal batteries, *Nat. Mater.* 12 (5) (May 2013) 452–457, <https://doi.org/10.1038/nmat3602>.
- [188] F. Croce, L.L. Persi, B. Scrosati, F. Serraino-Fiore, E. Plichta, M.A. Hendrickson, Role of the ceramic fillers in enhancing the transport properties of composite polymer electrolytes, *Electrochim. Acta* 46 (16) (May 2001) 2457–2461, [https://doi.org/10.1016/S0013-4686\(01\)00458-3](https://doi.org/10.1016/S0013-4686(01)00458-3).
- [189] J. Przyłuski, M. Siekierski, W. Wiczeorek, Effective medium theory in studies of conductivity of composite polymeric electrolytes, *Electrochim. Acta* 40 (13–14) (Oct. 1995) 2101–2108, [https://doi.org/10.1016/0013-4686\(95\)00147-7](https://doi.org/10.1016/0013-4686(95)00147-7).
- [190] E. Quartarone, P. Mustarelli, A. Magistris, PEO-based composite polymer electrolytes, *Solid State Ionics* 110 (1–2) (Jul. 1998) 1–14, [https://doi.org/10.1016/S0167-2738\(98\)00114-3](https://doi.org/10.1016/S0167-2738(98)00114-3).
- [191] J. Zheng, Y.Y. Hu, New insights into the compositional dependence of Li-ion transport in polymer-ceramic composite electrolytes, *ACS Appl. Mater. Interfaces* 10 (4) (Jan. 2018) 4113–4120, <https://doi.org/10.1021/acsami.7b17301>.
- [192] Y.-C. Jung, S.-M. Lee, J.-H. Choi, S.S. Jang, D.-W. Kim, All solid-state lithium batteries assembled with hybrid solid electrolytes, *J. Electrochem. Soc.* 162 (4) (Feb. 2015) A704–A710, <https://doi.org/10.1149/2.0731504jes>.
- [193] T. Yang, J. Zheng, Q. Cheng, Y.-Y. Hu, C.K. Chan, Composite polymer electrolytes with Li₇La₃Zr₂O₁₂ garnet-type nanowires as ceramic fillers: mechanism of conductivity enhancement and role of doping and morphology, *ACS Appl. Mater. Interfaces* 9 (26) (Jul. 2017) 21773–21780, <https://doi.org/10.1021/acsami.7b03806>.
- [194] J.H. Choi, C.H. Lee, J.H. Yu, C.H. Doh, S.M. Lee, Enhancement of ionic conductivity of composite membranes for all-solid-state lithium rechargeable batteries incorporating tetragonal Li₇La₃Zr₂O₁₂ into a polyethylene oxide matrix, *J. Power Sources* 274 (Jan. 2015) 458–463, <https://doi.org/10.1016/j.jpowsour.2014.10.078>.
- [195] W. Wang, E. Yi, A.J. Fici, R.M. Laine, J. Kieffer, Lithium ion conducting poly(ethylene oxide)-based solid electrolytes containing active or passive ceramic nanoparticles, *J. Phys. Chem. C* 121 (5) (Feb. 2017) 2563–2573, <https://doi.org/10.1021/acs.jpcc.6b11136>.
- [196] J. Zagórski, J.M. López del Amo, M.J. Cordill, F. Aguesse, L. Buannic, A. Llordés, "Garnet-Polymer composite electrolytes: new insights on local Li-ion dynamics and electrodeposition stability with Li metal anodes, *ACS Appl. Energy Mater.* 2 (3) (Mar. 2019) 1734–1746, <https://doi.org/10.1021/acsaem.8b01850>.
- [197] D. Li, L. Chen, T. Wang, L.-Z. Fan, 3D fiber-network-reinforced bicontinuous composite solid electrolyte for dendrite-free lithium metal batteries, *ACS Appl. Mater. Interfaces* 10 (8) (Feb. 2018) 7069–7078, <https://doi.org/10.1021/acsami.7b18123>.
- [198] Y. Sun, et al., Improving ionic conductivity with bimodal-sized Li₇La₃Zr₂O₁₂ fillers for composite polymer electrolytes, *ACS Appl. Mater. Interfaces* 11 (13) (Apr. 2019) 12467–12475, <https://doi.org/10.1021/acsami.8b21770>.
- [199] R. Fan, et al., Versatile strategy for realizing flexible room-temperature all-solid-state battery through a synergistic combination of salt affluent PEO and

- Li₆.75La₃Zr_{1.75}Ta_{0.25}O₁₂ nanofibers, *ACS Appl. Mater. Interfaces* 12 (6) (Feb. 2020) 7222–7231, <https://doi.org/10.1021/acsami.9b20104>.
- [200] X. Wang, et al., Rechargeable solid-state lithium metal batteries with vertically aligned ceramic nanoparticle/polymer composite electrolyte, *Nanomater. Energy* 60 (Jun. 2019) 205–212, <https://doi.org/10.1016/j.nanoen.2019.03.051>.
- [201] W. Liu, et al., Ionic conductivity enhancement of polymer electrolytes with ceramic nanowire fillers, *Nano Lett.* 15 (4) (Apr. 2015) 2740–2745, <https://doi.org/10.1021/acs.nanolett.5b00600>.
- [202] T. Jiang, P. He, G. Wang, Y. Shen, C. Nan, L. Fan, “Solvent-Free synthesis of thin, flexible, nonflammable garnet-based composite solid electrolyte for all-solid-state lithium batteries, *Adv. Energy Mater.* 10 (12) (Mar. 2020) 1903376, <https://doi.org/10.1002/aenm.201903376>.
- [203] N. Wu, et al., enhanced surface interactions enable fast Li⁺ conduction in oxide/polymer composite electrolyte, *Angew. Chem.* 132 (10) (Jan. 2020) 4160–4166, <https://doi.org/10.1002/ange.201914478>.
- [204] B. Zhang, et al., Solid-state lithium metal batteries enabled with high loading composite cathode materials and ceramic-based composite electrolytes, *J. Power Sources* 442 (Dec. 2019) 227230, <https://doi.org/10.1016/j.jpowsour.2019.227230>.
- [205] Y. Zhao, et al., Elastic and well-aligned ceramic LLZO nanofiber based electrolytes for solid-state lithium batteries, *Energy Storage Mater.* 23 (Dec. 2019) 306–313, <https://doi.org/10.1016/j.ensm.2019.04.043>.
- [206] W. Zhou, et al., Polymer lithium-garnet interphase for an all-solid-state rechargeable battery, *Nanomater. Energy* 53 (Nov. 2018) 926–931, <https://doi.org/10.1016/j.nanoen.2018.09.004>.
- [207] K. Liu, R. Zhang, J. Sun, M. Wu, T. Zhao, “Polyoxyethylene (PEO)|PEO-Perovskite|PEO composite electrolyte for all-solid-state lithium metal batteries, *ACS Appl. Mater. Interfaces* 11 (50) (Dec. 2019) 46930–46937, <https://doi.org/10.1021/acsami.9b16936>.
- [208] H. Duan, et al., “Extended electrochemical window of solid electrolytes via heterogeneous multilayered structure for high-voltage lithium metal batteries, *Adv. Mater.* 31 (12) (Mar. 2019) 1807789, <https://doi.org/10.1002/adma.201807789>.
- [209] S.-S. Chi, Y. Liu, N. Zhao, X. Guo, C.-W. Nan, L.-Z. Fan, Solid polymer electrolyte soft interface layer with 3D lithium anode for all-solid-state lithium batteries, *Energy Storage Mater.* 17 (Feb. 2019) 309–316, <https://doi.org/10.1016/j.ensm.2018.07.004>.
- [210] T. Ates, M. Keller, J. Kulisch, T. Adermann, S. Passerini, Development of an all-solid-state lithium battery by slurry-coating procedures using a sulfidic electrolyte, *Energy Storage Mater.* 17 (Feb. 2019) 204–210, <https://doi.org/10.1016/j.ensm.2018.11.011>.
- [211] J.W. Fergus, Recent developments in cathode materials for lithium ion batteries, *J. Power Sources* 195 (4) (15-Feb-2010) 939–954, <https://doi.org/10.1016/j.jpowsour.2009.08.089>. Elsevier.
- [212] L. Wang, B. Chen, J. Ma, G. Cui, L. Chen, Reviving lithium cobalt oxide-based lithium secondary batteries-toward a higher energy density, *Chem. Soc. Rev.* 47 (17) (07-Sep-2018) 6505–6602, <https://doi.org/10.1039/c8cs00322j>. Royal Society of Chemistry.
- [213] S.T. Myung, et al., Nickel-rich layered cathode materials for automotive lithium-ion batteries: achievements and perspectives, *ACS Energy Letters* 2 (1) (13-Jan-2017) 196–223, <https://doi.org/10.1021/acsenenergylett.6b00594>. American Chemical Society.
- [214] A. Ueda, “Solid-State redox reactions of LiNi[_{1/2}]Co[_{1/2}]O[₂] (R3m) for 4 volt secondary lithium cells,” *J. Electrochem. Soc.*, vol. 141, no. 8, p. 2010, 1994, doi: 10.1149/1.2055051.
- [215] C. Delmas, I. Saadoun, A. Rougier, The cycling properties of the Li_xNi_{1-x}CoO₂ electrode, *J. Power Sources* 44 (1–3) (Apr. 1993) 595–602, [https://doi.org/10.1016/0378-7753\(93\)80208-7](https://doi.org/10.1016/0378-7753(93)80208-7).
- [216] T. Ohzuku, “Synthesis and characterization of LiAl[_{1/4}]Ni[_{3/4}]O[₂] (R3m) for lithium-ion (shuttlecock) batteries, *J. Electrochem. Soc.* 142 (12) (1995) 4033, <https://doi.org/10.1149/1.2048458>.
- [217] M. Guilmard, A. Rougier, M. Grüne, L. Croguennec, C. Delmas, Effects of aluminum on the structural and electrochemical properties of LiNiO₂, *J. Power Sources* 115 (2) (Apr. 2003) 305–314, [https://doi.org/10.1016/S0378-7753\(03\)00012-0](https://doi.org/10.1016/S0378-7753(03)00012-0).
- [218] O. Srur-Lavi, et al., Studies of the electrochemical behavior of LiNi_{0.80}Co_{0.15}Al_{0.05}O₂ electrodes coated with LiAlO₂, *J. Electrochem. Soc.* 164 (13) (2017) A3266–A3275, <https://doi.org/10.1149/1.2631713jes>.
- [219] H.J. Noh, S. Youn, C.S. Yoon, Y.K. Sun, Comparison of the structural and electrochemical properties of layered Li[Ni_xCoyMnz]O₂ (x = 1/3, 0.5, 0.6, 0.7, 0.8 and 0.85) cathode material for lithium-ion batteries, *J. Power Sources* 233 (Jul. 2013) 121–130, <https://doi.org/10.1016/j.jpowsour.2013.01.063>.
- [220] S.M. Bak, et al., Structural changes and thermal stability of charged LiNi_xMnyCo_zO₂ cathode materials studied by combined in situ time-resolved XRD and mass spectroscopy, *ACS Appl. Mater. Interfaces* 6 (24) (Dec. 2014) 22594–22601, <https://doi.org/10.1021/am506712c>.
- [221] Y.K. Sun, et al., Nanostructured high-energy cathode materials for advanced lithium batteries, *Nat. Mater.* 11 (11) (Oct. 2012) 942–947, <https://doi.org/10.1038/nmat3435>.
- [222] D.W. Jun, C.S. Yoon, U.H. Kim, Y.K. Sun, High-energy density core-shell structured Li[Ni_{0.95}Co_{0.025}Mn_{0.025}]O₂ cathode for lithium-ion batteries, *Chem. Mater.* 29 (12) (Jun. 2017) 5048–5052, <https://doi.org/10.1021/acs.chemmater.7b01425>.
- [223] BMW iX3 to introduce Gen5 BMW eDrive technology; NMC-811 batteries - green Car Congress.” [Online]. Available: <https://www.greencarcongress.com/2019/12/bmw-ix3-to-introduce-gen5-bmw-edrive-technology-nmc-811-batterie-s.html>. [Accessed: 11-Mar-2020].
- [224] A.K. Padhi, Phospho-olivines as positive-electrode materials for rechargeable lithium batteries, *J. Electrochem. Soc.* 144 (4) (1997) 1188, <https://doi.org/10.1149/1.1837571>.
- [225] M. Armand, M. Gauthier, J.-F. Magnan, N. Ravet, “Method for Synthesis of Carbon-Coated Redox Materials with Controlled Size,” *World Patent WO 02/27823 A1*, 21-Sep-2002.
- [226] K. Amine, H. Yasuda, M. Yamachi, Olivine LiCoPO₄ as 4.8 V electrode material for lithium batteries, *Electrochem. Solid State Lett.* 3 (4) (Apr. 2000) 178–179, <https://doi.org/10.1149/1.1390994>.
- [227] A. Yamada, S.-C. Chung, “Crystal Chemistry of the Olivine-Type Li(Mn[_y]Fe[_{1-y}])PO[₄] and (Mn[_y]Fe[_{1-y}])PO[₄] as Possible 4 V Cathode Materials for Lithium Batteries, *J. Electrochem. Soc.* 148 (8) (Jul. 2001) A960, <https://doi.org/10.1149/1.1385377>.
- [228] C. Masquelier, L. Croguennec, Polymeric (phosphates, silicates, sulfates) frameworks as electrode materials for rechargeable Li (or Na) batteries, *Chem. Rev.* 113 (8) (14-Aug-2013) 6552–6591, <https://doi.org/10.1021/cr3001862>. American Chemical Society.
- [229] D.H. Jang, “Dissolution of spinel oxides and capacity losses in 4 V Li/Li[₂]O[₄] cells,” *J. Electrochem. Soc.* 143 (7) (1996) 2204, <https://doi.org/10.1149/1.1836981>.
- [230] N.J. Dudney, et al., “Nanocrystalline Li_xMn_{2-y}O₄ cathodes for solid-state thin-film rechargeable lithium batteries, *J. Electrochem. Soc.* 146 (7) (Jul. 1999) 2455–2464, <https://doi.org/10.1149/1.1391955>.
- [231] Y. Kobayashi, All-solid-state lithium secondary battery with ceramic/polymer composite electrolyte, *Solid State Ionics* 152 (153) (Dec. 2002) 137–142, [https://doi.org/10.1016/S0167-2738\(02\)00366-1](https://doi.org/10.1016/S0167-2738(02)00366-1).
- [232] A.A. Delluva, J. Dudoff, G. Teeter, A. Holewinski, Cathode interface compatibility of amorphous LiMn₂O₄ (LMO) and Li₇La₃Zr₂O₁₂ (LLZO) characterized with thin-film solid-state electrochemical cells, *ACS Appl. Mater. Interfaces* 12 (22) (Jun. 2020) 24992–24999, <https://doi.org/10.1021/acsami.0c03519>.
- [233] Y.S. Lee, M. Yoshio, Effect of Mn source and peculiar cycle characterization for LiAlO_{1.1}Mn_{1.9}O₄ material in the 3 V region, *Electrochem. Solid State Lett.* 4 (10) (Oct. 2001) A155, <https://doi.org/10.1149/1.1397935>.
- [234] K. Amine, H. Tukamoto, H. Yasuda, Y. Fujita, Preparation and electrochemical investigation of LiMn_{2-x}MexO₄ (Me: Ni, Fe, and x = 0.5, 1) cathode materials for secondary lithium batteries, *J. Power Sources* 68 (2) (Oct. 1997) 604–608, [https://doi.org/10.1016/S0378-7753\(96\)02590-6](https://doi.org/10.1016/S0378-7753(96)02590-6).
- [235] Q. Zhong, A. Bonakdarpour, M. Zhang, G. Y. D. J. R., “Synthesis and Electrochemistry of LiNi[_x]Mn[_{2-x}]O[₄], *J. Electrochem. Soc.* 144 (1) (1997) 205, <https://doi.org/10.1149/1.1837386>.
- [236] A. Manthiram, K. Chemelewski, E.S. Lee, A perspective on the high-voltage LiMn_{1.5}Ni_{0.5}O₄ spinel cathode for lithium-ion batteries, in: *Energy and Environmental Science* vol. 7, 2014, pp. 1339–1350, <https://doi.org/10.1039/c3ee42981d>, 4.
- [237] E.M. Erickson, W. Li, A. Dolocan, A. Manthiram, Insights into the cathode-electrolyte interphases of high-energy-density cathodes in lithium-ion batteries, *ACS Appl. Mater. Interfaces* (Mar. 2020), <https://doi.org/10.1021/acsami.0c00900> acsami.0c00900.
- [238] A. Mauger, C. Julien, Nanoscience supporting the research on the negative electrodes of Li-ion batteries, *Nanomaterials* 5 (4) (Dec. 2015) 2279–2301, <https://doi.org/10.3390/nano5042279>.
- [239] K.C. Moeller, Overview of battery systems, in: *Lithium-Ion Batteries: Basics and Applications*, Springer Berlin Heidelberg, 2018, pp. 3–9.
- [240] C. Fang, X. Wang, Y.S. Meng, Key issues hindering a practical lithium-metal anode, *Trends in Chemistry* 1 (2) (01-May-2019) 152–158, <https://doi.org/10.1016/j.trechm.2019.02.015>. Cell Press.
- [241] Kato Yamahira, Anzai, US5053297, 1991.
- [242] M. Winter, J. O. Besenhard, M. E. Spahr, and P. Novák, “Insertion electrode materials for rechargeable lithium batteries”.
- [243] S. Chae, S. Choi, N. Kim, J. Sung, J. Cho, “Integration of graphite and silicon anodes for the commercialization of high-energy lithium-ion batteries, *Angew. Chem. Int. Ed.* 59 (1) (Jan. 2020) 110–135, <https://doi.org/10.1002/anie.201902085>.
- [244] T. Ohzuku, “Zero-Strain insertion material of Li[Li[_{1/3}]Ti[_{5/3}]O[₄] for rechargeable lithium cells,” *J. Electrochem. Soc.* 142 (5) (1995) 1431, <https://doi.org/10.1149/1.2048592>.
- [245] C. Han, et al., A review of gassing behavior in Li₄Ti₅O₁₂-based lithium ion batteries, *J. Mater. Chem.* 5 (14) (04-Apr-2017) 6368–6381, <https://doi.org/10.1039/c7ta00303j>. Royal Society of Chemistry.
- [246] S. Yubuchi, et al., All-solid-state cells with Li₄Ti₅O₁₂/carbon nanotube composite electrodes prepared by infiltration with argyrodite sulfide-based solid electrolytes via liquid-phase processing, *J. Power Sources* 417 (Mar. 2019) 125–131, <https://doi.org/10.1016/j.jpowsour.2019.01.070>.
- [247] D.Y. Oh, D.H. Kim, S.H. Jung, J.G. Han, N.S. Choi, Y.S. Jung, Single-step wet-chemical fabrication of sheet-type electrodes from solid-electrolyte precursors for all-solid-state lithium-ion batteries, *J. Mater. Chem.* 5 (39) (2017) 20771–20779, <https://doi.org/10.1039/c7ta06873e>.
- [248] S. Ito, et al., A rocking chair type all-solid-state lithium ion battery adopting Li₂O-ZrO₂ coated LiNi_{0.8}Co_{0.15}Al_{0.05}O₂ and a sulfide based electrolyte, *J. Power Sources* 248 (Feb. 2014) 943–950, <https://doi.org/10.1016/j.jpowsour.2013.10.005>.
- [249] W. Ping, et al., A silicon anode for garnet-based all-solid-state batteries: interfaces and nanomechanics, *Energy Storage Mater.* 21 (Sep. 2019) 246–252, <https://doi.org/10.1016/j.ensm.2019.06.024>.

- [250] R.B. Cervera, et al., High performance silicon-based anodes in solid-state lithium batteries, *Energy Environ. Sci.* 7 (2) (Jan. 2014) 662–666, <https://doi.org/10.1039/c3ee43306d>.
- [251] M. Sakuma, K. Suzuki, M. Hirayama, R. Kanno, Reactions at the electrode/electrolyte interface of all-solid-state lithium batteries incorporating Li-M (M = Sn, Si) alloy electrodes and sulfide-based solid electrolytes, *Solid State Ionics* 285 (Feb. 2016) 101–105, <https://doi.org/10.1016/j.ssi.2015.07.010>.
- [252] A. Orue Mendizabal, N. Gomez, F. Aguesse, P. López-Aranguren, Designing spinel Li₄Ti₅O₁₂ electrode as anode material for poly(ethylene)oxide-based solid-state batteries, *Materials* 14 (5) (Mar. 2021) 1213, <https://doi.org/10.3390/ma14051213>.
- [253] F. Marchini, S. Saha, D. Alves Dalla Corte, J.M. Tarascon, Li-rich layered sulfide as cathode active materials in all-solid-state Li-metal batteries, *ACS Appl. Mater. Interfaces* 12 (13) (Apr. 2020) 15145–15154, <https://doi.org/10.1021/acsami.9b22937>.
- [254] X. Yao, et al., High-energy all-solid-state lithium batteries with ultralong cycle life, *Nano Lett.* 16 (11) (Nov. 2016) 7148–7154, <https://doi.org/10.1021/acs.nanolett.6b03448>.
- [255] Q. Zhang, et al., Nickel sulfide anchored carbon nanotubes for all-solid-state lithium batteries with enhanced rate capability and cycling stability, *J. Mater. Chem.* 6 (25) (2018) 12098–12105, <https://doi.org/10.1039/c8ta03449d>.
- [256] B.R. Shin, Y.J. Nam, J.W. Kim, Y.G. Lee, Y.S. Jung, Interfacial architecture for extra Li⁺ storage in all-solid-state lithium batteries, *Sci. Rep.* 4 (Jul. 2014) 5572, <https://doi.org/10.1038/srep05572>.
- [257] K. Aso, A. Sakuda, A. Hayashi, M. Tatsumisago, All-solid-state lithium secondary batteries using NiS-carbon fiber composite electrodes coated with Li₂S-P₂S₅ solid electrolytes by pulsed laser deposition, *ACS Appl. Mater. Interfaces* 5 (3) (Feb. 2013) 686–690, <https://doi.org/10.1021/am302164e>.
- [258] X. Han, et al., Negating interfacial impedance in garnet-based solid-state Li metal batteries, *Nat. Mater.* 16 (5) (Dec. 2016) 572–579, <https://doi.org/10.1038/nmat4821>.
- [259] T. Chartier, A. Bruneau, Aqueous tape casting of alumina substrates, *J. Eur. Ceram. Soc.* 12 (4) (Jan. 1993) 243–247, [https://doi.org/10.1016/0955-2219\(93\)90098-C](https://doi.org/10.1016/0955-2219(93)90098-C).
- [260] D. Hotza, P. Greil, Review: aqueous tape casting of ceramic powders, *Mater. Sci. Eng., A* 202 (1–2) (Nov. 1995) 206–217, [https://doi.org/10.1016/0921-5093\(95\)09785-6](https://doi.org/10.1016/0921-5093(95)09785-6).
- [261] L. Wang, G. Tang, Z.K. Xu, Preparation and electrical properties of multilayer ZnO varistors with water-based tape casting, *Ceram. Int.* 35 (1) (Jan. 2009) 487–492, <https://doi.org/10.1016/j.ceramint.2008.01.011>.
- [262] J. Marie, J. Bourret, P.M. Geffroy, A. Smith, V. Chaleix, T. Chartier, Eco-friendly alumina suspensions for tape-casting process, *J. Eur. Ceram. Soc.* 37 (16) (Dec. 2017) 5239–5248, <https://doi.org/10.1016/j.jeurceramsoc.2017.04.033>.
- [263] J. Kienemann, T. Chartier, C. Pagnoux, J.F. Baumard, M. Huger, J.M. Lamérand, Drying mechanisms and stress development in aqueous alumina tape casting, *J. Eur. Ceram. Soc.* 25 (9) (Jun. 2005) 1551–1564, <https://doi.org/10.1016/j.jeurceramsoc.2004.05.028>.
- [264] M. Michálek, G. Blugan, T. Graule, J. Kuebler, Comparison of aqueous and non-aqueous tape casting of fully stabilized ZrO₂ suspensions, *Powder Technol.* 274 (Apr. 2015) 276–283, <https://doi.org/10.1016/j.powtec.2015.01.036>.
- [265] L.H. Hu, Y.K. Wang, S.C. Wang, Aluminum nitride surface functionalized by polymer derived silicon oxycarbonitride ceramic for anti-hydrolysis, *J. Alloys Compd.* 772 (Jan. 2019) 828–833, <https://doi.org/10.1016/j.jallcom.2018.09.118>.
- [266] R.K. Nishihora, P.L. Rachadel, M.G.N. Quadri, D. Hotza, “Manufacturing porous ceramic materials by tape casting—a review, *J. Eur. Ceram. Soc.* 38 (4) (01-Apr-2018) 988–1001, <https://doi.org/10.1016/j.jeurceramsoc.2017.11.047>. Elsevier Ltd.
- [267] D. Hotza, R.K. Nishihora, R.A.F. Machado, P. Geffroy, T. Chartier, S. Bernard, Tape casting of preceramic polymers toward advanced ceramics: a review, *Int. J. Ceram. Eng. Sci.* 1 (1) (May 2019) 21–41, <https://doi.org/10.1002/ces2.10009>.
- [268] J. Kaiser, et al., Prozess- und Produktentwicklung von Elektroden für Li-Ionen-Zellen, *Chem. Ing. Tech.* 86 (5) (May 2014) 695–706, <https://doi.org/10.1002/cite.201300085>.
- [269] J. Lee, C.-L. Lee, K. Park, I.-D. Kim, Synthesis of an Al₂O₃-coated polyimide nanofiber mat and its electrochemical characteristics as a separator for lithium ion batteries, *J. Power Sources* 248 (Feb. 2014) 1211–1217, <https://doi.org/10.1016/j.jpowsour.2013.10.056>.
- [270] J. Zhang, et al., Renewable and superior thermal-resistant cellulose-based composite nonwoven as lithium-ion battery separator, *ACS Appl. Mater. Interfaces* 5 (1) (Jan. 2013) 128–134, <https://doi.org/10.1021/am302290n>.
- [271] M. Roeder, et al., Li₄Ti₅O₁₂ and LiMn₂O₄ thin-film electrodes on transparent conducting oxides for all-solid-state and electrochromic applications, *J. Power Sources* 301 (2016) 35–40, <https://doi.org/10.1016/j.jpowsour.2015.09.063>.
- [272] M. Bitzer, T. Van Gestel, S. Uhlenbruck, Hans-Peter-Buchkremer, Sol-gel synthesis of thin solid Li₇La₃Zr₂O₁₂ electrolyte films for Li-ion batteries, *Thin Solid Films* 615 (Sep. 2016) 128–134, <https://doi.org/10.1016/j.tsf.2016.07.010>.
- [273] L. Cheng-Bin, Y. Hong-Yun, W. Qiu-Xian, L. Jing-Xian, Y. Shu-Ting, Preparation and property of a novel heat-resistant ceramic composite solid-state electrolyte for lithium batteries, *J. Inorg. Mater.* 32 (8) (2017) 801, <https://doi.org/10.15541/jim20160617>.
- [274] K. Tadanaga, et al., Preparation of lithium ion conductive Al-doped Li₇La₃Zr₂O₁₂ thin films by a sol-gel process, *J. Power Sources* 273 (Jan. 2015) 844–847, <https://doi.org/10.1016/j.jpowsour.2014.09.164>.
- [275] R.-J. Chen, M. Huang, W.-Z. Huang, Y. Shen, Y.-H. Lin, C.-W. Nan, “Sol-gel derived Li-La-Zr-O thin films as solid electrolytes for lithium-ion batteries, *J. Mater. Chem.* 2 (33) (Jun. 2014) 13277, <https://doi.org/10.1039/C4TA02289K>.
- [276] Z. Zhang, et al., Stable cycling of all-solid-state lithium battery with surface amorphized Li_{1.5}Al_{0.5}Ge_{1.5}(PO₄)₃ electrolyte and lithium anode, *Electrochim. Acta* 297 (Feb. 2019) 281–287, <https://doi.org/10.1016/j.electacta.2018.11.206>.
- [277] C.-H. Park, M. Park, S.-I. Yoo, S.-K. Joo, A spin-coated solid polymer electrolyte for all-solid-state rechargeable thin-film lithium polymer batteries, *J. Power Sources* 158 (2) (Aug. 2006) 1442–1446, <https://doi.org/10.1016/j.jpowsour.2005.10.022>.
- [278] J. Zhang, S. Wang, D. Han, M. Xiao, L. Sun, Y. Meng, Lithium (4-styrenesulfonyl) (trifluoromethanesulfonyl) imide based single-ion polymer electrolyte with superior battery performance, *Energy Storage Mater.* 24 (Jan. 2020) 579–587, <https://doi.org/10.1016/j.ensm.2019.06.029>.
- [279] W. Zhou, et al., Double-layer polymer electrolyte for high-voltage all-solid-state rechargeable batteries, *Adv. Mater.* 31 (4) (Jan. 2019) 1805574, <https://doi.org/10.1002/adma.201805574>.
- [280] J. Zagórski, B. Silván, D. Saurel, F. Aguesse, A. Llordés, Importance of composite electrolyte processing to improve the kinetics and energy density of Li metal solid-state batteries, *ACS Appl. Energy Mater.* 3 (9) (Sep. 2020) 8344–8355, <https://doi.org/10.1021/acsaeam.0c00935>.
- [281] W. Zha, Y. Xu, F. Chen, Q. Shen, L. Zhang, Cathode/electrolyte interface engineering via wet coating and hot pressing for all-solid-state lithium battery, *Solid State Ionics* 330 (Feb. 2019) 54–59, <https://doi.org/10.1016/j.ssi.2018.12.008>.
- [282] D. Müller, J.-M. Chabagno, and M. Duval, “Process for Production of an Electrochemical Sub-assembly Comprising an Electrode and an Electrolyte, and the Sub-assembly Obtained in This Way,” no. US4968319A.
- [283] K. O. Macfadden, “Process to Produce Lithium-Polymer Batteries,” no. US5772934A.
- [284] H. Zeng, et al., Enhanced cycling performance for all-solid-state lithium ion battery with LiFePO₄ composite cathode encapsulated by poly (ethylene glycol) (PEG) based polymer electrolyte, *Solid State Ionics* 320 (Jul. 2018) 92–99, <https://doi.org/10.1016/j.ssi.2018.02.040>.
- [285] M. Martínez-Ibañez, et al., “Unprecedented improvement of single Li-ion conductive solid polymer electrolyte through salt additive, *Adv. Funct. Mater.* (Feb. 2020) 2000455, <https://doi.org/10.1002/adfm.202000455>.
- [286] A.I. Piñillas Martínez, et al., The cathode composition, A key player in the success of Li-metal solid-state batteries, *J. Phys. Chem. C* 123 (6) (2019) 3270–3278, <https://doi.org/10.1021/acs.jpcc.8b04626>.
- [287] X. Yu, A. Manthiram, “A long cycle life, all-solid-state lithium battery with a ceramic-polymer composite electrolyte, *ACS Appl. Energy Mater.* 3 (3) (Mar. 2020) 2916–2924, <https://doi.org/10.1021/acsaeam.9b02547>.
- [288] J. Liu, et al., Pathways for practical high-energy long-cycling lithium metal batteries, *Nat. Energy* 4 (3) (Mar. 2019) 180–186, <https://doi.org/10.1038/s41560-019-0338-x>.
- [289] C. Zhao, et al., “Rechargeable lithium metal batteries with an in-built solid-state polymer electrolyte and a high voltage/loading Ni-rich layered cathode, *Adv. Mater.* 32 (12) (Mar. 2020) 1905629, <https://doi.org/10.1002/adma.201905629>.
- [290] T. Inada, et al., All solid-state sheet battery using lithium inorganic solid electrolyte, thio-LISICON, *J. Power Sources* 194 (2) (Dec. 2009) 1085–1088, <https://doi.org/10.1016/j.jpowsour.2009.06.100>.
- [291] Y.-J. Nam, et al., Bendable and thin sulfide solid electrolyte film: a new electrolyte opportunity for free-standing and stackable high-energy all-solid-state lithium-ion batteries, *Nano Lett.* 15 (5) (May 2015) 3317–3323, <https://doi.org/10.1021/acs.nanolett.5b00538>.
- [292] K. Lee, et al., Selection of binder and solvent for solution-processed all-solid-state battery, *J. Electrochem. Soc.* 164 (9) (Jul. 2017) A2075–A2081, <https://doi.org/10.1149/2.1341709jes>.
- [293] N. Rippa, et al., Slurry-based processing of solid electrolytes: a comparative binder study, *J. Electrochem. Soc.* 165 (16) (Dec. 2018) A3993–A3999, <https://doi.org/10.1149/2.0961816jes>.
- [294] D.H. Kim, et al., Infiltration of solution-processable solid electrolytes into conventional Li-Ion-Battery electrodes for all-solid-state Li-ion batteries, *Nano Lett.* 17 (5) (May 2017) 3013–3020, <https://doi.org/10.1021/acs.nanolett.7b00330>.
- [295] D.H. Kim, Y.H. Lee, Y.B. Song, H. Kwak, S.Y. Lee, Y.S. Jung, Thin and flexible solid electrolyte membranes with ultrahigh thermal stability derived from solution-processable Li argyrodites for all-solid-state Li-ion batteries, *ACS Energy Lett.* 5 (3) (Mar. 2020) 718–727, <https://doi.org/10.1021/acsenergylett.0c00251>.
- [296] J. Schnell, F. Tietz, C. Singer, A. Hofer, N. Billot, G. Reinhart, Prospects of production technologies and manufacturing costs of oxide-based all-solid-state lithium batteries, *Energy Environ. Sci.* 12 (6) (Jun. 2019) 1818–1833, <https://doi.org/10.1039/c9ee02692k>.
- [297] E. Yi, W. Wang, J. Kieffer, R.M. Laine, Flame made nanoparticles permit processing of dense, flexible, Li⁺ conducting ceramic electrolyte thin films of cubic-Li₇La₃Zr₂O₁₂ (c-LLZO), *J. Mater. Chem.* 4 (33) (2016) 12947–12954, <https://doi.org/10.1039/c6ta04492a>.
- [298] K. Fu, et al., Three-dimensional bilayer garnet solid electrolyte based high energy density lithium metal-sulfur batteries, *Energy Environ. Sci.* 10 (7) (2017) 1568–1575, <https://doi.org/10.1039/C7EE01004D>.
- [299] S. Xu, et al., All-in-one lithium-sulfur battery enabled by a porous-dense-porous garnet architecture, *Energy Storage Mater.* 15 (Nov. 2018) 458–464, <https://doi.org/10.1016/j.ensm.2018.08.009>.

- [303] G.T. Hitz, et al., High-rate lithium cycling in a scalable trilayer Li-garnet-electrolyte architecture, *Mater. Today* 22 (Jan. 2019) 50–57, <https://doi.org/10.1016/j.mattod.2018.04.004>.
- [304] Z. Zhang, et al., Enabling high-areal-capacity all-solid-state lithium-metal batteries by tri-layer electrolyte architectures, *Energy Storage Mater.* 24 (Jan. 2020) 714–718, <https://doi.org/10.1016/j.ensm.2019.06.006>.
- [305] S. Ohta, S. Komagata, J. Seki, T. Saeki, S. Morishita, T. Asaoka, Short communication All-solid-state lithium ion battery using garnet-type oxide and Li₃BO₃ solid electrolytes fabricated by screen-printing, *J. Power Sources* 238 (Sep. 2013) 53–56, <https://doi.org/10.1016/j.jpowsour.2013.02.073>.
- [306] J. van den Broek, S. Afyon, J.L.M. Rupp, Interface-engineered all-solid-state Li-ion batteries based on garnet-type fast Li⁺ conductors, *Adv. Energy Mater.* 6 (19) (Oct. 2016) 1600736, <https://doi.org/10.1002/aenm.201600736>.
- [307] J.R. Kim, S.W. Choi, S.M. Jo, W.S. Lee, B.C. Kim, Electrospun PVDF-based fibrous polymer electrolytes for lithium ion polymer batteries, *Electrochim. Acta* 50 (1) (Nov. 2004) 69–75, <https://doi.org/10.1016/j.electacta.2004.07.014>.
- [308] G. Piana, F. Bella, F. Geobaldo, G. Meligrana, C. Gerbaldi, “PEO/LAGP hybrid solid polymer electrolytes for ambient temperature lithium batteries by solvent-free, ‘one pot’ preparation, *J. Energy Storage* 26 (Dec. 2019) 100947, <https://doi.org/10.1016/j.est.2019.100947>.
- [309] A. Miguel, F. González, V. Gregorio, N. García, P. Tiemblo, Solvent-free procedure for the preparation under controlled atmosphere conditions of phase-segregated thermoplastic polymer electrolytes, *Polymers* 11 (3) (Mar. 2019) 406, <https://doi.org/10.3390/polym11030406>.
- [310] P.-A. Lavoie, J. Dube, Y. Gagnon, and R. Laliberte, “EP1568090B1 - Co-extrusion manufacturing process of thin film electrochemical cell for lithium polymer batteries - google Patents.” [Online]. Available: <https://patents.google.com/patent/EP1568090B1/en>. [Accessed: 27-Feb-2020].
- [311] L. G. Johnson and D. K. Johnson, “EP3168914A1 - solid-state batteries and methods of fabrication thereof - google Patents.” [Online]. Available: <https://patents.google.com/patent/EP3168914A1>. [Accessed: 27-Feb-2020].
- [312] J. A. Cook, G. B. Park, R. H. McLoughlin, and W. J. Whitcher, “Method for Making a Polymeric Electrolyte,” no. US5013619A.
- [313] M. Duval, “Process of Coating by Melt Extrusion a Solid Polymer Electrolyte on Positive Electrode of Lithium Battery,” no. US5348824A.
- [314] M. Duval and G. St-Amant, “Process for Assembling LPB Batteries,” no. US5536278A.
- [315] M. Gueguen, M. Billion, and H. Majastre, “Method of Manufacturing a Multilayer Electrochemical Assembly Comprising an Electrolyte between Two Electrodes, and an Assembly Made Thereby,” no. US5593462.
- [316] P.-A. Lavoie, R. Laliberté, J. Dubé, and Y. Gagnon, “Co-extrusion Manufacturing Process of Thin Film Electrochemical Cell for Lithium Polymer Batteries and Apparatus Therefor,” no. US7700019B2.
- [317] F. González, et al., High performance polymer/ionic liquid thermoplastic solid electrolyte prepared by solvent free processing for solid state lithium metal batteries, *Membranes* 8 (3) (Aug. 2018) 55, <https://doi.org/10.3390/membranes8030055>.
- [318] F. González, et al., Synergy of inorganic fillers in composite thermoplastic polymer/ionic liquid/LiTFSI electrolytes, *J. Electrochem. Soc.* 167 (7) (Feb. 2020), <https://doi.org/10.1149/1945-7111/AB6BC1>, 070519.
- [319] Z. Huang, R. Tong, J. Zhang, L. Chen, C.-A. Wang, Blending Poly(ethylene oxide) and Li₆.4La₃Zr_{1.4}Ta_{0.6}O₁₂ by Haake Rheomixer without any solvent: a low-cost manufacture method for mass production of composite polymer electrolyte, *J. Power Sources* 451 (Mar. 2020) 227797, <https://doi.org/10.1016/j.jpowsour.2020.227797>.
- [320] S. P. Herle and J. G. Gordon, “Solid State Battery Fabrication,” no. US20140060723A1.
- [321] S. Kuppan and R. Subbaraman, “HOT MELT EXTRUDED SOLID STATE BATTERY COMPONENTS,” no. WO2019170467A1.
- [322] K.-H. Choi, D.B. Ahn, S.-Y. Lee, Current status and challenges in printed batteries: toward form factor-free, monolithic integrated power sources, *ACS Energy Lett.* 3 (1) (Jan. 2018) 220–236, <https://doi.org/10.1021/acsenenergylett.7b01086>.
- [323] C.M. Costa, R. Gonçalves, S. Lancers-Méndez, Recent advances and future challenges in printed batteries, *Energy Storage Mater.* 28 (Jun. 2020) 216–234, <https://doi.org/10.1016/j.ensm.2020.03.012>.
- [324] S.-H. Kim, K.-H. Choi, S.-J. Cho, S. Choi, S. Park, S.-Y. Lee, Printable solid-state lithium-ion batteries: a new route toward shape-conformable power sources with aesthetic versatility for flexible electronics, *Nano Lett.* 15 (8) (Aug. 2015) 5168–5177, <https://doi.org/10.1021/acs.nanolett.5b01394>.
- [325] S.-H. Kim, K.-H. Choi, S.-J. Cho, J. Yoo, S.-S. Lee, S.-Y. Lee, Flexible/shape-versatile, bipolar all-solid-state lithium-ion batteries prepared by multistage printing, *Energy Environ. Sci.* 11 (2) (2018) 321–330, <https://doi.org/10.1039/C7EE01630A>.
- [326] S. Yu, A. Mertens, H. Tempel, R. Schierholz, H. Kungl, R.A. Eichel, Monolithic all-phosphate solid-state lithium-ion battery with improved interfacial compatibility, *ACS Appl. Mater. Interfaces* 10 (26) (Jul. 2018) 22264–22277, <https://doi.org/10.1021/acsami.8b05902>.
- [327] S. Zekoll, et al., Hybrid electrolytes with 3D bicontinuous ordered ceramic and polymer microchannels for all-solid-state batteries, *Energy Environ. Sci.* 11 (1) (2018) 185–201, <https://doi.org/10.1039/C7EE02723K>.
- [328] Y. He, S. Chen, L. Nie, Z. Sun, X. Wu, W. Liu, Stereolithography three-dimensional printing solid polymer electrolytes for all-solid-state lithium metal batteries, *Nano Lett.* 20 (10) (Oct. 2020) 7136–7143, <https://doi.org/10.1021/acs.nanolett.0c02457>.
- [329] L.J. Deiner, T. Jenkins, T. Howell, M. Rottmayer, “Aerosol jet printed polymer composite electrolytes for solid-state Li-ion batteries, *Adv. Eng. Mater.* 21 (12) (Dec. 2019) 1900952, <https://doi.org/10.1002/adem.201900952>.
- [330] A. Maurel, et al., “Poly(Ethylene Oxide)–LiTFSI solid polymer electrolyte filaments for fused deposition modeling three-dimensional printing, *J. Electrochem. Soc.* 167 (7) (Mar. 2020), <https://doi.org/10.1149/1945-7111/ab7c38>, 070536.
- [331] H. Ragones, et al., On the road to a multi-coaxial-cable battery: development of a novel 3D-printed composite solid electrolyte, *J. Electrochem. Soc.* 167 (7) (Dec. 2020), <https://doi.org/10.1149/2.0032007jes>, 070503.
- [332] D.W. McOwen, et al., 3D-Printing electrolytes for solid-state batteries, *Adv. Mater.* 30 (18) (May 2018) 1707132, <https://doi.org/10.1002/adma.201707132>.
- [333] H.A. Kuhn, B.L. Ferguson, Pseudo-isostatic powder metallurgy densification process, in *SAE Technical Papers* (1983), <https://doi.org/10.4271/830362>.
- [334] S. Hans, Cold-pressing process and apparatus, U.S. Patent and Trademark Office, Washington, DC, Oct. 1966. U.S. Patent No. 3,280,613.
- [335] C. Meyer, H. Bockholt, W. Haselrieder, A. Kwade, Characterization of the calendaring process for compaction of electrodes for lithium-ion batteries, *J. Mater. Process. Technol.* 249 (Nov. 2017) 172–178, <https://doi.org/10.1016/j.jmatprotec.2017.05.031>.
- [336] G.B. Appetecchi, J. Hassoun, B. Scrosati, F. Croce, F. Cassel, M. Salomon, Hot-pressed, solvent-free, nanocomposite, PEO-based electrolyte membranes. II. All solid-state Li/LiFePO₄ polymer batteries, *J. Power Sources* 124 (1) (Oct. 2003) 246–253, [https://doi.org/10.1016/S0378-7753\(03\)00611-6](https://doi.org/10.1016/S0378-7753(03)00611-6).
- [337] L. Wang, X. Li, W. Yang, Enhancement of electrochemical properties of hot-pressed poly(ethylene oxide)-based nanocomposite polymer electrolyte films for all-solid-state lithium polymer batteries, *Electrochim. Acta* 55 (2010) 1895–1899, <https://doi.org/10.1016/j.electacta.2009.11.003>.
- [338] T. Okumura, et al., LISICON-based amorphous oxide for bulk-type All-solid-state lithium-ion battery, *ACS Appl. Energy Mater.* 3 (4) (Apr. 2020) 3220–3229, <https://doi.org/10.1021/acsaem.9b01949>.
- [339] X. Kuang, G. Carotenuto, L. Nicolais, Review of ceramic sintering and suggestions on reducing sintering temperatures, *Adv. Perform. Mater.* 4 (3) (Jul. 1997) 257–274, <https://doi.org/10.1023/A:1008621020555>.
- [340] L. Miara, et al., About the compatibility between high voltage spinel cathode materials and solid oxide electrolytes as a function of temperature, *ACS Appl. Mater. Interfaces* 8 (40) (Oct. 2016) 26842–26850, <https://doi.org/10.1021/acsami.6b09059>.
- [341] A. Paoletta, et al., “Toward an all-ceramic cathode–electrolyte interface with low-temperature pressed NASICON Li 1.5 Al 0.5 Ge 1.5 (PO 4) 3 electrolyte,” *Adv. Mater. Interfaces* 7 (12) (Jun. 2020) 2000164, <https://doi.org/10.1002/admi.202000164>.
- [342] Y. Suzuki, et al., Transparent cubic garnet-type solid electrolyte of Al₂O₃-doped Li₇La₃Zr₂O₁₂, *Solid State Ionics* 278 (Jun. 2015) 172–176, <https://doi.org/10.1016/j.ssi.2015.06.009>.
- [343] E.C. Bucharsky, K.G. Schell, A. Hintennach, M.J. Hoffmann, Preparation and characterization of sol-gel derived high lithium ion conductive NZP-type ceramics Li₁ + x Al₂Ti₂ - X(PO₄)₃, *Solid State Ionics* 274 (Jun. 2015) 77–82, <https://doi.org/10.1016/j.ssi.2015.03.009>.
- [344] I. Lisenker, C.R. Stoldt, Improving NASICON sinterability through crystallization under high-frequency electrical fields, *Front. Energy Res.* 4 (MAR) (Mar. 2016) 13, <https://doi.org/10.3389/fenrg.2016.00013>.
- [345] M. Oghbaei, O. Mirzaei, Microwave versus conventional sintering: a review of fundamentals, advantages and applications, *J. Alloys Compd.* 494 (1–2) (Oct–Apr 2010) 175–189, <https://doi.org/10.1016/j.jallcom.2010.01.068>. Elsevier.
- [346] L. Hallopeau, et al., Microwave-assisted reactive sintering and lithium ion conductivity of Li_{1.3}Al_{0.3}Ti_{1.7}(PO₄)₃ solid electrolyte, *J. Power Sources* 378 (Feb. 2018) 48–52, <https://doi.org/10.1016/j.jpowsour.2017.12.021>.
- [347] H.X. Geng, A. Mei, C. Dong, Y.H. Lin, C.W. Nan, Investigation of structure and electrical properties of Li_{0.5}La_{0.5}TiO₃ ceramics via microwave sintering, *J. Alloys Compd.* 481 (1–2) (Jul. 2009) 555–558, <https://doi.org/10.1016/j.jallcom.2009.03.038>.
- [348] S.W. Baek, J.M. Lee, T.Y. Kim, M.S. Song, Y. Park, Garnet related lithium ion conductor processed by spark plasma sintering for all solid state batteries, *J. Power Sources* 249 (2014) 197–206, <https://doi.org/10.1016/j.jpowsour.2013.10.089>.
- [349] A. Aboulaich, et al., A new approach to develop safe all-inorganic monolithic lithium-ion batteries, *Adv. Energy Mater.* 1 (2) (Mar. 2011) 179–183, <https://doi.org/10.1002/aenm.201000050>.
- [350] X. Wei, J. Rehtin, E.A. Olevsky, The fabrication of all-solid-state lithium-ion batteries via spark plasma sintering, *Metals* 7 (9) (Sep. 2017), <https://doi.org/10.3390/met7090372>.
- [351] G. Zhong, et al., Rapid, high-temperature microwave soldering toward a high-performance cathode/electrolyte interface, *Energy Storage Mater.* 30 (Sep. 2020) 385–391, <https://doi.org/10.1016/j.ensm.2020.05.015>.
- [352] A.M. Laptev, H. Zheng, M. Bram, M. Finsterbusch, O. Guillon, High-pressure field assisted sintering of half-cell for all-solid-state battery, *Mater. Lett.* 247 (Jul. 2019) 155–158, <https://doi.org/10.1016/j.matlet.2019.03.109>.
- [353] E.Y. Gutmanas, A. Rabinkin, M. Roitberg, Cold sintering under high pressure, *Scripta Metall.* 13 (1) (Jan. 1979) 11–15, [https://doi.org/10.1016/0036-9748\(79\)90380-6](https://doi.org/10.1016/0036-9748(79)90380-6).
- [354] N. Yamasaki, K. Yanagisawa, M. Nishioka, S. Kanahara, A hydrothermal hot-pressing method: apparatus and application, *J. Mater. Sci. Lett.* 5 (3) (Mar. 1986) 355–356, <https://doi.org/10.1007/BF01748104>.

- [357] H. Guo, A. Baker, J. Guo, C.A. Randall, Cold sintering process: a novel technique for low-temperature ceramic processing of ferroelectrics, *J. Am. Ceram. Soc.* 99 (11) (2016) 3489–3507, <https://doi.org/10.1111/jace.14554>.
- [358] J.P. Maria, et al., Cold sintering: current status and prospects, *J. Mater. Res.* 32 (17) (14-Sep-2017) 3205–3218, <https://doi.org/10.1557/jmr.2017.262>. Cambridge University Press.
- [360] S.S. Berbano, J. Guo, H. Guo, M.T. Lanagan, C.A. Randall, Cold sintering process of $\text{Li}_{1.5}\text{Al}_{0.5}\text{Ge}_{1.5}(\text{PO}_4)_3$ solid electrolyte, *J. Am. Ceram. Soc.* 100 (5) (May 2017) 2123–2135, <https://doi.org/10.1111/jace.14727>.
- [361] H. Nakaya, M. Iwasaki, C.A. Randall, Thermal-assisted cold sintering study of a lithium electrolyte: $\text{Li}_{13.9}\text{Sr}_{0.1}\text{Zn}(\text{GeO}_4)_4$, *J. Electroceram.* 44 (1–2) (Apr. 2020) 16–22, <https://doi.org/10.1007/s10832-019-00196-1>.
- [362] J.H. Seo, et al., Cold sintering of a Li-ion cathode: LiFePO_4 -composite with high volumetric capacity, *Ceram. Int.* 43 (17) (Dec. 2017) 15370–15374, <https://doi.org/10.1016/j.ceramint.2017.08.077>.
- [363] J.H. Seo, K. Verlinde, R. Rajagopalan, E.D. Gomez, T.E. Mallouk, C.A. Randall, Cold sintering process for fabrication of a high volumetric capacity $\text{Li}_4\text{Tl}_5\text{O}_{12}$ anode, *Mater. Sci. Eng. B Solid-State Mater. Adv. Technol.* 250 (Nov. 2019) 114435, <https://doi.org/10.1016/j.mseb.2019.114435>.
- [364] D.M. Mattox, D.M. Mattox, Vacuum evaporation and vacuum deposition, *Handb. Phys. Vap. Depos. Process.* (Jan. 2010) 195–235, <https://doi.org/10.1016/B978-0-8155-2037-5.00006-X>.
- [365] K. Wasa, *Sputtering Systems*, in: *Handbook of Sputter Deposition Technology: Fundamentals and Applications for Functional Thin Films, Nano-Materials and MEMS*, second ed., William Andrew Publishing, 2012, pp. 77–139.
- [366] R.W. Johnson, A. Hultqvist, S.F. Bent, A brief review of atomic layer deposition: from fundamentals to applications, *Mater. Today* (2014), <https://doi.org/10.1016/j.mattod.2014.04.026>.
- [367] J.S. Park, et al., “Effects of crystallinity and impurities on the electrical conductivity of Li-La-Zr-O thin films, *Thin Solid Films* 576 (2015) 55–60, <https://doi.org/10.1016/j.tsf.2014.11.019>.
- [368] H. Katsui, T. Goto, Preparation of cubic and tetragonal $\text{Li}_7\text{La}_3\text{Zr}_{12}\text{O}_{22}$ film by metal organic chemical vapor deposition, *Thin Solid Films* 584 (Jun. 2015) 130–134, <https://doi.org/10.1016/j.tsf.2014.11.094>.
- [369] J.B. Bates, N.J. Dudney, B. Neudecker, A. Ueda, C.D. Evans, Thin-film lithium and lithium-ion batteries, *Solid State Ionics* 135 (1–4) (Nov. 2000) 33–45, [https://doi.org/10.1016/S0167-2738\(00\)00327-1](https://doi.org/10.1016/S0167-2738(00)00327-1).
- [370] C.M. Julien, A. Mauger, Pulsed laser deposited films for microbatteries, *Coatings* 9 (6) (01-Jun-2019) 386, <https://doi.org/10.3390/COATINGS9060386>. MDPI AG.
- [371] A. Rambabu, S.B. Krupanidhi, P. Barpanda, An overview of nanostructured Li-based thin film micro-batteries, *Proc Indian Natn Sci Acad* 85 (1) (2019) 121–142, <https://doi.org/10.16943/ptinsa/2018/49472>.
- [372] R. Xu, et al., Artificial interphases for highly stable lithium metal anode, *Matter* 1 (2) (07-Aug-2019) 317–344, <https://doi.org/10.1016/j.matt.2019.05.016>. Cell Press.
- [373] J.B. Bates, et al., Electrical properties of amorphous lithium electrolyte thin films, *Solid State Ionics* 53 (1992) 647–654, [https://doi.org/10.1016/0167-2738\(92\)90442-R](https://doi.org/10.1016/0167-2738(92)90442-R).
- [374] R. Pfenninger, M. Struzik, I. Garbayo, E. Stulp, J.L.M. Rupp, A low ride on processing temperature for fast lithium conduction in garnet solid-state battery films, *Nat. Energy* (May 2019) 1, <https://doi.org/10.1038/s41560-019-0384-4>.
- [375] F. Aguesse, et al., Microstructure and ionic conductivity of LLTO thin films: influence of different substrates and excess lithium in the target, *Solid State Ionics* 272 (Apr 2015) 1–8, <https://doi.org/10.1016/j.ssi.2014.12.005>, 0.
- [376] C. Wang, et al., Conformal, nanoscale ZnO surface modification of garnet-based solid-state electrolyte for lithium metal anodes, *Nano Lett.* 17 (1) (Jan. 2017) 565–571, <https://doi.org/10.1021/acs.nanolett.6b04695>.
- [377] Z. Fan, et al., Solid/solid interfacial architecture of solid polymer electrolyte-based all-solid-state lithium-sulfur batteries by atomic layer deposition, *Small* (Sep. 2019) 1903952, <https://doi.org/10.1002/smll.201903952>.
- [378] M. Nagao, A. Hayashi, M. Tatsumisago, Bulk-type lithium metal secondary battery with indium thin layer at interface between Li electrode and $\text{Li}_2\text{S-P2S}_5$ solid electrolyte, *Electrochemistry* 80 (10) (Oct. 2012) 734–736, <https://doi.org/10.5796/electrochemistry.80.734>.
- [379] K. Kelvin, Fu, et al., “Toward garnet electrolyte-based Li metal batteries: an ultrathin, highly effective, artificial solid-state electrolyte/metallic Li interface, *Sci. Adv.* 3 (4) (Apr. 2017), e1601659, <https://doi.org/10.1126/sciadv.1601659>.
- [380] K.K. Fu, et al., “Transient behavior of the metal interface in lithium metal-garnet batteries, *Angew. Chem. Int. Ed.* 56 (47) (Nov. 2017) 14942–14947, <https://doi.org/10.1002/anie.201708637>.
- [381] C.-L. Tsai, et al., $\text{Li}_7\text{La}_3\text{Zr}_{12}\text{O}_{22}$ interface modification for Li dendrite prevention, *ACS Appl. Mater. Interfaces* 8 (16) (Apr. 2016) 10617–10626, <https://doi.org/10.1021/acsami.6b00831>.
- [382] J. Wakasugi, H. Munakata, K. Kanamura, effect of gold layer on interface resistance between lithium metal anode and $\text{Li}_{6.25}\text{Al}_{0.25}\text{La}_3\text{Zr}_{12}\text{O}_{22}$ solid electrolyte, *J. Electrochem. Soc.* 164 (6) (Jan. 2017) A1022–A1025, <https://doi.org/10.1149/2.0471706jes>.
- [383] L. Wang, et al., Long lifespan lithium metal anodes enabled by Al_2O_3 sputter coating, *Energy Storage Mater.* 10 (Jan. 2018) 16–23, <https://doi.org/10.1016/J.ENSM.2017.08.001>.
- [384] K. Liu, R. Zhang, M. Wu, H. Jiang, T. Zhao, Ultra-stable lithium plating/stripping in garnet-based lithium-metal batteries enabled by a SnO_2 nanolayer, *J. Power Sources* 433 (Sep. 2019) 226691, <https://doi.org/10.1016/J.JPOWSOUR.2019.226691>.
- [385] M. Rawlence, et al., “Effect of gallium substitution on lithium-ion conductivity and phase evolution in sputtered $\text{Li}_{7-3x}\text{Ga}_x\text{La}_3\text{Zr}_{12}\text{O}_{22}$ thin films, *ACS Appl. Mater. Interfaces* 10 (16) (Apr. 2018) 13720–13728, <https://doi.org/10.1021/acsami.8b03163>.
- [386] H.C.M. Knoop, M.E. Donders, M.C.M. van de Sanden, P.H.L. Notten, W.M. M. Kessels, Atomic layer deposition for nanostructured Li-ion batteries, *J. Vac. Sci. Technol. A Vacuum, Surfaces, Film.* 30 (1) (Jan. 2012), <https://doi.org/10.1116/1.3660699>, 010801.
- [387] J. Liu, et al., Rational design of atomic-layer-deposited LiFePO_4 as a high-performance cathode for lithium-ion batteries, *Adv. Mater.* 26 (37) (Oct. 2014) 6472–6477, <https://doi.org/10.1002/adma.201401805>.
- [388] M.E. Donders, W.M. Arnoldbik, H.C.M. Knoop, W.M.M. Kessels, P.H.L. Notten, Atomic layer deposition of LiCoO_2 thin-film electrodes for all-solid-state Li-ion micro-batteries, *J. Electrochem. Soc.* 160 (5) (Mar. 2013) A3066–A3071, <https://doi.org/10.1149/2.011305jes>.
- [389] G. Wang, et al., Toward ultrafast lithium ion capacitors: a novel atomic layer deposition seeded preparation of $\text{Li}_4\text{Tl}_5\text{O}_{12}$ /graphene anode, *Nanomater. Energy* 36 (Jun. 2017) 46–57, <https://doi.org/10.1016/j.nanoen.2017.04.020>.
- [390] M. Nisula, Y. Shindo, H. Koga, M. Karppinen, Atomic layer deposition of lithium phosphorus oxynitride, *Chem. Mater.* 27 (20) (Oct. 2015) 6987–6993, <https://doi.org/10.1021/acs.chemmater.5b02199>.
- [391] A.C. Kozen, A.J. Pearce, C.F. Lin, M. Noked, G.W. Rubloff, Atomic layer deposition of the solid electrolyte LiPON , *Chem. Mater.* 27 (15) (Jul. 2015) 5324–5331, <https://doi.org/10.1021/acs.chemmater.5b01654>.
- [392] E. Kazayak, et al., Atomic layer deposition of the solid electrolyte garnet $\text{Li}_7\text{La}_3\text{Zr}_{12}\text{O}_{22}$, *Chem. Mater.* 29 (8) (Apr. 2017) 3785–3792, <https://doi.org/10.1021/acs.chemmater.7b00944>.
- [393] W. Lu, et al., Recent progresses and development of advanced atomic layer deposition towards high-performance Li-ion batteries, *Nanomaterials* 7 (10) (Oct. 2017) 325, <https://doi.org/10.3390/nano7100325>.
- [394] J. Liu, H. Zhu, M.H.A. Shiraz, Toward 3D solid-state batteries via atomic layer deposition approach, *Front. Energy Res.* 6 (2018), <https://doi.org/10.3389/fenrg.2018.00010>. MAR, Mar.
- [395] X. Li, et al., Atomic layer deposition of solid-state electrolyte coated cathode materials with superior high-voltage cycling behavior for lithium ion battery application, *Energy Environ. Sci.* 7 (2) (Jan. 2014) 768–778, <https://doi.org/10.1039/c3ee42704h>.
- [396] J. Lau, R.H. DeBlock, D.M. Butts, D.S. Ashby, C.S. Choi, B.S. Dunn, Sulfide solid electrolytes for lithium battery applications, *Adv. Energy Mater.* 8 (27) (Sep. 2018) 1800933, <https://doi.org/10.1002/aenm.201800933>.
- [397] J.B. Goodenough, K.S. Park, The Li-ion rechargeable battery: a perspective, *J. Am. Chem. Soc.* 135 (4) (Jan-2013) 1167–1176, <https://doi.org/10.1021/ja3091438>. American Chemical Society.
- [398] N. Ohta, K. Takada, L. Zhang, R. Ma, M. Osada, T. Sasaki, Enhancement of the high-rate capability of solid-state lithium batteries by nanoscale interfacial modification, *Adv. Mater.* 18 (17) (Sep. 2006) 2226–2229, <https://doi.org/10.1002/adma.200502604>.
- [399] D. Grazioli, O. Veners, V. Zadin, D. Brandell, A. Simone, Electrochemical-mechanical modeling of solid polymer electrolytes: impact of mechanical stresses on Li-ion battery performance, *Electrochim. Acta* 296 (2019) 1122–1141, <https://doi.org/10.1016/j.electacta.2018.07.234>.
- [400] R. Koerver, et al., Capacity fade in solid-state batteries: interphase formation and chemomechanical processes in nickel-rich layered oxide cathodes and lithium thiophosphate solid electrolytes, *Chem. Mater.* 29 (13) (Jul. 2017) 5574–5582, <https://doi.org/10.1021/acs.chemmater.7b00931>.
- [401] Y. Xiao, L.J. Miara, Y. Wang, G. Ceder, Computational Screening of Cathode Coatings for Solid-State Batteries, 2019, <https://doi.org/10.1016/j.joule.2019.02.006>.
- [402] G. Oh, M. Hirayama, O. Kwon, K. Suzuki, R. Kanno, Bulk-type All solid-state batteries with 5 v class $\text{LiNi}_0.5\text{Mn}_{1.5}\text{O}_4$ cathode and $\text{Li}_10\text{GeP}_2\text{S}_{12}$ solid electrolyte, *Chem. Mater.* 28 (8) (May 2016) 2634–2640, <https://doi.org/10.1021/acs.chemmater.5b04940>.
- [403] F. Mizuno, A. Hayashi, K. Tadanaga, M. Tatsumisago, Effects of conductive additives in composite positive electrodes on charge-discharge behaviors of all-solid-state lithium secondary batteries, *J. Electrochem. Soc.* 152 (8) (Jun. 2005) A1499, <https://doi.org/10.1149/1.1939633>.
- [404] K. Borzutzki, M. Winter, G. Brunklaus, Improving the NMC111/Polymers electrolyte interface by cathode composition and processing, *J. Electrochem. Soc.* 167 (7) (2020) 70546, <https://doi.org/10.1149/1945-7111/ab7fb5>.
- [405] J. Sakamoto, More pressure needed, *Nature Energy* 4 (10) (01-Oct-2019) 827–828, <https://doi.org/10.1038/s41560-019-0478-z>. Nature Publishing Group, pp.
- [406] X. Zhang, Q.J. Wang, K.L. Harrison, S.A. Roberts, S.J. Harris, Pressure-driven interface evolution in solid-state lithium metal batteries, *Cell Reports Phys. Sci.* 1 (2) (Feb. 2020) 100012, <https://doi.org/10.1016/j.xcrp.2019.100012>.
- [407] E. Yi, et al., All-solid-state batteries using rationally designed garnet electrolyte frameworks, *ACS Appl. Energy Mater.* 3 (1) (Jan. 2020) 170–175, <https://doi.org/10.1021/acs.aem.9b02101>.
- [408] Y. Tian, et al., Compatibility issues between electrodes and electrolytes in solid-state batteries, *Energy Environ. Sci.* 10 (5) (May 2017) 1150–1166, <https://doi.org/10.1039/c7ee00534b>.
- [409] S. Kaboli, et al., Behavior of solid electrolyte in Li-polymer battery with NMC cathode via in-situ scanning electron microscopy, *Nano Lett.* 20 (3) (Mar. 2020) 1607–1613, <https://doi.org/10.1021/acs.nanolett.9b04452>.

- [410] K. Nie, et al., Increasing poly(ethylene oxide) stability to 4.5 V by surface coating of the cathode, *ACS Energy Lett.* 5 (3) (Mar. 2020) 826–832, <https://doi.org/10.1021/acseenergylett.9b02739>.
- [411] H. Vishal, S. Fujiki, Y. Aihara, T. Watanabe, Y. Park, S. Doo, The influence of the carbonate species on $\text{LiNi}_0.8\text{Co}_0.15\text{Al}_0.05\text{O}_2$ surfaces for all-solid-state lithium ion battery performance, *J. Power Sources* 269 (Dec. 2014) 396–402, <https://doi.org/10.1016/j.jpowsour.2014.07.021>.
- [412] D. Wang, et al., Mitigating the interfacial degradation in cathodes for high-performance oxide-based solid-state lithium batteries, *ACS Appl. Mater. Interfaces* 11 (5) (Feb. 2019) 4954–4961–243, <https://doi.org/10.1021/acsami.8b17881>.
- [413] X. Li, et al., Constructing double buffer layers to boost electrochemical performances of NCA cathode for ASSLB, *Energy Storage Mater.* 18 (2019 Mar) 100–106–1325, <https://doi.org/10.1016/j.ensm.2018.10.003>.
- [414] S. Wang, S. Li, B. Wei, X. Lu, Interfacial Engineering at Cathode/LATP Interface for High-Performance Solid-State Batteries, *J. Electrochem. Soc.* 167 (10) (Jun. 2020) 100528, <https://doi.org/10.1149/1945-7111/ab9a00>.
- [415] X. Li, et al., Unravelling the chemistry and microstructure evolution of a cathodic interface in sulfide-based all-solid-state Li-ion batteries, *ACS Energy Lett.* 4 (10) (Oct. 2019) 2480–2488, <https://doi.org/10.1021/acseenergylett.9b01676>.
- [416] Z. Bi, et al., Surface coating of LiMn_2O_4 cathodes with garnet electrolytes for improving cycling stability of solid lithium batteries, *J. Mater. Chem. A* 8 (8) (2020) 4252–4256, <https://doi.org/10.1039/C9TA11203K>.
- [417] C. Wang, et al., Manipulating interfacial nanostructure to achieve high-performance all-solid-state lithium-ion batteries, *Small Methods* 3 (10) (Oct. 2019) 1900261, <https://doi.org/10.1002/smd.201900261>.
- [418] J. Liang, et al., Engineering the conductive carbon/PEO interface to stabilize solid polymer electrolytes for all-solid-state high voltage LiCoO_2 batteries, *J. Mater. Chem. A* 8 (5) (2020) 2769–2776, <https://doi.org/10.1039/C9TA08607B>.
- [419] G.-L. Xu, et al., Building ultraconformal protective layers on both secondary and primary particles of layered lithium transition metal oxide cathode, *Nat. Energy* 4 (6) (Jul. 2019) 484–494, <https://doi.org/10.1038/s41560-019-0387-1>.
- [420] C. Chen, et al., Atomically ordered and epitaxially grown surface structure in core-shell NCA/ NiAl_2O_4 enabling high voltage cyclic stability for cathode application, *Electrochim. Acta* 300 (Mar. 2019) 437–444, <https://doi.org/10.1016/j.electacta.2019.01.144>.
- [421] X. Yu, J. Li, A. Manthiram, Rational design of a laminated dual-polymer/polymer–ceramic composite electrolyte for high-voltage all-solid-state lithium batteries, *ACS Mater. Lett.* (2020) 317–324, <https://doi.org/10.1021/acsmaterialslett.9b00535>.
- [422] J. Ju, et al., Integrated interface strategy toward room temperature solid-state lithium batteries, *ACS Appl. Mater. Interfaces* 10 (16) (2018) 13588–13597, <https://doi.org/10.1021/acsami.8b02240>.
- [423] J. Liu, et al., Nonflammable and high-voltage-tolerated polymer electrolyte achieving high stability and safety in 4.9 V-class lithium metal battery, *ACS Appl. Mater. Interfaces* 11 (48) (Dec. 2019) 45048–45056, <https://doi.org/10.1021/acsami.9b14147>.
- [424] T. Nakamura, K. Amezawa, J. Kulisch, W.G. Zeier, J. Janek, Guidelines for all-solid-state battery design and electrode buffer layers based on chemical potential profile calculation, *ACS Appl. Mater. Interfaces* 11 (22) (Jun. 2019) 19968–19976, <https://doi.org/10.1021/acsami.9b03053>.
- [425] S. Seki, Y. Kobayashi, H. Miyashiro, Y. Mita, T. Iwahori, Fabrication of high-voltage, high-capacity all-solid-state lithium polymer secondary batteries by application of the polymer electrolyte/inorganic electrolyte composite concept, *Chem. Mater.* 17 (8) (Apr. 2005) 2041–2045, <https://doi.org/10.1021/cm047846c>.
- [426] H. Miyashiro, et al., Fabrication of all-solid-state lithium polymer secondary batteries using Al_2O_3 -coated LiCoO_2 , *Chem. Mater.* 17 (23) (Nov. 2005) 5603–5605, <https://doi.org/10.1021/cm0517115>.
- [427] Y. Kobayashi, S. Seki, M. Tabuchi, H. Miyashiro, Y. Mita, T. Iwahori, High-performance genuine lithium polymer battery obtained by fine-ceramic-electrolyte coating of LiCoO_2 , *J. Electrochem. Soc.* 152 (10) (2005) A1985, <https://doi.org/10.1149/1.2007207>.
- [428] T. Kobayashi, et al., Oxidation reaction of polyether-based material and its suppression in lithium rechargeable battery using 4 V class cathode, $\text{LiNi}_{1/3}\text{Mn}_{1/3}\text{Co}_{1/3}\text{O}_2$, *ACS Appl. Mater. Interfaces* 5 (23) (Dec. 2013) 12387–12393, <https://doi.org/10.1021/am403304j>.
- [429] Z. Li, et al., Interfacial engineering for stabilizing polymer electrolytes with 4V cathodes in lithium metal batteries at elevated temperature, *Nanomater. Energy* 72 (Jun. 2020) 104655, <https://doi.org/10.1016/j.nanoen.2020.104655>.
- [430] J. Qiu, L. Yang, G. Sun, X. Yu, H. Li, L. Chen, A stabilized PEO-based solid electrolyte via a facile interfacial engineering method for a high voltage solid-state lithium metal battery, *Chem. Commun.* 56 (42) (2020) 5633–5636, <https://doi.org/10.1039/D0CC01829E>.
- [431] K. Takahashi, et al., All-solid-state lithium battery with LiBH_4 solid electrolyte, *J. Power Sources* 226 (Mar. 2013) 61–64, <https://doi.org/10.1016/j.jpowsour.2012.10.079>.
- [432] N. Ohta, et al., LiNbO_3 -coated LiCoO_2 as cathode material for all solid-state lithium secondary batteries, *Electrochem. Commun.* 9 (7) (Jul. 2007) 1486–1490, <https://doi.org/10.1016/j.elecom.2007.02.008>.
- [434] Q. Zhao, P. Chen, S. Li, X. Liu, L.A. Archer, Solid-state polymer electrolytes stabilized by task-specific salt additives, *J. Mater. Chem.* 7 (13) (2019) 7823–7830, <https://doi.org/10.1039/C8TA12008K>.
- [436] M. Yamada, T. Watanabe, T. Gunji, J. Wu, F. Matsumoto, Review of the design of current collectors for improving the battery performance in lithium-ion and post-lithium-ion batteries, *Electrochemistry* 1 (2) (2020) 124–159, <https://doi.org/10.3390/electrochem1020011>.
- [437] S.T. Myung, Y. Hitoshi, Y.K. Sun, Electrochemical behavior and passivation of current collectors in lithium-ion batteries, *J. Mater. Chem.* 21 (27) (21-Jul-2011) 9891–9911, <https://doi.org/10.1039/c0jm04353b>. The Royal Society of Chemistry.
- [438] K. Kanamura, T. Okagawa, Z. ichiro Takehara, Electrochemical oxidation of propylene carbonate (containing various salts) on aluminium electrodes, *J. Power Sources* 57 (1–2) (Sep. 1995) 119–123, [https://doi.org/10.1016/0378-7753\(95\)02265-1](https://doi.org/10.1016/0378-7753(95)02265-1).
- [439] J.W. Braithwaite, et al., Corrosion of Lithium-Ion Battery Current Collectors, 1999.
- [440] T. Ma, et al., Revisiting the corrosion of the aluminum current collector in lithium-ion batteries, *J. Phys. Chem. Lett.* 8 (5) (Mar. 2017) 1072–1077, <https://doi.org/10.1021/acs.jpclett.6b02933>.
- [441] M. Morita, T. Shibata, N. Yoshimoto, M. Ishikawa, Anodic behavior of aluminum current collector in LiTFSI solutions with different solvent compositions, in: *Journal of Power Sources*, vols. 119–121, 2003, pp. 784–788, [https://doi.org/10.1016/S0378-7753\(03\)00253-2](https://doi.org/10.1016/S0378-7753(03)00253-2).
- [442] L.J. Krause, et al., Corrosion of aluminum at high voltages in non-aqueous electrolytes containing perfluoroalkylsulfonate imides; new lithium salts for lithium-ion cells, *J. Power Sources* 68 (2) (Oct. 1997) 320–325, [https://doi.org/10.1016/S0378-7753\(97\)02517-2](https://doi.org/10.1016/S0378-7753(97)02517-2).
- [443] H. Yang, K. Kwon, T.M. Devine, J.W. Evans, Aluminum corrosion in lithium batteries: an investigation using the electrochemical quartz crystal microbalance, *J. Electrochem. Soc.* 147 (12) (2000) 4399, <https://doi.org/10.1149/1.1394077>.
- [444] K. Matsumoto, K. Inoue, K. Nakahara, R. Yuge, T. Noguchi, K. Utsugi, Suppression of aluminum corrosion by using high concentration LiTFSI electrolyte, *J. Power Sources* 231 (Jun. 2013) 234–238, <https://doi.org/10.1016/j.jpowsour.2012.12.028>.
- [445] Y. Zhou, J. Hu, P. He, Y. Zhang, J. Xu, X. Wu, Corrosion suppression of aluminum metal by optimizing lithium salt concentration in solid-state imide salt-based polymer plastic crystal electrolyte membrane, *ACS Appl. Energy Mater.* 1 (12) (Dec. 2018) 7022–7027, <https://doi.org/10.1021/acsaem.8b01443>.
- [446] M. Wetjen, G.T. Kim, M. Joost, G.B. Appetecchi, M. Winter, S. Passerini, Thermal and electrochemical properties of PEO-LiTFSI-Pyr 14TFSI-based composite cathodes, incorporating 4 V-class cathode active materials, *J. Power Sources* 246 (Jan. 2014) 846–857, <https://doi.org/10.1016/j.jpowsour.2013.08.037>.
- [447] H. Louis, Y.G. Lee, K.M. Kim, W. Il Cho, J.M. Ko, Suppression of aluminum corrosion in lithium bis(trifluoromethanesulfonyl) imidebased electrolytes by the addition of fumed silica, *Bull. Kor. Chem. Soc.* 34 (6) (Jun. 2013) 1795–1799, <https://doi.org/10.5012/bkcs.2013.34.6.1795>.
- [448] V. Wurster, C. Engel, H. Graebe, T. Ferber, W. Jaegermann, R. Hausbrand, characterization of the interfaces in $\text{LiFePO}_4/\text{PEO-LiTFSI}$ composite cathodes and to the adjacent layers, *J. Electrochem. Soc.* 166 (3) (Jan. 2019) A5410–A5420, <https://doi.org/10.1149/2.0621903jes>.
- [449] I.L. Olsen, Polymeric Current Collector for Solid State Electrochemical Device, 1996, p. 5578399.
- [450] R. Koerver, et al., Redox-active cathode interphases in solid-state batteries, *J. Mater. Chem.* 5 (43) (Nov. 2017) 22750–22760, <https://doi.org/10.1039/c7ta07641j>.
- [451] S. Choi, J. Kim, M. Eom, X. Meng, D. Shin, Application of a carbon nanotube (CNT) sheet as a current collector for all-solid-state lithium batteries, *J. Power Sources* 299 (Dec. 2015) 70–75, <https://doi.org/10.1016/j.jpowsour.2015.08.081>.
- [452] B. De, A. Yadav, S. Khan, K.K. Kar, A facile methodology for the development of a printable and flexible all-solid-state rechargeable battery, *ACS Appl. Mater. Interfaces* 9 (23) (Jun. 2017) 19870–19880, <https://doi.org/10.1021/acsami.7b04112>.
- [453] X. Chen, H. Huang, L. Pan, T. Liu, M. Niederberger, “Fully integrated design of a stretchable solid-state lithium-ion full battery, *Adv. Mater.* 31 (43) (Oct. 2019) 1904648, <https://doi.org/10.1002/adma.201904648>.
- [454] A.N. Filippin, et al., Chromium nitride as a stable cathode current collector for all-solid-state thin film Li-ion batteries, *RSC Adv.* 7 (43) (May 2017) 26960–26967, <https://doi.org/10.1039/c7ra03580b>.
- [455] A.N. Filippin, et al., Ni-Al-Cr superalloy as high temperature cathode current collector for advanced thin film Li batteries, *RSC Adv.* 8 (36) (May 2018) 20304–20313, <https://doi.org/10.1039/c8ra02461h>.
- [456] X.Q. Zhang, X.B. Cheng, Q. Zhang, Advances in interfaces between Li metal anode and electrolyte, *Advanced Materials Interfaces* 5 (2) (23-Jan-2018), <https://doi.org/10.1002/admi.201701097>. Wiley-VCH Verlag.
- [457] X. Ke, Y. Wang, L. Dai, C. Yuan, Cell failures of all-solid-state lithium metal batteries with inorganic solid electrolytes: lithium dendrites, *Energy Storage Mater.* 33 (March) (2020) 309–328, <https://doi.org/10.1016/j.ensm.2020.07.024>.
- [458] W. Manalastas, et al., Mechanical failure of garnet electrolytes during Li electrodeposition observed by in-operando microscopy, *J. Power Sources* 412 (Feb. 2019) 287–293, <https://doi.org/10.1016/j.jpowsour.2018.11.041>.
- [459] P. Barai, A.T. Ngo, B. Narayanan, K. Higa, L.A. Curtiss, V. Srinivasan, The role of local inhomogeneities on dendrite growth in LLZO-based solid electrolytes, *J. Electrochem. Soc.* 167 (10) (Jun. 2020) 100537, <https://doi.org/10.1149/1945-7111/ab9b08>.
- [460] S. Wang, H. Xu, W. Li, A. Dolocan, A. Manthiram, Interfacial chemistry in solid-state batteries: formation of interphase and its consequences, *J. Am. Chem. Soc.* 140 (1) (Jan. 2018) 250–257, <https://doi.org/10.1021/jacs.7b09531>.

- [461] K. Takada, et al., Solid state batteries with sulfide-based solid electrolytes, in: *Solid State Ionics* vol. 172, 2004, pp. 25–30, <https://doi.org/10.1016/j.ssi.2004.02.027>, 1–4 SPEC. ISS., pp.
- [462] Q. Tu, L. Barroso-Luque, T. Shi, G. Ceder, Electrodeposition and mechanical stability at lithium-solid electrolyte interface during plating in solid-state batteries, *Cell Reports Phys. Sci.* 1 (7) (Jul. 2020) 100106, <https://doi.org/10.1016/j.xcrp.2020.100106>.
- [463] R.H. Basappa, T. Ito, H. Yamada, Contact between garnet-type solid electrolyte and lithium metal anode: influence on charge transfer resistance and short circuit prevention, *J. Electrochem. Soc.* 164 (4) (2017) A666–A671, <https://doi.org/10.1149/2.0841704jes>.
- [464] X. Yang, et al., Suppressed dendrite formation realized by selective Li deposition in all-solid-state lithium batteries, *Energy Storage Mater.* 27 (May 2020) 198–204, <https://doi.org/10.1016/j.ensm.2020.01.031>.
- [465] M.D. Tikekar, S. Choudhury, Z. Tu, L.A. Archer, Design principles for electrolytes and interfaces for stable lithium-metal batteries, *Nat. Energy* 1 (9) (Sep. 2016) 16114, <https://doi.org/10.1038/nenergy.2016.114>.
- [466] S. Choudhury, D. Vu, A. Warren, M.D. Tikekar, Z. Tu, L.A. Archer, Confining electrodeposition of metals in structured electrolytes, *Proc. Natl. Acad. Sci. Unit. States Am.* 115 (26) (Jun. 2018) 6620–6625, <https://doi.org/10.1073/pnas.1803385115>.
- [467] D. Sharon, P. Bennington, S.N. Patel, P.F. Nealey, Stabilizing dendritic electrodeposition by limiting spatial dimensions in nanostructured electrolytes, *ACS Energy Lett.* 5 (9) (Sep. 2020) 2889–2896, <https://doi.org/10.1021/acscenergylett.0c01543>.
- [468] Z.D. Gordon, T. Yang, G.B. Gomes Morgado, C.K. Chan, Preparation of nano- and microstructured garnet Li₇La₃Zr₂O₁₂ solid electrolytes for Li-ion batteries via cellulose templating, *ACS Sustain. Chem. Eng.* 4 (12) (Dec. 2016) 6391–6398, <https://doi.org/10.1021/acssuschemeng.6b01032>.
- [469] Z. Jiang, Q. Han, S. Wang, H. Wang, “Reducing the interfacial resistance in all-solid-state lithium batteries based on oxide ceramic electrolytes, *ChemElectroChem* 6 (12) (Jun. 2019) 2970–2983, <https://doi.org/10.1002/celec.201801898>.
- [470] A. Sharaifi, H.M. Meyer, J. Nanda, J. Wolfenstine, J. Sakamoto, Characterizing the Li₇La₃Zr₂O₁₂ interface stability and kinetics as a function of temperature and current density, *J. Power Sources* 302 (Jan. 2016) 135–139, <https://doi.org/10.1016/j.jpowsour.2015.10.053>.
- [471] Y. Liu, et al., Transforming from planar to three-dimensional lithium with flowable interphase for solid lithium metal batteries, *Sci. Adv.* 3 (10) (Oct. 2017) eaao0713, <https://doi.org/10.1126/sciadv.aao0713>.
- [472] Y. Zhang, et al., High-capacity, low-tortuosity, and channel-guided lithium metal anode, *Proc. Natl. Acad. Sci. U.S.A.* 114 (14) (Apr. 2017) 3584–3589, <https://doi.org/10.1073/pnas.1618871114>.
- [473] R. Zhang, N.W. Li, X.B. Cheng, Y.X. Yin, Q. Zhang, Y.G. Guo, Advanced micro/nanostructures for lithium metal anodes, *Adv. Sci.* 4 (3) (Mar. 2017), <https://doi.org/10.1002/advs.201600445>.
- [474] Y.G. Lee, et al., “High-energy long-cycling all-solid-state lithium metal batteries enabled by silver–carbon composite anodes, *Nat. Energy* 5 (4) (Mar. 2020) 299–308, <https://doi.org/10.1038/s41560-020-0575-z>.
- [475] Y. Zhao, G. Li, Y. Gao, D. Wang, Q. Huang, D. Wang, Stable Li metal anode by a hybrid lithium polysulfidophosphate/polymer cross-linking film, *ACS Energy Lett.* 4 (6) (Jun. 2019) 1271–1278, <https://doi.org/10.1021/acscenergylett.9b00539>.
- [476] Z. Tong, S.-B. Wang, Y.-K. Liao, S.-F. Hu, R.-S. Liu, Interface between solid-state electrolytes and Li-metal anodes: issues, materials, and processing routes, *ACS Appl. Mater. Interfaces* 12 (42) (Oct. 2020) 47181–47196, <https://doi.org/10.1021/acsaami.0c13591>.
- [477] A. Gutiérrez-Pardo, F. Aguesse, F. Fernández-Carretero, A.I. Siriwardana, A. García-Luis, A. Llordés, Improved electromechanical stability of the Li metal/garnet ceramic interface by a solvent-free deposited OIPC soft layer, *ACS Appl. Energy Mater.* 4 (3) (Mar. 2021) 2388–2397, <https://doi.org/10.1021/acsaem.0c02439>.
- [478] A. Santiago, et al., Improvement of lithium metal polymer batteries through a small dose of fluorinated salt, *J. Phys. Chem. Lett.* 11 (15) (Aug. 2020) 6133–6138, <https://doi.org/10.1021/acs.jpclett.0c01883>.
- [479] X. Fan, et al., Fluorinated solid electrolyte interphase enables highly reversible solid-state Li metal battery, *Sci. Adv.* 4 (12) (Dec. 2018) eaau9245, <https://doi.org/10.1126/sciadv.aau9245>.
- [480] K. Shi, et al., “In situ construction of an ultra-stable conductive composite interface for high-voltage all-solid-state lithium metal batteries, *Angew. Chem. Int. Ed.* 59 (29) (Jul. 2020) 11784–11788, <https://doi.org/10.1002/anie.202000547>.
- [481] W.E. Tenhaeff, X. Yu, K. Hong, K.A. Perry, N.J. Dudney, Ionic transport across interfaces of solid glass and polymer electrolytes for lithium ion batteries, *J. Electrochem. Soc.* 158 (10) (2011) A1143, <https://doi.org/10.1149/1.3625281>.
- [482] H. Xu, et al., Li₃N-modified garnet electrolyte for all-solid-state lithium metal batteries operated at 40 °C, *Nano Lett.* 18 (11) (Nov. 2018) 7414–7418, <https://doi.org/10.1021/acs.nanolett.8b03902>.
- [484] Y. Huang, et al., “Graphitic carbon nitride (g-C₃N₄): an interface enabler for solid-state lithium metal batteries, *Angew. Chem. Int. Ed.* 59 (9) (Feb. 2020) 3699–3704, <https://doi.org/10.1002/anie.201914417>.
- [485] M. Yan, et al., Stabilizing polymer–lithium interface in a rechargeable solid battery, *Adv. Funct. Mater.* 31 (2019) 1908047, <https://doi.org/10.1002/adfm.201908047>.
- [486] J. Lopez, A. Pei, J.Y. Oh, G.-J.N. Wang, Y. Cui, Z. Bao, Effects of polymer coatings on electrodeposited lithium metal, *J. Am. Chem. Soc.* 140 (37) (2018) 11735–11744, <https://doi.org/10.1021/jacs.8b06047>.
- [487] X. Kong, P.E. Rudnicki, S. Choudhury, Z. Bao, J. Qin, Dendrite suppression by a polymer coating: a coarse-grained molecular study, *Adv. Funct. Mater.* (2020) 1910138, <https://doi.org/10.1002/adfm.201910138>.
- [489] W. Zhou, S. Wang, Y. Li, S. Xin, A. Manthiram, J.B. Goodenough, Plating a dendrite-free lithium anode with a polymer/ceramic/polymer sandwich electrolyte, *J. Am. Chem. Soc.* 138 (30) (Aug. 2016) 9385–9388, <https://doi.org/10.1021/jacs.6b05341>.
- [490] C. Wang, et al., Suppression of lithium dendrite formation by using LAGP-PEO (LiTFSI) composite solid electrolyte and lithium metal anode modified by PEO (LiTFSI) in all-solid-state lithium batteries, *ACS Appl. Mater. Interfaces* 9 (15) (2017) 13694–13702, <https://doi.org/10.1021/acsaami.7b00336>.
- [491] B. Liu, et al., Garnet solid electrolyte protected Li-metal batteries, *ACS Appl. Mater. Interfaces* 9 (22) (2017) 18809–18815, <https://doi.org/10.1021/acsaami.7b03887>.
- [492] Y. Zhu, et al., “Dopant-Dependent stability of garnet solid electrolyte interfaces with lithium metal, *Adv. Energy Mater.* 9 (12) (Mar. 2019) 1803440, <https://doi.org/10.1002/aenm.201803440>.
- [493] Y. Kim, et al., “Electrochemical stability of Li_{6.5}La₃Zr_{1.5}M_{0.5}O₁₂ (M = Nb or Ta) against metallic lithium, *Front. Energy Res.* 4 (MAY) (May 2016) 20, <https://doi.org/10.3389/fenrg.2016.00020>.
- [494] S. Kumazaki, et al., High lithium ion conductive Li₇La₃Zr₂O₁₂ by inclusion of both Al and Si, *Electrochem. Commun.* 13 (5) (May 2011) 509–512, <https://doi.org/10.1016/j.elecom.2011.02.035>.
- [495] R.H. Brugge, et al., The origin of chemical inhomogeneity in garnet electrolytes and its impact on the electrochemical performance, *J. Mater. Chem.* 8 (28) (Jul. 2020) 14265–14276, <https://doi.org/10.1039/d0ta04974c>.
- [496] A. Paoletta, et al., “Understanding the reactivity of a thin Li_{1.5}Al_{0.5}Ge_{1.5}(PO₄)₃ solid-state electrolyte toward metallic lithium anode, *Adv. Energy Mater.* (Jul. 2020) 2001497, <https://doi.org/10.1002/aenm.202001497>.
- [497] Y. Liu, et al., Germanium thin film protected lithium aluminum germanium phosphate for solid-state Li batteries, *Adv. Energy Mater.* 8 (16) (Jun. 2018) 1702374, <https://doi.org/10.1002/aenm.201702374>.
- [498] Q. Liu, et al., Self-healing janus interfaces for high-performance LAGP-based lithium metal batteries, *ACS Energy Lett.* 5 (5) (May 2020) 1456–1464, <https://doi.org/10.1021/acscenergylett.0c00542>.
- [499] Q. Yu, et al., Constructing effective interfaces for Li_{1.5}Al_{0.5}Ge_{1.5}(PO₄)₃ pellets to achieve room-temperature hybrid solid-state lithium metal batteries, *ACS Appl. Mater. Interfaces* 11 (10) (Mar. 2019) 9911–9918, <https://doi.org/10.1021/acsaami.8b20413>.
- [501] S. Siculo, M. Fingerle, R. Hausbrand, K. Albe, Interfacial instability of amorphous LiPON against lithium: a combined Density Functional Theory and spectroscopic study, *J. Power Sources* 354 (Jun. 2017) 124–133, <https://doi.org/10.1016/j.jpowsour.2017.04.005>.
- [502] J.M. Whiteley, J.H. Woo, E. Hu, K.-W. Nam, S.-H. Lee, Empowering the lithium metal battery through a silicon-based superionic conductor, *J. Electrochem. Soc.* 161 (12) (2014) A1812–A1817, <https://doi.org/10.1149/2.0501412jes>.
- [503] S. Yubuchi, M. Uematsu, C. Hotehama, A. Sakuda, A. Hayashi, M. Tatsumisago, An argyrodite sulfide-based superionic conductor synthesized by a liquid-phase technique with tetrahydrofuran and ethanol, *J. Mater. Chem.* 7 (2) (2019) 558–566, <https://doi.org/10.1039/c8ta09477b>.
- [504] C. Wang, et al., Stabilizing interface between Li₁₀SnP₂S₁₂ and Li metal by molecular layer deposition, *Nanomater. Energy* 53 (Nov. 2018) 168–174, <https://doi.org/10.1016/j.nanoen.2018.08.030>.
- [505] A.L. Davis, et al., Electro-chemo-mechanical evolution of sulfide solid electrolyte/Li metal interfaces: operando analysis and ALD interlayer effects, *J. Mater. Chem.* 8 (13) (Apr. 2020) 6291–6302, <https://doi.org/10.1039/c9ta11508k>.
- [506] S.J. Visco, V. Nimon, I. Wogan, Y.S. Nimon, L.C. De Jonghe, B.D. Katz, *Solid-state Laminate Electrode Assemblies and Methods of Making*, 2020. “US10707536B2.
- [507] G.B. Appetecchi, S. Scaccia, S. Passerini, Investigation on the stability of the lithium-polymer electrolyte interface, *J. Electrochem. Soc.* 147 (12) (2000) 4448, <https://doi.org/10.1149/1.1394084>.
- [508] B. Sun, C. Xu, J. Mindemark, T. Gustafsson, K. Edström, D. Brandell, At the polymer electrolyte interfaces: the role of the polymer host in interphase layer formation in Li-batteries, *J. Mater. Chem.* 3 (26) (2015) 13994–14000, <https://doi.org/10.1039/C5TA02485D>.
- [511] G.B. Appetecchi, F. Croce, B. Scrosati, Kinetics and stability of the lithium electrode in poly(methylmethacrylate)-based gel electrolytes, *Electrochim. Acta* 40 (8) (Jun. 1995) 991–997, [https://doi.org/10.1016/0013-4686\(94\)00345-2](https://doi.org/10.1016/0013-4686(94)00345-2).
- [512] F. Groce, F. Gerace, G. Dautzemberg, S. Passerini, G.B. Appetecchi, B. Scrosati, Synthesis and characterization of highly conducting gel electrolytes, *Electrochim. Acta* 39 (14) (Oct. 1994) 2187–2194, [https://doi.org/10.1016/0013-4686\(94\)E0167-X](https://doi.org/10.1016/0013-4686(94)E0167-X).
- [513] A. Manuel, Stephan, “Review on gel polymer electrolytes for lithium batteries, *Eur. Polym. J.* 42 (1) (Jan. 2006) 21–42, <https://doi.org/10.1016/j.eurpolymj.2005.09.017>.
- [514] A. Manuel Stephan, S. Gopu Kumar, N.G. Renganathan, M. Anbu Kulandainathan, “Characterization of poly(vinylidene fluoride–hexafluoropropylene) (PVDF–HFP) electrolytes complexed with different lithium salts, *Eur. Polym. J.* 41 (1) (Jan. 2005) 15–21, <https://doi.org/10.1016/j.eurpolymj.2004.09.001>.
- [515] H. Huo, Y. Chen, J. Luo, X. Yang, X. Guo, X. Sun, “Rational design of hierarchical “Ceramic-in-Polymer” and “Polymer-in-Ceramic” electrolytes for dendrite-free solid-state batteries, *Adv. Energy Mater.* 9 (17) (2019) 1804004, <https://doi.org/10.1002/aenm.201804004>.

- [516] T. Abe, M. Ohtsuka, F. Sagane, Y. Iriyama, Z. Ogumi, Lithium ion transfer at the interface between lithium-ion-conductive solid crystalline electrolyte and polymer electrolyte, *J. Electrochem. Soc.* 151 (11) (2004) A1950, <https://doi.org/10.1149/1.1804813>.
- [517] F. Langer, M.S. Palagonia, I. Bardenhagen, J. Glenneberg, F. La Mantia, R. Kun, Impedance spectroscopy analysis of the lithium ion transport through the Li₇La₃Zr₂O₁₂/P(EO)₂₀Li interface, *J. Electrochem. Soc.* 164 (12) (2017) A2298–A2303, <https://doi.org/10.1149/2.0381712jes>.
- [518] A. Gupta, J. Sakamoto, Controlling ionic transport through the PEO-LiTFSI/LLZTO interface, *Electrochem. Soc. Interface* 28 (2) (2019) 63–69, <https://doi.org/10.1149/2.F06192if>.
- [519] H. Huo, et al., Li₂CO₃ effects: new insights into polymer/garnet electrolytes for dendrite-free solid lithium batteries, *Nanomater. Energy* 73 (Jul. 2020) 104836, <https://doi.org/10.1016/j.nanoen.2020.104836>.
- [520] Y. Li, et al., Hybrid polymer/garnet electrolyte with a small interfacial resistance for lithium-ion batteries, *Angew. Chem. Int. Ed.* 56 (3) (Jan. 2017) 753–756, <https://doi.org/10.1002/anie.201608924>.
- [521] Z. Li, et al., Ionic conduction in composite polymer electrolytes: case of PEO:Ga-LLZO composites, *ACS Appl. Mater. Interfaces* 11 (1) (Jan. 2019) 784–791, <https://doi.org/10.1021/acsami.8b17279>.
- [522] W. Zaman, N. Hortance, M.B. Dixit, V. De Andrade, K.B. Hatzell, “Visualizing percolation and ion transport in hybrid solid electrolytes for Li-metal batteries, *J. Mater. Chem.* 7 (41) (2019) 23914–23921, <https://doi.org/10.1039/C9TA05118J>.
- [523] D. Brogioli, F. Langer, R. Kun, F. La Mantia, Space-charge effects at the Li₇La₃Zr₂O₁₂/Poly(ethylene oxide) interface, *ACS Appl. Mater. Interfaces* 11 (12) (2019) 11999–12007, <https://doi.org/10.1021/acsami.8b19237>.
- [524] X. Zhang, et al., Synergistic coupling between Li_{6.75}La₃Zr_{1.75}Ta_{0.25}O₁₂ and poly(vinylidene fluoride) induces high ionic conductivity, mechanical strength, and thermal stability of solid composite electrolytes, *J. Am. Chem. Soc.* 139 (39) (Oct. 2017) 13779–13785, <https://doi.org/10.1021/jacs.7b06364>.
- [525] N. Rippa, B. Stiasny, H. Beyer, S. Indris, H.A. Gasteiger, S.J. Sedlmaier, “Editors’ choice—understanding chemical stability issues between different solid electrolytes in all-solid-state batteries, *J. Electrochem. Soc.* 166 (6) (2019) A975–A983, <https://doi.org/10.1149/2.0351906jes>.
- [526] F.J. Simon, M. Hanauer, A. Henss, F.H. Richter, J. Janek, Properties of the interphase formed between argyrodite-type Li₆PS₅Cl and polymer-based PEO10:LiTFSI, *ACS Appl. Mater. Interfaces* 11 (45) (2019) 42186–42196, <https://doi.org/10.1021/acsami.9b14506>.
- [527] D. Liu, et al., Review of recent development of in situ/operando characterization techniques for lithium battery research, *Adv. Mater.* 31 (28) (Jul. 2019) 1806620, <https://doi.org/10.1002/adma.201806620>.
- [528] S. Krachkovskiy, M.L. Trudeau, K. Zaghib, Application of magnetic resonance techniques to the in situ characterization of Li-ion batteries: a review, *Materials* 13 (7) (Apr. 2020) 1694, <https://doi.org/10.3390/ma13071694>.
- [529] A. Mauger, M. Armand, C.M. Julien, K. Zaghib, Challenges and issues facing lithium metal for solid-state rechargeable batteries, *J. Power Sources* 353 (15–Jun-2017) 333–342, <https://doi.org/10.1016/j.jpowsour.2017.04.018>. Elsevier B.V.